TRANSMEMBRANE PROTEASE TMPRSS11B PROMOTES LUNG CANCER GROWTH BY ENHANCING LACTATE EXPORT AND GLYCOLYTIC METABOLISM

APPROVED BY SUPERVISORY COMMITTEE

Kathryn O'Donnell, Ph.D. _____

Michael Buszczak, Ph.D. _____

Josh Mendell, M.D. Ph.D. _____

Sean Morrison, Ph.D. _____

DEDICATION

This body of work is dedicated to my family for their continuous support. I would like to thank my sister, Jaimie, and nephew, Hendrix, for bringing so much happiness to my life. My parents, Karen and Bob, have given me the opportunity and means to pursue whatever I want in life and I hope this work, in some way, thanks them for that opportunity. Lastly, I am fortunate to have had the support of my graduate mentor, Kate O'Donnell, and undergraduate mentors, Jason Collier and Susan Burke, for their help in guiding my scientific career.

TRANSMEMBRANE PROTEASE TMPRSS11B PROMOTES LUNG CANCER GROWTH BY ENHANCING LACTATE EXPORT AND GLYCOLYTIC METABOLISM

by

BARRETT LOGAN UPDEGRAFF

DISSERTATION

Presented to the Faculty of the Graduate School of Biomedical Sciences at The University of Texas Southwestern Medical Center at Dallas In Partial Fulfillment of the Requirements for the Degree of

DOCTOR OF PHILOSOPHY

The University of Texas Southwestern Medical Center at Dallas

Dallas, Texas

December 7, 2018

TRANSMEMBRANE PROTEASE TMPRSS11B PROMOTES LUNG CANCER GROWTH BY ENHANCING LACTATE EXPORT AND GLYCOLYTIC METABOLISM

BARRETT LOGAN UPDEGRAFF

The University of Texas Southwestern Medical Center at Dallas, 2018

KATHRYN A. O'DONNELL, Ph.D.

Abstract

Pathways underlying metabolic reprogramming in cancer remain incompletely understood. We identified the Transmembrane Serine Protease *TMPRSS11B* as a novel gene that promotes transformation of immortalized human bronchial epithelial cells. *TMPRSS11B* is upregulated in human lung squamous cell cancers and high expression is associated with poor survival of non-small cell lung cancer patients. TMPRSS11B depletion in human lung squamous cell cancer reduced transformation and tumor growth. TMPRSS11B harbors an extracellular protease domain and we hypothesized that catalysis of a membrane bound substrate modulates tumor progression. Interrogation of a set of soluble receptors revealed that wild-type, but not catalytic mutants of TMPRSS11B promotes membrane release of Basigin, an obligate

chaperone of the lactate monocarboxylate transporters MCT1 and MCT4. To investigate whether TMPRSS11B regulates lactate transport, we monitored intracellular lactate content and lactate secretion. Our data suggest TMPRSS11B regulates cellular lactate levels by interacting and co-localizing with Basigin and MCT4 at the plasma membrane to enhance their lactate export efficiency. Specifically, TMPRSS11B expression promoted lactate secretion concomitant with reduced levels of intracellular lactate content. Conversely, TMPRSS11B depletion in lung squamous cell cancer lines resulted in substantial accumulation of intracellular lactate. We detail a novel metabolic role of TMPRSS11B and this work identifies an oncogenic transmembrane protease that promotes tumorigenesis, thereby uncovering a new enzymatic activity that may be targeted for cancer therapy. Interrogation of lactate metabolism *in vivo* will ultimately guide these therapies and contribute to our growing knowledge of lactate biology.

Table of contents

Prior publications

1. Burke SJ, Goff MR, **Updegraff BL**, Lu D, Brown PL, Minkin SC Jr, Biggerstaff JP, Zhao L, Karlstad MD, Collier JJ. Regulation of the CCL2 gene in pancreatic beta-cells by IL-1β and glucocorticoids: role of MKP-1. 2012. PLoS ONE. PMID: 23056550
2. Salomon D, Gonzalez H, **Updegraff BL**, Orth K. Vibrio parahaemolyticus type VI secretion system 1 is activated in marine conditions to target bacteria, and is differentially regulated from system 2. 2013. PLoS ONE. PMID: 23613791
3. Burke SJ, **Updegraff BL**, Bellich RM, Goff MR, Lu D, Minkin SC Jr, Karlstad MD, Collier JJ. Regulation of iNOS gene transcription by IL-1b and IFN-g requires a coactivator exchange mechanism. 2013. Molecular Endocrinology. PMID: 24014650
4. **Updegraff BL**, O'Donnell KA. Stressing the Importance of CHOP in Liver Cancer. (Mini-review).2013. PLoS Genetics. PMID: 24367283
5. Guo Y, **Updegraff BL**, Park S, Durakoglugil D, Cruz VH, Maddux S, Hwang TH, O'Donnell KA. Comprehensive ex vivo transposon mutagenesis identifies genes that promote growth factor independence and leukemogenesis. 2016. Cancer Research. PMID: 26676752
6. Zhou X, **Updegraff BL**, Guo Y, Peyton M, Girard L, Larsen JE, Xie XJ, Zhou Y, Hwang TH, Xie Y, Rodriguez-Canales J, Villalobos P, Behrens C, Wistuba II, Minna JD, O'Donnell KA. Protocadherin 7 acts through SET and PP2A to potentiate MAPK signaling by EGFR and KRAS during lung tumorigenesis. 2017. Cancer Research. PMID: 27821484

7. O'Donnell KA*, Guo Y, Suresh S, **Updegraff BL**, Zhou X. Ex vivo transposon-mediated genetic screens for cancer gene discovery. (Invited chapter, *corresponding author). 2018. Methods in Molecular Biology, in press
8. **Updegraff BL**, Zhou X, Guo Y, Padanad MS, Chen P, Yang C, Sudderth J, Rodriguez-Tirado C, Girard L, Minna JD, Mishra P, DeBerardinis RJ, O'Donnell KA. Transmembrane protease TMPRSS11B promotes lung cancer growth by enhancing lactate export and glycolytic metabolism. 2018. Cell Reports.

Figures

Chapter I: Cancer metabolism

Lung squamous cell cancer (LSCC) in mouse and man

Lung squamous cell cancer kills 400,000 people annually and is the second most common subtype of non-small cell lung cancer (NSCLC) after lung adenocarcinoma (LUAD) (Cancer Genome Atlas Research, 2012). Somatic mutations driving these disease subtypes are distinct, with common LUAD therapies showing little efficacy in LSCC patients (Rekhtman et al., 2012). Recurrent losses of the genomic region harboring *TP53* are common in both types of NSCLC, but additional "driver" mutations separate these into two very different cancers (Cancer Genome Atlas Research, 2012). A common genomic alteration in human LSCC is amplification of a small region of chromosome arm 3q (Bass et al., 2009). This region harbors several genes implicated in LSCC progression and squamous differentiation including the oncogene SRY-box 2 (SOX2), phosphoinositol-3-OH kinase (PIK3CA), and the transcription factor p63 (Bass et al., 2009, Massion et al., 2003). p63 and the cytokeratin KRT5, among other markers of squamous differentiation, are used for histopathological identification of LSCC tumors (Gurda et al., 2015).

Mouse models of cancer are indispensable tools for pre-clinical studies. In mice, the conditional expression of an oncogenic variant of Kras ($Kras^{G12D}$) leads to the development and progression of NSCLC consisting of predominantly LUAD (Meuwissen et al., 2001, Johnson et al., 2001). Another model involving intratracheal delivery of virus encoding Cre recombinase allowed researchers to simultaneously delete *Stk11*

(LKB1) and activate *Kras*^{G12D} in lung epithelia and this promoted the development of both LSCC and LUAD lesions (DuPage et al., 2009). This *Kras*^{G12D}/*Stk11*$^{fl/fl}$ (KL) genetically engineered mouse model (GEMM) makes it possible to study the differential impact of therapies on the development of one or both subtypes of NSCLC. A mouse model of NSCLC that predominantly gives rise to LSCC after the combined deletion of liver kinase B1 (LKB1; mouse gene *Stk11*) and phosphatase and tensin homolog (PTEN; mouse gene *Pten*) develops LSCCs with histopathology consistent with human LSCC samples (Xu et al., 2014). Human LSCC is characterized by the presence of "pearls" rich in cytokeratin proteins, expression of p63, and absence of thyroid transcription factor 1 (TTF1) which is expressed in LUAD samples (Xu et al., 2014). Interestingly, *Stk11* deletion in the *Kras*^{G12D} model gives rise to mixed subtypes of lung cancer with spontaneous LSCC formation in ~56% of mice analyzed (Ji et al., 2007). Another GEMM involving knock-in of a kinase-dead variant of inhibitor of NFκB alpha (Ikk$\alpha^{K44A/K44A}$) spontaneously develop LSCC at a reported 100% incidence rate (Xiao et al., 2013). These models will be important for pre-clinical studies on the efficacy of therapies for LSCC.

Recent evidence suggests that the glucose transporter, GLUT1, can serve as a distinguishing marker of LSCC lesions in the KL mouse model of NSCLC and in human NSCLC tissues (Goodwin et al., 2017). The biological relevance of enhanced GLUT1 expression is reflected by the avidity of LSCC for glucose as revealed by its enhanced uptake of the fluorinated glucose analog ^{18F}-fluorodeoxyglucose identified through positron emission tomography (FDG-PET) compared to non-cancerous tissue (Inoue et al., 1995). FDG-PET has been indispensable in the clinical identification of tumors and

metastases of several cancers due to their enhanced glucose uptake (Som et al., 1980). Not surprisingly, researchers are studying these and other metabolic alterations in cancer to identify and exploit pathways critical to tumor progression.

Cancer metabolism

Proliferative tissues in the body, as well as tumors, utilize metabolic pathways to fuel cellular division (Figure - **Introduction to Cancer Metabolism)**. Our growing knowledge of metabolism in cancer has been confounded by differences in the metabolism of cultured cancer cells in medium replete with high concentrations of glucose and other nutrients compared to the metabolic environment encountered by tumors *in vivo* (DeBerardinis and Chandel, 2016, Hensley et al., 2016). One of the earliest molecular findings in regards to tumors is their profound avidity for glucose and their rapid aerobic fermentation of pyruvate into the easily excretable metabolite lactate (Warburg et al., 1927). In addition to tumors, proliferative cells in the body sometimes ferment glucose into lactate and secrete it instead of completely oxidizing it to carbon dioxide in the tricarboxylic acid (TCA) cycle (Munyon and Merchant, 1959, Hedeskov, 1968, Greiner et al., 1994). Paradoxically, tumors and many healthy tissues import and oxidize lactate rather than utilizing lactate immediately derived from glucose within the cell (Faubert et al., 2017, Hui et al., 2017). This suggests whole-body and subcellular partitioning or compartmentalization of lactate production, transport, and oxidation, but this is poorly understood.

Nutrient labeling experiments have shown glucose-derived carbons contribute to a wide variety of anabolic processes important for proliferation in culture, but *in vivo* labeling and metabolomic approaches will ultimately be necessary to understand

pathways important for tumor progression (Zu and Guppy, 2004, Lunt and Vander Heiden, 2011). The detailed molecular processes governing glucose metabolism remain incompletely understood, however data suggest that tumors acquire and metabolize glucose at rates exceeding their mitochondrial oxidative capacity (Hanahan and Weinberg, 2011). Several investigators, including Otto Warburg, postulated that this enhanced aerobic glycolysis was due to impaired mitochondrial function in cancer. However, mitochondria retain function in cancer and furthermore, partial oxidation of glucose in mitochondria yields precursors for fatty acid and nucleic acid biosynthesis, among other building blocks required for proliferation (Zu and Guppy, 2004, DeBerardinis et al., 2008, Weinberg et al., 2010).

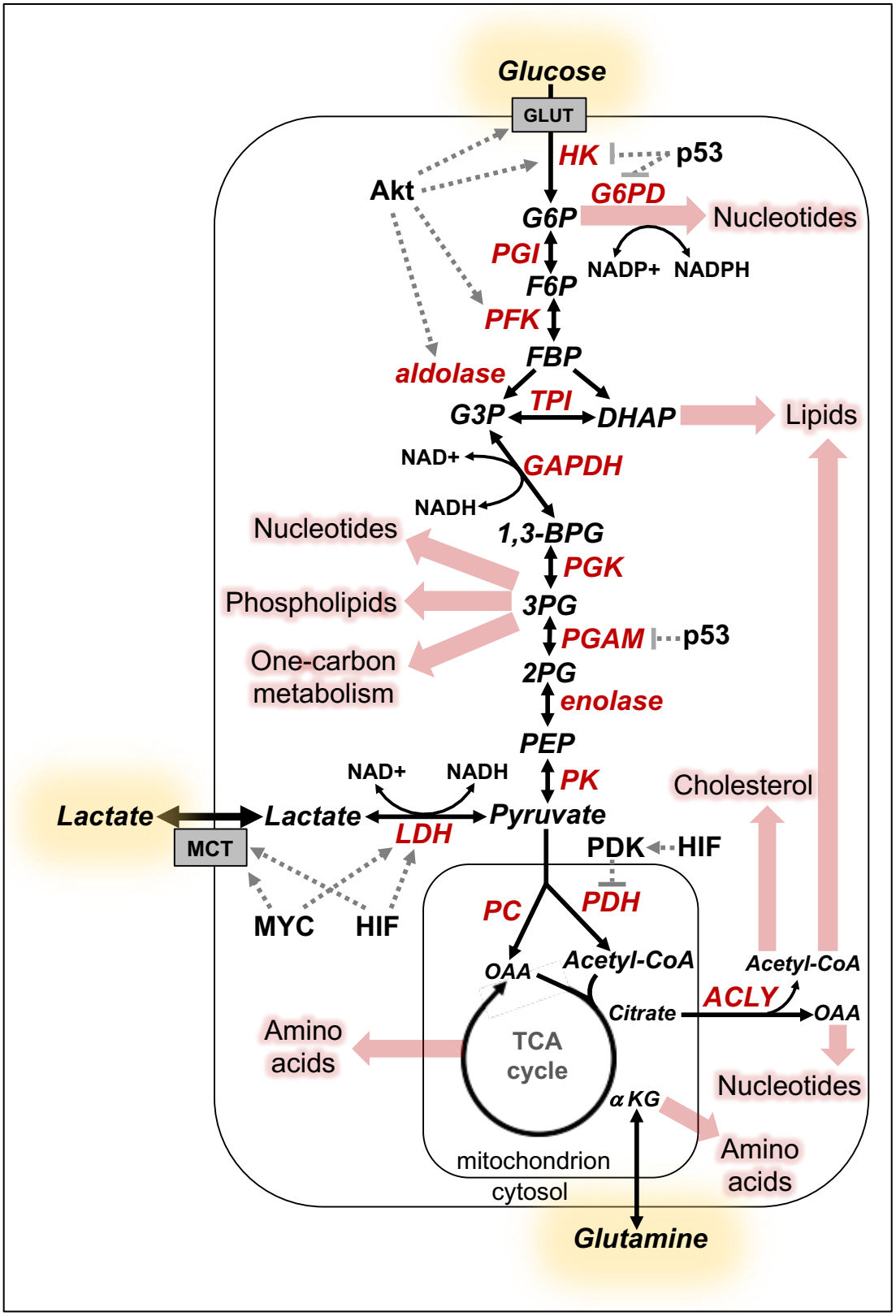
Glucose
GLUT
HK
p53
Akt
G6PD
G6P
Nucleotides
PGI
NADP+
NADPH
F6P
PFK
FBP
aldolase
TPI
G3P
DHAP
Lipids
NAD+
GAPDH
NADH
Nucleotides
1,3-BPG
PGK
Phospholipids
3PG
PGAM
p53
One-carbon metabolism
2PG
enolase
PEP
NAD+
NADH
PK
Cholesterol
Lactate
Lactate
Pyruvate
LDH
MCT
PDK
HIF
MYC
HIF
PC
PDH
OAA
Acetyl-CoA
Acetyl-CoA
ACLY
Citrate
OAA
Amino acids
TCA cycle
Nucleotides
α KG
Amino acids
mitochondrion
cytosol
Glutamine

Introduction to Cancer metabolism. Schematic of metabolic pathways altered in tumors. Enzymes are italicized and maroon, metabolites are italicized and black, and anabolic pathways are in pink. Metabolite abbreviations: G6P, glucose-6-phosphate; F6P, fructose-6-phosphate; FBP, fructose-1,6-bisphosphate; G3P, glyceraldehyde-3-phosphate; DHAP, dihydroxyacetone phosphate; 1,3-BPG, 1,3-bisphosphoglycerate; 3PG, 3-phosphoglycerate; 2PG, 2-phosphoglycerate; PEP, phosphoenol pyruvate; OAA, oxaloacetate; Acetyl-CoA, acetyl coenzyme A; αKG, alphaketoglutarate; NAD, nicotinamide adenine dinucleotide; TCA, tricarboxylic acid. Protein abbreviations: GLUT, glucose transporter; HK, hexokinase; G6PD, glucose-6-phosphate dehydrogenase; PGI: phosphoglucose isomerase; PFK, phosphofructose kinase; TPI, triosephosphate isomerase; GAPDH, glyceraldehyde-3-phosphate dehydrogenase; PGK, phosphoglycerate kinase; PGAM, phosphoglycerate mutase; PK, pyruvate kinase; LDH, lactate dehydrogenase; PC, pyruvate carboxylase; PDH, pyruvate dehydrogenase; MCT, monocarboxylate transporter; ACLY, ATP-citrate lyase; HIF, hypoxia-inducible factor.

Glycolysis supports anabolism and cellular division

Although aerobic glycolysis generates far less ATP from glucose (2 ATP) than complete oxidation in mitochondria (36 ATP), flux through this pathway increases cellular pools of metabolites that can be used for biosynthetic purposes. Glycolytic ATP production contributes minimally to cellular ATP pools, accounting for ~17% of ATP production in a panel of cultured cancer cell lines (Zu and Guppy, 2004). This suggests mitochondrial oxidative phosphorylation supplies the majority of cellular ATP and this is supported by the efficacy of drugs targeting the electron transport chain (ETC), contradicting the notion that impaired mitochondrial metabolism is an inherent feature of cancer (Weinberg and Chandel, 2015). These data demonstrate that upregulation of glycolysis in cancer likely serves biosynthetic, rather than bioenergetic needs. Glycolysis supplies substrate pools for diverse anabolic reactions that are required for cellular division (**Introduction Figure 1**). Elegant labeling experiments have revealed the fate of glucose in cultured cancer cells and tumors by tracing the fate of heavy isotopomers such as $^{13/14}$C-glucose and ^{3}H-glucose (Jang et al., 2018). These studies have shed light on anabolic reactions that utilize metabolites from the glycolytic pathway and will be discussed in detail in the following section.

Anabolic fates of glycolytic metabolites

FDG-PET has revealed high rates of glucose uptake in both primary tumors and metastases and this has proven essential for guiding patient treatment. Tumors use glucose and other metabolites for anabolic reactions required for cell division (**Introduction Figure 1**). ***Glucose*** enters cells through dedicated transporters (GLUTs) and is retained upon phosphorylation by hexokinases (Wood and Trayhurn, 2003,

Meyerhof, 1927, Cahill et al., 1958). Following glucose capture, cells can utilize glucose carbons for biosynthetic or bioenergetic purposes. Phosphorylated glucose, ***glucose-6-phosphate (G6P)*** can either proceed through glycolysis or can enter the oxidative pentose phosphate pathway (PPP) by G6P dehydrogenase (G6PD)-catalyzed oxidation to the metabolite 6-phospho-D-glucono-1,5-lactone (Najjar, 1948, Utter, 1958). This redox reaction reduces NADP+ to NADPH along with the oxidation of ***G6P*** to ribose-5-phosphate (R5P) (Gumaa and McLean, 1969). NADPH, among other roles, serves as a cofactor for a myriad of anabolic reactions in the cell including fatty acid, nucleotide, amino acid, and cholesterol biosynthesis (Lewis et al., 2014). Interestingly, the tumor suppressor p53 has been shown to directly bind G6PD to inhibit its dimerization and enzymatic activity, resulting in reduced PPP flux and NAPDH production (Jiang et al., 2011).

Glucose carbon is used in *de novo* synthesis of nucleotides through the PPP. R5P, upon phosphorylation to 5-phosphoribosyl-α-pyrophosphate (PRPP), can serve as substrate for nucleotide biosynthesis by supplying up to 9 carbons to purine and pyrimidine nucleotides (Tong et al., 2009). Adenosine triphosphate (ATP) sustains virtually all metabolic and replicative processes in the cell such as transcription, translation, and cellular division. Researchers have found that incorporation of ^{3}H-thymidine into DNA increases with higher glucose concentrations in culture and glycolytic enzyme activities are highest during the S phase of the cell cycle (Hume et al., 1978, Marjanovic et al., 1988). Of interest, the oncoprotein Myc has been shown to regulate many genes involved in nucleotide biosynthesis such as the inosine monophosphate dehydrogenases IMPDH1 and IMPDH2, whose expression are

required for Myc-induced proliferation of cultured cancer cells, and experimental tumor growth of subsets of small-cell lung cancer (Liu et al., 2008, Huang et al., 2018).

Glucose carbon, via ***G6P***, that is not diverted toward the PPP proceeds through glycolysis and its isomerization yields ***fructose-6-phosphate (F6P)*** (Slein, 1950). Phosphofructokinase 1 (PFK1) then phosphorylates ***F6P*** yielding ***fructose-1,6-bisphosphate (FBP)*** (Passonneau and Lowry, 1962). Glycosylation of PFK1 impairs its catalytic activity and has been shown to reduce glycolytic flux while promoting diversion of the upstream metabolite ***G6P*** towards the PPP and, paradoxically, this event is important for experimental tumor growth (Yi et al., 2012). The gluconeogenic enzyme fructose-1,6-bisphosphatase (FBP1) also antagonizes glycolytic flux by dephosphorylating ***FBP*** to the upstream ***fructose-6-phosphate (F6P)*** and is almost ubiquitously deleted in clear cell renal cell carcinoma (ccRCC) (Li et al., 2014). This suggests that antagonizing glycolytic flux is tumor suppressive in some cancers.

Aldolase and GAPDH are critical feedback nodes regulating glycolytic flux. Aldolase catalyzes the cleavage of 6-carbon ***FBP*** into two 3-carbon molecules: ***dihydroxyacetone phosphate (DHAP)*** and ***glyceraldehyde-3-phosphate (G3P)*** (Sibley and Lehninger, 1949). Aldolase is frequently up-regulated in LSCC and its expression is associated with poor prognosis (Du et al., 2014). ***G3P*** can undergo reversible isomerization by triose-phosphate isomerase (TPI) to ***DHAP*** which can serve as substrate for phospholipid and triacylglycerol biosynthesis upon reduction to glycerol-3-phosphate, or be interconverted back to ***G3P*** for use in glycolysis (Wu and Racker, 1959). GADPH-catalyzed dehydrogenation of ***G3P*** yields 1,***3-bisphosphoglycerate (1,3-BPG)*** (Cori et al., 1948). In *BRAF* and *KRAS* mutant colorectal cancer cells,

enhanced uptake of oxidized vitamin C (dehydroascorbate) burdens the glutathione antioxidant system leading to the accumulation of reactive oxygen species, impairment of GAPDH activity, and reduced glycolytic flux (Yun et al., 2015). Moreover, GAPDH activity is regulated by both the redox status and abundance of NAD, both of which are deregulated in cancer (Chiarugi et al., 2012).

Phosphoglycerate kinase (PGK) exchanges the phosphoryl group at carbon 1 of ***1,3-BPG*** to ADP, yielding 3-phosphoglycerate (***3PG***) and 2 mole ATP per mole glucose (Banks et al., 1979). One-carbon metabolism of ***3PG***-derived serine is upregulated in human tumors, and has been the target of chemotherapies for decades (DeBerardinis, 2011). ***3PG*** can be oxidized to 3-phosphohydroxypyruvate (PHP) by phosphoglycerate dehydrogenase (PHGDH) and ultimately serine after the actions of two more enzymes (Locasale, 2013). PHGDH is commonly amplified in estrogen receptor negative breast cancer and its depletion impairs serine biosynthesis and proliferation (Possemato et al., 2011). Serine can supply carbons for protein and sphingolipid synthesis or be converted to glycine by serine hydroxymethyltransferase (SHMT) (DeBerardinis, 2011). SHMT donates a methyl group to tetrahydrofolate (THF) producing 5,10-methylene-THF which supplies 2 essential carbons to thymidine, and this activity bolsters the proliferative capacity of cultured cells deficient for Myc (Nikiforov et al., 2002). Glycine supplies 2 carbons to purine nucleotides and inhibition of glycine uptake or synthesis selectively impairs survival of highly proliferative cancer cells in culture (Jain et al., 2012). The enhanced demand for nucleotide synthesis in proliferative cells is exploited in chemotherapy regimens that target folate metabolism with agents such as pemetrexed or methotrexate (Locasale, 2013).

3PG and ***lactate*** labeling patterns in human lung tumors after intraoperative infusion of [U^{13}C] ***glucose*** and/or [1^{13}C] ***lactate*** indicate that a high ratio of labeled ***lactate*** to the upstream metabolite ***3PG*** is associated with poor patient prognosis (Faubert et al., 2017). In addition to serine, the nonessential amino acids glycine, cysteine, and alanine can be generated from ***3PG*** and be used in a variety of anabolic processes (Eagle, 1959). The enzyme phosphoglycerate mutase 1 (PGAM1) uses inorganic phosphate to exchange the phosphate at carbon 3 of ***3PG*** to carbon 2 yielding the product ***2-phosphoglycerate (2PG)*** (Sutherland et al., 1949). PGAM1 regulates glycolytic flux and is up-regulated in cells deficient for p53 (Hitosugi et al., 2012). Dehydration of ***2PG*** by the enzyme enolase yields ***phosphoenolpyruvate (PEP)*** (Wold and Ballou, 1957). Pyruvate kinase generates 1 molecule of ATP (2 per mole glucose) by transferring the phosphate group of ***PEP*** to ADP in a reaction that also yields ***pyruvate***. Numerous studies suggest tumors predominantly express the embryonic splice isoform of pyruvate kinase, pyruvate kinase M2 (PKM2), which has been shown to promote glycolytic flux and tumorigenesis (Christofk et al., 2008).

Pyruvate has several metabolic fates, with lactate dehydrogenase (LDH)-mediated reduction to ***lactate*** being the predominant fate in cancer cells (DeBerardinis et al., 2008). ***Pyruvate*** can also be imported into mitochondria and fuel TCA cycle anaplerosis after pyruvate carboxylase (PC) mediated conversion to oxaloacetate (OAA) in mitochondria, or through partial oxidation by pyruvate dehydrogenase (PDH) to the 2-carbon metabolite acetyl-CoA (Utter and Keech, 1963, Patel and Roche, 1990). Mitochondrial oxidation is suppressed during hypoxia by the action of PDH kinases that phosphorylate and suppress the PDH-mediated entry of acetyl-CoA into the TCA cycle

(Kim et al., 2006). Interestingly, import and oxidation of ***lactate*** outpaces oxidation of ***pyruvate*** derived from cell-autonomous glycolysis in the TCA cycle, suggesting glycolysis and the TCA cycle are uncoupled at the level of ***lactate*** transport and that the millimolar levels of circulating lactate are not merely an abundant waste product of glycolysis (Faubert et al., 2017, Hui et al., 2017).

Bioenergetic (catabolic) metabolism of pyruvate

Mitochondrial acetyl-CoA is condensed with OAA by citrate synthase to initiate the TCA cycle (Karpusas et al., 1990). Aconitase catalyzes isomerization of citrate into isocitrate and subsequent oxidation of isocitrate to αKG by isocitrate dehydrogenase generates the first oxidizable cofactor of the TCA cycle, NADH, to be used by the electron transport chain to ultimately generate ATP (Balaban, 1990). Further oxidation of alpha-ketoglutarate (αKG) yields succinyl-CoA coupled to the reduction of another molecule of NAD+ (Sheu and Blass, 1999). Succinyl-CoA synthetase then splits succinyl-CoA into succinate and CoA-SH (Wider de Xifra and Battle, 1973). Fumarase catalyzes the hydration of succinate to produce malate, in a reaction that also reduces oxidized flavin adenine dinucleotide (FAD+) supplying $FADH_2$ to the ETC for use in oxidative phosphorylation (Racker, 1950). Malate then is fully oxidized to OAA yielding another molecule of NADH and completing one round of the TCA cycle (Green, 1936).

Biosynthetic (anabolic) metabolism of pyruvate

Citrate produced from the condensation of OAA and pyruvate-derived acetyl-CoA can be shuttled to the cytosol where the enzyme ATP-citrate lyase (ACLY) utilizes ATP to cleave it back to OAA and acetyl-CoA (Currie et al., 2013). Cytosolic acetyl-CoA serves as substrate for cholesterol and fatty acid biosynthesis, and inhibition or

depletion of ACLY impairs the growth of experimental tumors (Hatzivassiliou et al., 2005, Bauer et al., 2005). Citrate remaining in mitochondria is converted to isocitrate and further oxidized to αKG. Interestingly, in cells deficient in mitochondrial function, oxidation of αKG is required for reductive carboxylation of glutamine into citrate to meet biosynthetic needs (Mullen et al., 2014). αKG can be exported from mitochondria, converted to glutamate, and serve as substrate for *de novo* glutamine, proline, and arginine synthesis (Brosnan, 2000). Further oxidation and decarboxylation of αKG yields OAA, completing a round of the TCA cycle. Aspartate synthesis from OAA supports nucleotide and amino acid synthesis and is required in cells treated with ETC inhibitors (Birsoy et al., 2015).

Lactate

In cancer cells, most ***pyruvate*** from glycolysis is reduced to ***lactate*** by lactate dehydrogenase (LDH) in a reaction that regenerates oxidized NAD+, which, in theory, helps maintain glycolytic flux by providing reducing equivalents for glyceraldehyde-3-phosphate dehydrogenase (GAPDH) (DeBerardinis et al., 2008). Detailed studies on the fate of LDH-mediated oxidation of NADH will refine this theory and explore other theories of compartmentalized LDH activity. Lactate production accounts for >90% of glucose uptake in cultured cells with the remainder being used in biosynthetic reactions (DeBerardinis et al., 2007). LDHA is up-regulated or amplified in several human cancers and its expression is associated with poor prognosis, and its depletion in cancer cell lines reduces tumorigenicity (Koukourakis et al., 2009, Fantin et al., 2006). *LDHB* is up-regulated or amplified in KRAS-mutant lung adenocarcinoma, and its depletion suppresses xenograft tumor growth (McCleland et al., 2013). In cultured

cancer cells, both MYC and hypoxia inducible factor (HIF) promote transcription of many glycolytic genes including *LDHA* (Shim et al., 1997, Stine et al., 2015, Dang and Semenza, 1999, Kim et al., 2004) (discussed in **Regulation of glycolysis**).

LDH exists as a tetramer that catalyzes reduction of ***pyruvate*** to ***lactate*** and the reverse reaction. The two predominant LDH isoforms, LDHA and LDHB (originally designated LDH-M and LDH-H for muscle and heart, respectively), exist in both mixed and homotetrameric complexes that have distinct tissue expression patterns. It is hypothesized that different tetramers have differential oxidative and reductive function, but this remains poorly understood. Interestingly, LDH purified from organs with active gluconeogenesis such as the liver, favors oxidation of lactate into pyruvate (Dawson et al., 1964). Protons from the oxidation of lactate are important for the function of vacuolar ATPase in lysosomal acidification, and this was impaired by LDHB, but not LDHA, inhibition (Brisson et al., 2016). Other *in vitro* enzymatic studies show similar reaction rates between different stoichiometric preparations of LDHA and LDHB (Goto et al., 2016, Vesell et al., 1968). Ultimately this will be refined by the use of xenograft or GEMM models involving conditional deletion of *LDHA* and *LDHB,* coupled with *in vivo* isotope tracing.

Tumors import and oxidize ***lactate*** (Faubert et al., 2017), suggesting differences in enzymatic activities of LDH may be imposed by tetramer composition, post-translational modifications, or subcellular localization. Interestingly, LDHA can be phosphorylated at residues Y10 and Y83 by the receptor tyrosine kinase fibroblast growth factor receptor 1 (FGFR1) and these modifications are associated with increased LDH tetramer formation and enhanced reduction of ***pyruvate*** into ***lactate***

(Fan et al., 2011). Conversely, LDHA can be acetylated at residue K5 suppressing enzymatic function and promoting its lysosomal degradation (Zhao et al., 2013). LDHA mRNA is subject to microRNA-mediated regulation by miR-30-a-5p whose expression suppresses glucose uptake, lactate production and secretion, and tumorigenicity of breast cancer cells (Li et al., 2017). There are likely other post-transcriptional modifications and interacting factors contributing to the tumorigenic function of LDH *in vivo*.

Glutamine

Tumors are able to derive carbon from multiple sources in response to changes in nutrient availability in their local environment, but some cancers have distinct preferences for carbon sources. A notable example is that of glutamine metabolism in *KRAS*-mutant pancreatic cancers, which mirrors the metabolic preference of its tissue of origin (Hui et al., 2017, Mayers et al., 2016). Interestingly, a major source of glutamine in pancreatic tumors comes from macropinocytosis of proteins from extracellular space, highlighting the diversity of how tumors obtain nutrients (Commisso et al., 2013). Among other metabolic pathways, amplification of the Myc oncoprotein stimulates glutaminolysis and usage of glutamine for bioenergetic needs (Wise et al., 2008). In small subsets of small-cell lung cancer (SCLC), glutamine is used in the synthesis of nucleotide monophosphates (Huang et al., 2018). Cancer cell lines in culture do not faithfully recapitulate the *in vivo* environment of a tumor, and not surprisingly have radically different metabolic activities in each setting. Cells cultured in media replete with supraphysiological concentrations of nutrients use glutamine as a major source of carbon (Yuneva et al., 2007, Reitzer et al., 1979). *In vivo*, glucose-derived lactate is the

preferred carbon sources for TCA cycle oxidation in NSCLC (Faubert et al., 2017). This highlights the need to interrogate metabolism *in vivo* to understand and develop new therapies.

Redox balance

The oxidative state of cancer cells influences nutrient metabolism. Not surprisingly, cells adapt to disturbances in redox balance through the activity of multiple enzymes and nutrient transporters. Oxidative stress has been shown to limit melanoma metastasis, suggesting redox metabolism presents a bottleneck for cancer progression (Piskounova et al., 2015). Molecular insight into the cellular processes regulating oxidative stress are numerous; Cysteine derived from SLC7A11-mediated cystine/glutamate transport is used to maintain the reductive capacity of glutathione, an important cellular antioxidant system (Harris et al., 2015, Hui et al., 2017, Lunt and Vander Heiden, 2011). Beyond the glutathione system are several transporters dedicated to exchanging H+ with extracellular space in order to buffer cellular pH, as well as a host of enzymes with pH buffering capacity (Webb et al., 2011).

Alterations in expression of redoxin proteins and reduced mitochondrial oxidative metabolism represent two examples of adaptations to oxidative stress in cancer (Panieri and Santoro, 2016). A major regulator of adaptation to oxidative stress, NFE2-related factor 2 (NRF2), responds to oxidative stress by activating the transcription of genes containing antioxidant response elements (AREs) to mitigate oxidative stress, and this is important for the progression of pancreatic and NSCLC tumors (Sporn and Liby, 2012, DeNicola et al., 2011, Homma et al., 2009). NRF2 is also hyperactivated by the kelch-like ECH-associated protein KEAP1 and this is important for mutant KRAS-

driven LUAD (Romero et al., 2017). Therapies guided by the understanding of oxidative stress in cancers will ultimately improve patient treatment (Gorrini et al., 2013).

Chapter II: Regulation of glycolysis in cancer

Regulation of glycolysis

Glycolysis supplies carbon and hydrogen for biosynthetic and bioenergetic purposes (**Introduction Figure 1**). Enhancing flux along this pathway supports bioenergetic needs and provides ample substrate for biosynthetic reactions. Proliferation is tightly coupled to glucose metabolism in both healthy and pathophysiological contexts. Several factors have been shown to regulate glycolysis that are deregulated in cancer, and notable examples not included in the previous section will be included.

PI3K/Akt and mTOR

Phosphatidylinositol-3-OH kinase (PI3K) is a major regulator of glycolysis that is important for the progression of multiple cancers (Shaw and Cantley, 2006). Somatic mutations and amplifications of a catalytic subunit of PI3K, PIK3CA, are abundant in cancers and its ectopic expression promotes tumor growth in experimental settings (Karakas et al., 2006, Dogruluk et al., 2015). The predominant downstream effector of PI3K is the mammalian homolog of retrovirus AKT8 kinase (Akt) which has been shown to enhance glycolysis through multiple mechanisms: (i) activation of hexokinases, (ii) phosphorylation and activation of PFK2, (iii) promoting aldolase activity through regulation of its cellular localization, and (iv) enhancing the translation of GLUT1 and GLUT4 (Hu et al., 2016, Deprez et al., 1997, Gottlob et al., 2001, Taha et al., 1999). PI3K phosphorylation and activation of Akt enhances glycolytic flux among other metabolic pathways. Cells expressing constitutively active variants of Akt show

enhanced glycolytic flux and susceptibility to glucose limitation (Elstrom et al., 2004). Interestingly, in some cancer cell lines glucose limitation leads to the outgrowth of cells harboring oncogenic mutations to *KRAS* and *BRAF* (Yun et al., 2009).

Phosphorylation of tuberous sclerosis complex 2 (TSC2, tuberin) by Akt inhibits its ability to suppress activation of ribosomal S6 kinase S6K1 and protein synthesis via suppressing mammalian target of rapamycin (mTOR) activation (Manning et al., 2002, Inoki et al., 2002). Adenosine monophosphate-activated protein kinase (AMPK) opposes the actions of mTOR and is critical for regulation of nutrient metabolism in response to starvation (Hardie, 2007, Gwinn et al., 2008). Loss-of-function or deletion of the alpha-1 subunit of AMPK stimulates aerobic glycolysis, and its function as a tumor suppressor is well documented (Faubert et al., 2013, Luo et al., 2010). Recently it has been shown that aldolase A senses the glycolytic metabolite fructose-1,6-bisphosphate at the surface of lysosomes and glucose starvation (reflected by depletion of fructose-1,6-bisphosphate) promotes the formation of a complex comprising aldolase, AMPK, and LKB1 and this association promotes phosphorylation and activation of AMPK (Zhang et al., 2017). Downstream effectors of activated mTOR remodel cellular metabolism to sustain adequate energy, such as increased fatty acid oxidation and reduced cholesterol biosynthesis (Carling et al., 1989, Davies et al., 1989).

P53

The tumor suppressor p53 regulates many metabolic processes and is lost or mutated in the majority of human cancers. Upstream of glycolysis, p53-mediated repression of transcription of the glucose transporters GLUT1 and GLUT4 suppresses glucose uptake, and loss of p53 results in enhanced membrane expression of these

transporters concomitant with increased glucose consumption (Schwartzenberg-Bar-Yoseph et al., 2004). Interestingly, oncogenic gain-of-function mutations to p53 promote constitutive membrane translocation of GLUT1 and enhanced glucose uptake (Zhang et al., 2013). The p53-regulated protein TP53-induced glycolysis and apoptosis regulator (TIGAR) encodes a fructose-2,6-bisphosphatase which impedes glycolytic flux by dephosphorylating the glycolytic metabolite fructose-2,6-bisphosphate, returning it to the upstream metabolite fructose-6-phosphate and promoting diversion of glucose carbons towards the PPP (Bensaad et al., 2006). In some cells, p53 induces the transcription of hexokinase 2 (HK2) and stimulates glycolytic flux (Mathupala et al., 1997). Phosphoglycerate mutase (PGAM1), which catalyzes the conversion of 3PG into 2PG during glycolysis, is transcriptionally repressed by p53 (Kondoh et al., 2005). Loss of p53 results in reduced expression of the cytochrome C oxidase SCO2, suppressing oxygen consumption and TCA cycle activity (Matoba et al., 2006). These and the majority of studies on the regulation of glycolysis by p53 implicate it as a repressor, but approaches such as metabolic flux analysis (MFA) modeling may yield insight into pathways disturbed upon loss of p53 or other metabolic tumor suppressors.

MYC

The oncoprotein Myc is commonly translocated or amplified in human cancers and orchestrates the activation of many metabolic genes required for anabolic growth (Stine et al., 2015). Myc regulates most genes involved in glucose and glutamine metabolism, a notable example being *LDHA* transcription and subsequent lactate production (Hu et al., 2011). The Myc-regulated thioredoxin-interacting protein (TXNIP) regulates the reduction of disulfide bonds, and subsequent activity, of the

tumor suppressor PTEN to antagonize metabolism induced by PI3K/Akt signaling (Hui et al., 2008). Myc induces expression of the lactate transporter MCT1 and inhibition of its activity impairs growth of grafted murine Eμ-*Myc* B cells (Doherty et al., 2014). Pathways regulated by Myc are numerous and comprise thousands of publications confirming its role as an oncogene.

Hypoxia inducible factors (HIFs)

HIFs coordinate the induction of genes involved in anaerobic glycolysis and suppress those involved in mitochondrial metabolism in the absence of oxygen (Gordan et al., 2007). HIF1α induces expression of many glycolytic enzymes, including specific isoforms with higher activity, to enhance glycolytic ATP production in the absence of oxidative phosphorylation (Marin-Hernandez et al., 2009). The enzymes LDH, aldolase, and enolase are all transcriptionally up-regulated by HIF in response to hypoxia (Semenza et al., 1996). In the absence of oxygen, HIF1α induces the expression of the PDH-inhibitory kinase, PDK1, to halt entry of pyruvate into the TCA cycle and subsequent oxidation (Kim et al., 2006). However, HIFs are stabilized in normoxic conditions in an Akt-dependent manner in cells lacking the tumor suppressor phosphatase and tensin homolog (PTEN) (Zundel et al., 2000). Similarly, loss of the E3 ubiquitin ligase Von Hippel-Lindau (VHL) impairs the degradation of HIF subunits in the presence of oxygen, leading to accumulation of HIFs and up-regulation of genes involved in anaerobic glycolytic metabolism (Maxwell et al., 1999).

The diverse ways tumors use glucose and other nutrients to fuel their growth presents a challenge for researchers and clinicians, and furthermore, metabolic

pathways important for tumor initiation and those important for metastasis are likely different, suggesting the need for concurrent therapies.

Chapter III: Lactate transport by Basigin and monocarboxylate transporters

MCTs and lactate transport

Lactate is transported through dedicated membrane H^+-coupled monocarboxylate transporters (MCTs) (Dimmer et al., 2000, Halestrap and Price, 1999). The MCT family comprises 14 members and all members except MCT8 and MCT10 mediate proton-coupled transport of monocarboxylates including lactate, pyruvate, and ketone bodies (Halestrap, 2012). MCTs are 12 pass transmembrane proteins whose plasma membrane targeting requires the ubiquitously expressed glycoprotein Basigin, and to a lesser extent other members of the Basigin protein family including Embigin and Neuroplastin (discussed below in the **Basigin/CD147** subsection of this chapter) (Halestrap, 2012, Muramatsu and Miyauchi, 2003). MCTs 1-4 have documented lactate transport function, whereas the remaining ten MCTs have specificities towards other monocarboxylates and diverse molecules, including thyroid hormone transport by MCT8 and MCT10 which is not H^+-coupled (Halestrap, 2012, Visser et al., 2008). Transport by the H^+-coupled MCTs relies on a gradient of monocarboxylates between intracellular and extracellular space to drive the energetically unfavorable transport of H^+ (Broer et al., 1998, Dimmer et al., 2000).

Expression of MCT1 and MCT4 have both been implicated in contributing to cancer progression (Semenza, 2008). Due to experimental observations of the different binding kinetics of MCT1 and MCT4, MCT4 has been thought to predominantly export lactate and this is supported by its physiological up-regulation in hypoxia and in highly

glycolytic tissues which export lactate at high rates (Dimmer et al., 2000, Ullah et al., 2006, Bonen, 2001). Conversely, lactate import and oxidation in lung tumor xenografts was shown to rely on MCT1 (Faubert et al., 2017). These transporters are not unidirectional however; MCT1 and MCT4 can both mediate lactate/H^+ export, buffering protons generated by the high flux of GAPDH-catalyzed dehydrogenation of G3P during glycolysis to maintain appropriate intracellular pH, and in some tumors, impairing MCT1/4-mediated lactate export decreases intracellular pH, tumor growth, and glycolytic flux (Le Floch et al., 2011).

Lactate fuels mitochondrial oxidation (Sonveaux et al., 2008, Chen et al., 2016, Faubert et al., 2017, Hui et al., 2017). Although imported lactate and cell autonomous glycolysis contribute roughly equally to cellular pyruvate pools, pyruvate from imported lactate is preferentially oxidized through the TCA cycle (Faubert et al., 2017). This suggests aerobic glycolysis is uncoupled from the TCA cycle at the level of lactate production and secretion, indicating distinct cellular pools of lactate destined for export and lactate destined for oxidation likely exist.

Non-metabolic roles of lactate

Several observations contribute to our knowledge of lactate biology beyond metabolism in both normal physiology and in pathophysiological contexts. A major consequence of enhanced lactate production in tumors is its effect on different immune cell populations that regulate cancer progression, in large part due to acidification of the tumor microenvironment. Treatment of cells with buffered lactic acid (sodium lactate) has minimal effects on immune cells *in vitro*, whereas lactic acid treatment markedly affects immune populations; Tumor-derived lactate has been shown to blunt immune

cell proliferation and effector function through acidification of the microenvironment and upregulation of tumor PD-L1 expression (Feng et al., 2017, Fischer et al., 2007). Lactic acidification drives an inflammatory pro-tumorigenic response in macrophages and antigen presenting cells involving in their production and secretion of the cytokine interleukin 23 (IL-23) (Shime et al., 2008). Mice lacking the IL-23 receptor (*Il23r*$^{-/-}$) have reduced chemically-induced tumor incidence and reduced growth of transplanted tumors, and this reduced tumorigenicity is associated with enhanced infiltration of cytotoxic CD8+ T cells, suggesting lactic acidification would suppress the infiltration of T cells (Langowski et al., 2006). Secretion of tumor necrosis factor (TNF) and glycolytic metabolism in human monocytes is suppressed by lactic acid (Dietl et al., 2010). In a spheroid culture model, melanoma spheroid-derived lactate suppressed the differentiation of co-cultured monocytes into dendritic cells whose function is important for T cell activation (Gottfried et al., 2006). Lactic acidosis also suppresses the lytic function of cytotoxic T cell cells in culture (Mendler et al., 2012). The majority of studies on the effects of lactic acidosis on the function of immune cells have been in cultured cells, necessitating study of lactic acidosis *in vivo* in more immunocompetent and autochthonous mouse models of cancer. Although not attributed to the suppression of immune cell function, the lactate content of tumors is positively correlated with radiation resistance, metastasis, and patient mortality (Quennet et al., 2006, Sattler et al., 2010, Walenta et al., 2000).

Basigin/CD147

Cell surface expression of MCT1 and MCT4 is facilitated by the transmembrane glycoprotein Basigin/CD147 (Kirk et al., 2000). The rat homolog of Basigin, CE9, was

originally identified in rat hepatocytes as a polarity factor (Hubbard et al., 1985). Further work in mammalian systems have shown that Basigin is broadly expressed throughout the body and plays an essential role in retinal development, embryo implantation, and spermatogenesis (Hori et al., 2000, Igakura et al., 1998). Basigin is also expressed highly across numerous cancer types and has been shown to promote tumor growth and metastasis (Hori et al., 2000, Igakura et al., 1998, Zucker et al., 2001). However, the mechanisms through which Basigin promotes tumorigenesis remain incompletely understood, with reports implicating its interactions with extracellular matrix (ECM) factors, regulation of matrix metalloproteases (MMPs), and hyaluronan production (Marieb et al., 2004, Kanekura et al., 2002). Notably, Basigin plays a well-established role in trafficking MCTs to the plasma membrane for proper function (Yurchenko et al., 2002, Li et al., 2001, Marieb et al., 2004, Izumi et al., 2003). To understand the protumorigenic function of Basigin, Le Floch *et al* (2011) designed a series of elegant experiments; first, they created knock-outs of Basigin and MCT4 in colon adenocarcinoma cell lines and modified these cells to inducibly knock-down MCT1 to find that while Basigin deletion reduced tumor growth, combined depletion of MCT1 and MCT4 phenocopied this growth defect. Secondly, as Basigin knock-out results in impaired membrane trafficking of MCT1 and MCT4, researchers rescued this trafficking defect by introducing cDNA of rat Embigin. Embigin belongs to the same glycoprotein family as Basigin, and has documented MCT-trafficking function but does not promote tumorigenesis (Lain et al., 2009). Rat Embigin expression restored MCT1 and MCT4 expression and activity, and tumorigenicity of Basigin knock-out cells, suggesting the predominant tumorigenic function of Basigin is facilitating MCT activity (Le Floch et al.,

2011). These data are contradictory to the widely held view that Basigin-mediated induction of MMPs is the predominant function of Basigin in tumorigenesis, but this requires more study.

Basigin regulation and trafficking

Plasma membrane expression of Basigin is regulated by several proteins. Basigin protein folding, stability, and membrane localization is assisted by interaction with glycosyltransferases within the endoplasmic reticulum. Several asparagine residues (N44, N152, and N186) of Basigin are glycosylated by ER- and golgi-resident N-acetylglucosaminyltransferases (Tang et al., 2004, Yu et al., 2008). The N-acetylglucosaminyltransferase MGAT1 is one of several glycosyltransferases that adds glycans to Basigin and this function prevents its degradation by ER-associated degradation (ERAD) factors (Biswas et al., 2018). While the significance of glycosylation at N44 of Basigin remains unknown, glycosylation at N152 prevents its retention and degradation within the ER and is essential for membrane localization, and glycosylation of N152 and N186 is required for homooligomerization of Basigin whose function is poorly studied (Li et al., 2016).

Basigin interacts with multiple factors along its travel from the ER to the plasma membrane. The cytoplasmic tail of Basigin is recognized by the dynein-like effector Hook1 and this interaction promotes recycling through the endocytic pathway (Maldonado-Baez et al., 2013). The small GTPase Rab22a is also necessary for endocytic transport of Basigin along microtubules, ultimately regulating its recycling to the plasma membrane (Zhou et al., 2017). Interestingly, a component of the CUL4-RBX1-DDB1 (CRL4, also known as DCX) ubiquitin ligase complex, cereblon (CRBN),

moonlights as a chaperone for Basigin independently of its substrate recognition function in the CRL4 complex (Eichner et al., 2016). Ubiquitination pathways independent of the ubiquitin-proteasome system regulate signaling, stability, and localization of Basigin; tumor necrosis factor receptor-associated factor 6 (TRAF6), a well-known activator of Akt, uses its ubiquitin ligase activity to add lysine 63 (K63)-linked polyubiquitin chains to Basigin, which enhances its trafficking to the plasma membrane (Luo et al., 2016).

In this study, we describe the unexpected finding that a poorly characterized transmembrane serine protease transmembrane protease, serine 11B (TMPRSS11B) promotes Basigin/MCT4-mediated lactate export through interacting with and enhancing release of Basigin into extracellular space.

Chapter IV: Transmembrane serine proteases

TMPRSS and other type II transmembrane serine proteases (TTSPs)

TTSPs are proteolytic enzymes that catalyze the cleavage of peptide bonds of substrate proteins, and are responsible for the activation of inactive zymogens and extracellular factors (Bugge et al., 2009). Ivan Pavlov discovered the first TTSP, enteropeptidase (first designated enterokinase), in 1903 which he purified from digestive glands and demonstrated its proteolytic processing of inactive trypsinogen into active trypsin (Light and Janska, 1989). Moses Kunitz carried on this work to uncover components of chymotrypsinogen activation as well as decades of work on protease inhibitor function (Blow, 2000). All TTSPs share (i) signal peptide-independent transmembrane insertion, (ii) a C-terminal serine protease domain containing catalytic histidine, aspartic acid, and serine residues, (iii) multiple conserved disulfide bonds, and (iv) N-linked glycosylation (Bugge et al., 2009, Clements et al., 2001).

Serine proteolysis involves coordination of three conserved residues (**His**, **Asp**, **Ser**), the catalytic triad: (i) hydrogen bonding of **Asp** to a nitrogen of the imidazole ring of **His** results in a labile deprotonated **Ser** sidechain ($OH \rightarrow O^-$), (ii) the negatively charged **Asp** sidechain at the bottom of the substrate binding (S1) pocket interacts with the positively charged sidechain of substrate arginines or lysines (iii) **Ser** nucleophilic attack of substrate arginine or lysine and peptide bond scission, and (iv) ionization of water and release of cleaved peptide (Hedstrom, 2002). The specificity of trypsin-like proteases is provided by the negative charge of the **Asp** in the bottom of the substrate

binding pocket, which only accepts substrates with positively charged sidechains (arginine and lysine).

There are 17 human TTSPs that belong to four families: the human airway trypsin-like/differentially expressed in squamous cell cancer (HAT/DESC), Hepsin, Matriptase, and Corin families (Bugge et al., 2009). TTSPs have vast roles in organismal metabolism through activation of inactive pancreatic zymogens including trypsinogen, chymotrypsinogen, proelastase, prolipase, and procarboxypeptidase, which are all processed through a proteolytic cascade initiated by enteropeptidase (Light and Janska, 1989). The TTSP Corin regulates blood pressure and cardiac function by processing the inactive pro-form of atrial natriuretic peptide (proANP) into the biologically active ANP, and the absence of corin leads to loss of processed ANP (Knappe et al., 2004). Several TTSPs regulate the multi-subunit epithelial sodium channel (ENaC) (Rossier and Stutts, 2009). Although multiple cleavage events have been identified in ENaC subunits, attribution of these events to serine proteases is controversial, as expression of catalytically active or inactive variants of the membrane-anchored protease prostasin (PRSS8) can enhance ENaC channel activity that can be abrogated by serine protease inhibitors (Bruns et al., 2007). This suggests an alternative, unidentified protease likely carries out ENaC proteolysis, and this event is bolstered by the presence of prostasin regardless of its proteolytic activity. Interestingly, several TTSPs including matriptase, TMPRSS3, and TMPRSS4 are capable of activating ENaC (Szabo and Bugge, 2011). TMPRSS6 plays an essential role in regulating systemic iron homeostasis by cleavage and membrane release of hemojuvelin: soluble hemojuvelin is an activating co-receptor for bone morphogenetic

protein 6 (BMP6) that enhances Smad-dependent transcription of the iron-regulatory hormone hepcidin (Babitt et al., 2006, Silvestri et al., 2008, Du et al., 2008).

TMPRSS11 proteases

TMPRSS11B belongs to the HAT/DESC/TMPRSS11 subfamily of TTSPs. All members of the TMPRSS11 family belong to a cluster on chromosome 4 in humans and chromosome 5 in mice. The human TMPRSS11 family comprises TMPRSS11A, TMPRSS11B, TMPRSS11D, TMPRSS11E, and TMPRSS11F. Interestingly, mouse Tmprss11c and Tmprss11g exist as pseudogenes in primates, and Tmprss11b exists as both a protein coding TMPRSS11B and a non-coding pseudogene *TMPRSS11BNL*. These proteases have very short 10-15aa cytoplasmic tails, a single-pass transmembrane segment, and a common sea urchin sperm protein/enteropeptidase/agrin (SEA) domain between the transmembrane and extracellular serine protease domains. Although unknown in TMPRSS11 family members, the SEA domain found in the TTSPs matriptase and enteropeptidase contains a pro-enzyme cleavage sequence that is a point of regulation of their maturation and activity (Menou et al., 2017). Missense mutations to the SEA domain of TMPRSS6 are found in a rare autosomal recessive disease, iron-refractory iron-deficiency anaemia, and experimental interrogation of the mutant protein demonstrated the SEA domain of TMPRSS6 is essential for its autoactivation (Altamura et al., 2010). TMPRSS11D, hepsin, and likely other TTSPs are synthesized as inactive zymogens that undergo an activating cleavage event at a conserved arginine immediately preceding the serine protease domain that is hypothesized to occur in other TMPRSS11 family members (Yasuoka et al., 1997, Leytus et al., 1988). Interestingly, following

autocatalytic cleavage, the serine protease domain of TMPRSS11D can be released from cells or remain associate by a disulfide bond, suggesting redox regulation of its release by cellular or extracellular redoxins (Checconi et al., 2015).

The first and most extensively studied of the HAT/DESC family of TTSPs, TMPRSS11D (human airway trypsin-like), was purified and characterized in 1997 by Yasuoka *et al*. from the sputum of patients with chronic obstructive pulmonary disease (COPD) (Yasuoka et al., 1997). Using affinity chromatography with the reversible competitive serine protease inhibitor benzamidine they purified protease activity from the sputum of COPD patients and identified the N-terminal sequence of TMPRSS11D. TMPRSS11D is inhibited by classical serine protease inhibitors such as chemical irreversible sulfonylating agents and recombinant protein inhibitors such as aprotinin (bovine protein trypsin inhibitor) and soybean trypsin inhibitor (Yasuoka et al., 1997). This work also uncovered a strong substrate preference of TMPRSS11D for arginines over lysines, however the preference of TMPRSS11B is unknown. TMPRSS11D has been shown to regulate several factors including (i) urokinase plasminogen activator receptor (uPAR) through catalytic and non-catalytic mechanisms, (ii) cleavage of an extracellular portion of protease activated receptor 2 (PAR2) to initiate G protein signaling, and (iii) cleavage macrophage signaling protein (MSP) to enhance its biological function on macrophages (Beaufort et al., 2007, Menou et al., 2017, Orikawa et al., 2012). Interestingly, multiple TTSPs are able to cleave PAR2 including matriptase, TMPRSS2, and TMPRSS4 (Camerer et al., 2010, Szabo et al., 2009). TMPRSS11D and TMPRSS11E (also known as DESC1) can cleave recombinant fibrinogen into fibrin, but their role in blood clotting is unknown (Viloria et al., 2007,

Yasuoka et al., 1997). TTSPs also have non-endogenous substrates as well; TMPRSS11A and TMPRSS11E can both cleave the spike protein (S-protein) of severe acute respiratory syndrome coronavirus (SARS-CoV), enhancing virus entry into airway epithelial cells (Kam et al., 2009, Zmora et al., 2014). TMPRSS11A, TMPRSS11D, and TMPRSS11E can cleave hemagglutinin of influenza virus, and TMPRSS11A can also cleave the S-protein of Middle East respiratory syndrome coronavirus (MERS-CoV) (Zmora et al., 2018). All of these proteases are expressed in tracheal and lung epithelia, and are exploited by respiratory viruses. Substrates of TMPRSS11B remain unknown, and our approach to uncover its biological function will be discussed below in the **Results** section.

Inhibitors of serine proteases

TTSPs are inhibited by endogenous serine protease inhibitors such as Kunitz-type inhibitors and serine protease inhibitors (Serpins) which competitively inhibit substrate binding to limit proteolysis. Serpins form covalent bonds with their protease partners to form SDS-resistant complexes adding levels of complexity to the regulation of TTSPs (Potempa et al., 1994). Interestingly, some serpins have been shown to promote brain metastasis by inhibiting cleavage of plasminogen activator (PA) in genetically engineered mouse models of cancer (Valiente et al., 2014). Moreover, pathogenic mutations found in the *SERPINA1* locus (encoding alpha-1-antitrypsin) are overrepresented in patients with emphysema and other forms COPD (Denden et al., 2010).

Effective inhibitors of serine proteases share a common mechanism: irreversible sulfonylation of the active site serine sidechain of serine proteases. The most common

chemical inhibitors include phenylmethylsulfonyl fluoride (PMSF) and diisopropyl fluorophosphate (DFP), but the biological activity of these inhibitors has been markedly improved in terms of water solubility to produce the potent inhibitor 4-(2-aminoethyl)benzenesulfonyl fluoride (AEBSF). Of note, these inhibitors are cell permeant and thus inhibit a broad spectrum of serine proteases, suggesting that extracellular recombinant Serpins would have greater specificity to extracellular or transmembrane serine proteases. The importance of many serine proteases inhibitors in cancer is not well understood. The following section details mechanistic studies of TMPRSS11B physiological and pathophysiological function. The study presented herein demonstrates novel roles for TMPRSS11B LSCC and the next chapter will discuss our experimental approach and results.

Chapter V: Results

Experimental strategy

To identify new genes that promote transformation of human bronchial epithelial cells (HBECs), we performed *Sleeping Beauty* (*SB*)-mediated transposon mutagenesis of immortalized HBECs stably expressing CDK4, hTERT, and shRNA targeting *TP53* (HBEC-shp53). These cells progress to full malignancy upon overexpression of oncogenes such as $KRAS^{G12V}$ and *MYC* (Sato et al., 2013). We transfected cells with the mutagenic *T2/Onc* transposon and the *SB100* transposase, as previously described (Guo et al., 2016). Following *SB* mutagenesis, transformation was assessed by the ability to efficiently form large colonies in soft agar. Genomic DNA extracted from ~300 large colonies served as a template for ligation-mediated PCR (LM-PCR) followed by deep sequencing to identify transposon insertions. Common insertion site (CIS) analysis was then performed, revealing candidate genes that may promote transformation in this system (**Appendix table 1)**. Among the putative oncogenes identified in this screen, we were particularly interested in cell surface proteins since they might represent therapeutic targets that are accessible to antibody-based therapies. One of the identified CIS genes encodes the transmembrane serine protease TMPRSS11B which lacks known physiologic substrates. Interestingly, several TMPRSS11 family members were identified in the screen, and we selected TMPRSS11B as a representative family member for functional studies. We found that *TMPRSS11B* expression is highly upregulated in lung squamous cancer (LSCC) compared to normal lung tissue or other subtypes of non-small cell lung cancer

(NSCLC) including adenocarcinoma (**Figure 1A**). Moreover, high expression of *TMPRSS11B* mRNA correlates with poor overall survival in NSCLC patients, warranting further investigation of the role of this enzyme in tumorigenesis (**Figure 1B**) (Lee et al., 2008).

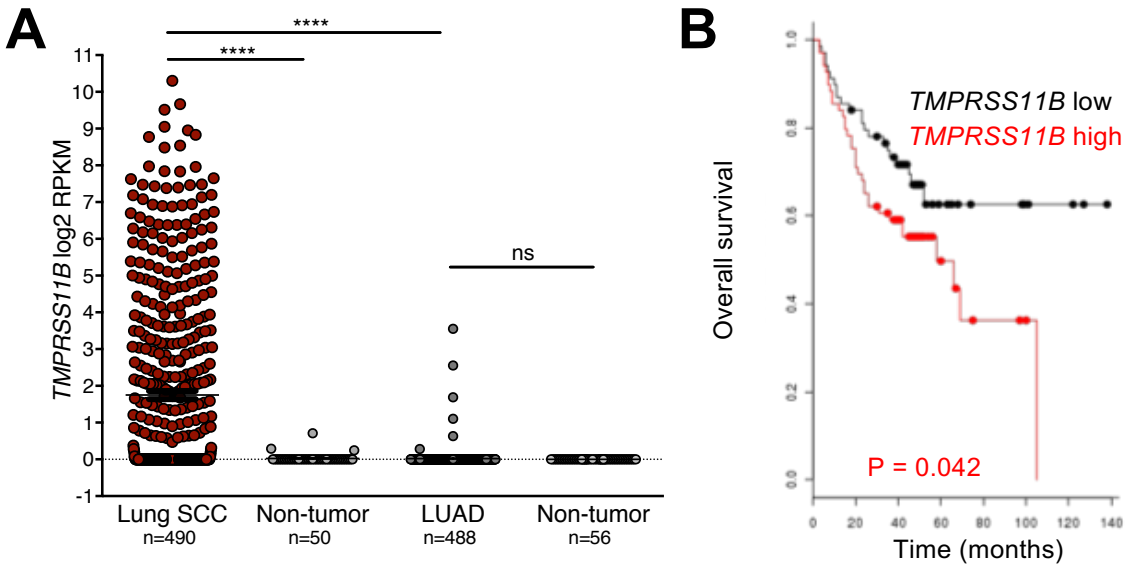

Figure 1: TMPRSS11B is up-regulated in lung squamous cell cancer and its expression portends worse survival in non-small cell lung cancer (NSCLC) patients. **A**) *TMPRSS11B* mRNA expression from The Cancer Genome Atlas (TCGA) of lung squamous cell cancer (LSCC) and lung adenocarcinoma (LUAD). RPKM: reads per kilobase million. **B**) NSCLC patients binned into high (red) or low (black) *TMPRSS11B* mRNA expression plotted against survival time in months. Unpaired t-test; **** P<0.0001.

TMPRSS11B promotes transformation and tumorigenesis

We first examined the extent of N-linked glycosylation of TMPRSS11B by treating lysate from HBEC-shp53 cells expressing a tagged TMPRSS11B construct with protein N-glycosylase F (PNGase F), to find that N-linked glycans account for ~1/3 of the molecular weight of TMPRSS11B (**Figure 2**). To confirm that TMPRSS11B promotes transformation of bronchial epithelial cells, we stably expressed the protein in HBEC-shp53 cells and assessed proliferation and colony formation in soft agar to find that TMPRSS11B promotes proliferation and transformation *in vitro* (**Figure 3**). To test whether catalytic function is necessary for this transforming activity, we mutated residues in the catalytic triad of this family of proteases to find that expression of wild-type TMPRSS11B robustly stimulated anchorage-independent growth and this effect was strongly impaired by catalytic mutations (**Figures 3B and 4**) (Miller et al., 2014). Expression of V5-tagged TMPRSS11B proteins was confirmed by western blotting (**Figure 4**). Notably, the S366A mutation resulted in faster migration of the protein, consistent with disruption of a nearby N-linked glycosylation site (**Figures 4B and 5A**). Interestingly, flow cytometry analysis of non-permeabilized HBEC-shp53 cells using anti-V5 or isotype control antibodies revealed that TMPRSS11B^{S366A} fails to be expressed at the plasma membrane, whereas TMPRSS11B^{D270N} and wild-type TMPRSS11B are present at the plasma membrane (**Figure 5B**). Moreover, stable ectopic expression of TMPRSS11B enhanced proliferation of HBEC-shp53 cells (**Figure 3**) and promoted growth in soft agar in several human LSCC lines (**Figure 6**). These data suggest that TMPRSS11B exhibits oncogenic activity in lung epithelial and LSCC cells.

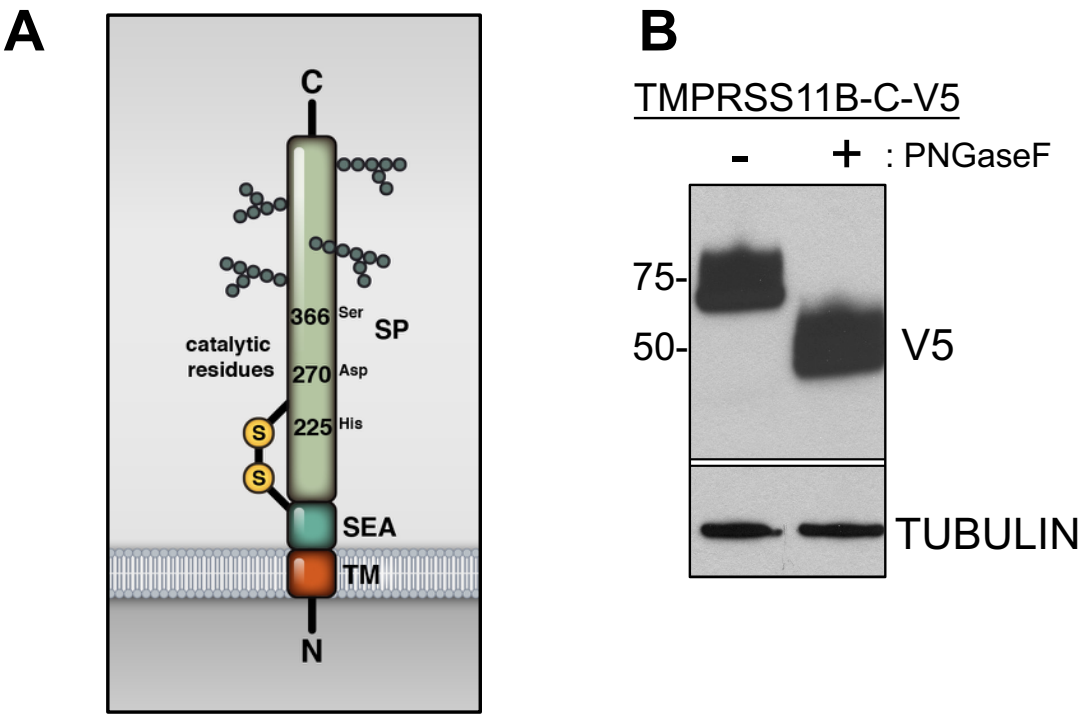

Figure 2: TMPRSS11B is a glycosylated transmembrane protein. **A**) Schematic representation of TMPRSS11B; TM: transmembrane, SEA: sea urchin sperm protein/enterokinase/agrin, SP: serine protease, S: disulfide bond. **B**) HBEC-shp53 cells expressing C-terminally V5 tagged TMPRSS11B treated with and without protein N-glycosylase F (PNGase F), tubulin is used as a loading control.

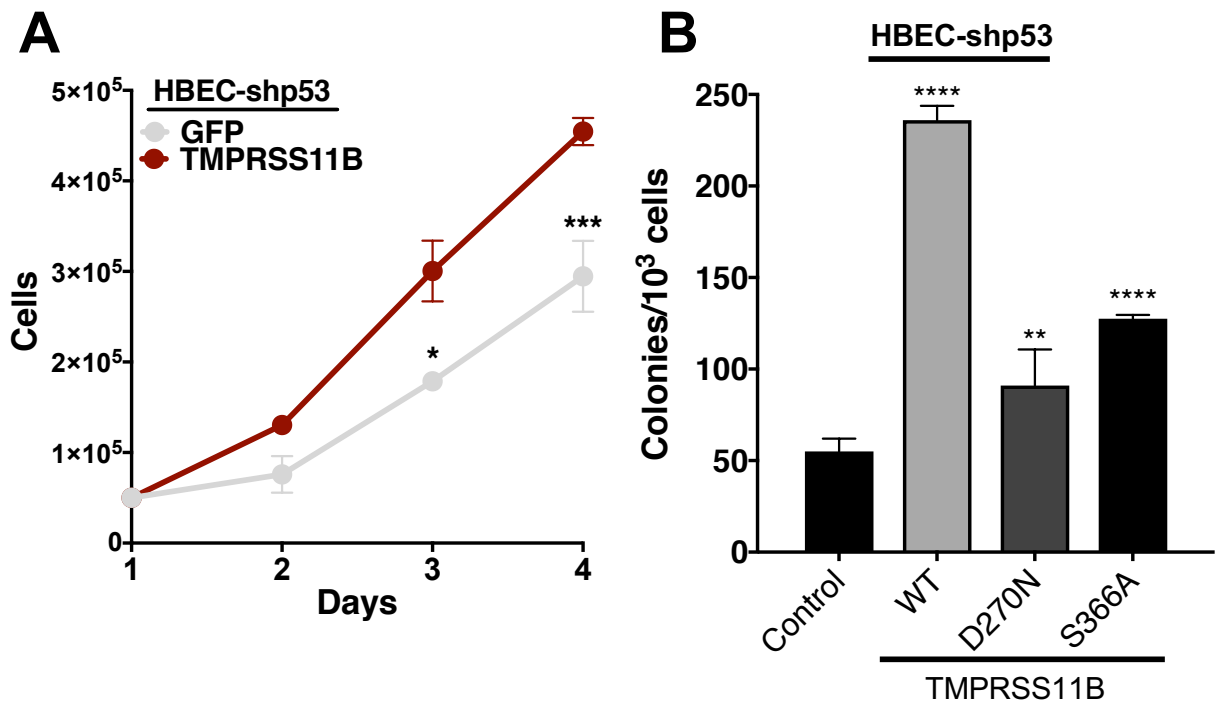

Figure 3: TMPRSS11B expression promotes proliferation and colony formation in soft agar. A) Proliferation assay of HBEC-shp53 cells expressing either GFP control (grey) or TMPRSS11B (red). **B**) Soft agar colony formation assay of HBEC-shp53 cells expressing control GFP or TMPRSS11B^{D270N}, TMPRSS11B^{S366A}, or wild-type TMPRSS11B constructs. Unpaired t-test; *P<0.05, **P< 0.01, ***P<0.001, ****P<0.0001.

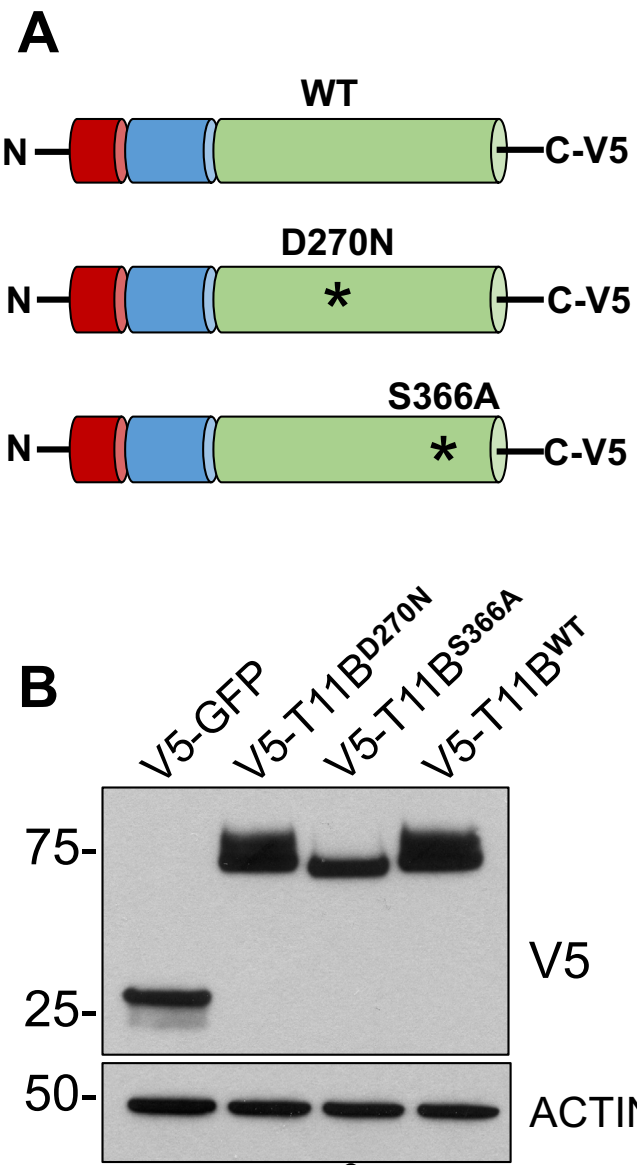

Figure 4: TMPRSS11B expression in HBEC-shp53 cells. **A**) Schematic diagram of wild-type and catalytic mutant TMPRSS11B constucts **B**) Western blot using anti-V5 antibody. Actin is used as a loading control.

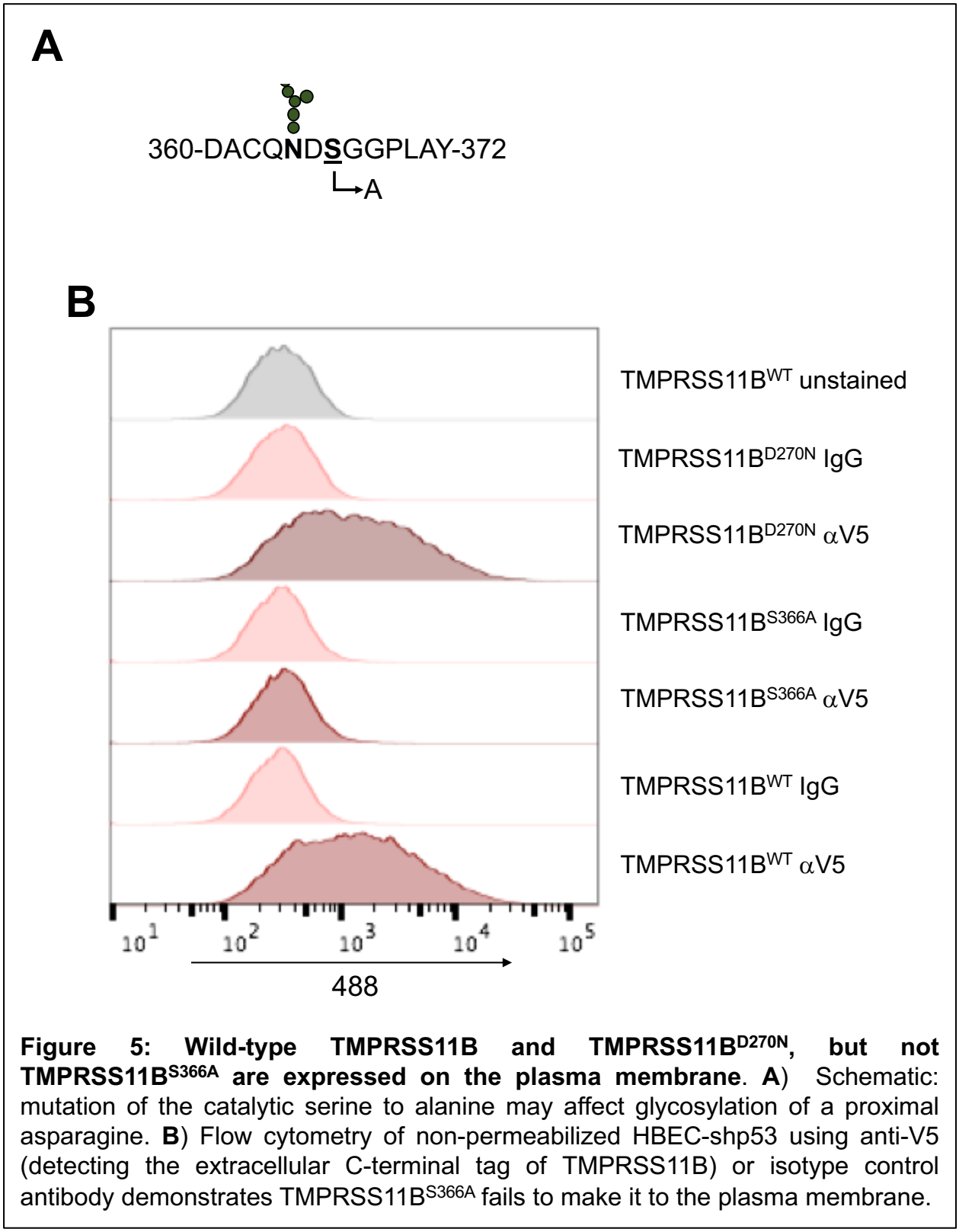

Figure 5: Wild-type TMPRSS11B and TMPRSS11B^{D270N}, but not TMPRSS11B^{S366A} are expressed on the plasma membrane. **A**) Schematic: mutation of the catalytic serine to alanine may affect glycosylation of a proximal asparagine. **B**) Flow cytometry of non-permeabilized HBEC-shp53 using anti-V5 (detecting the extracellular C-terminal tag of TMPRSS11B) or isotype control antibody demonstrates TMPRSS11B^{S366A} fails to make it to the plasma membrane.

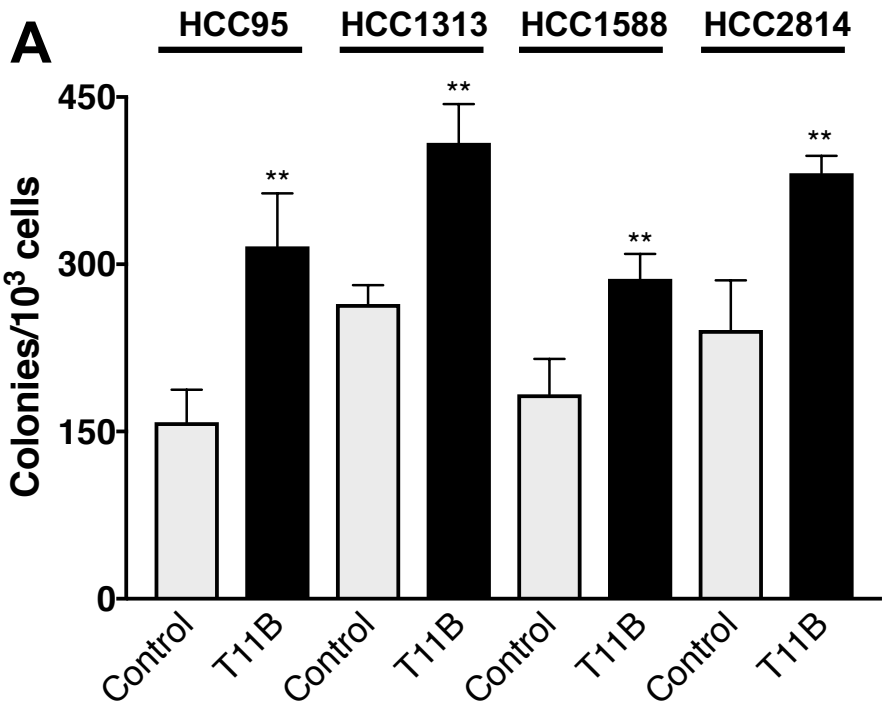

Figure 6: TMPRSS11B expression promotes colony formation of LSCC cell lines. **A**) Soft agar colony formation assay of lung squamous cell cancer lines expressing either mCherry control or TMPRSS11B. Unpaired t-test;
**P< 0.01

To determine whether inhibition of TMPRSS11B limits tumor growth, we performed loss-of-function studies using shRNA-mediated knockdown and CRISPR-mediated genome editing. First, lentivirally-delivered shRNA was used to deplete *TMPRSS11B* in the LSCC lines HCC2814 and H157, and the prostate cancer line DU145 (**Figure 7**), which expressed high levels of *TMPRSS11B* mRNA (Barretina et al., 2012). Xenograft assays in immunocompromised NOD/SCID Il2r$\gamma^{-/-}$ (NSG) mice demonstrated a strong impairment of tumorigenesis following depletion of *TMPRSS11B* in each of these cell lines (**Figures 8-11**). We used both shRNA mediated depletion and edited the endogenous *TMPRSS11B* locus using CRISPR-mediated genome-editing in HCC2814 cells. In CRISPR-edited cells this resulted in greatly reduced tumor growth, an effect that could be rescued by ectopic expression of TMPRSS11B (**Figure 10**). Taken together, these data demonstrate that inhibition of TMPRSS11B impairs tumorigenesis, raising the possibility that targeting TMPRSS11B may provide a novel therapeutic strategy in LSCC.

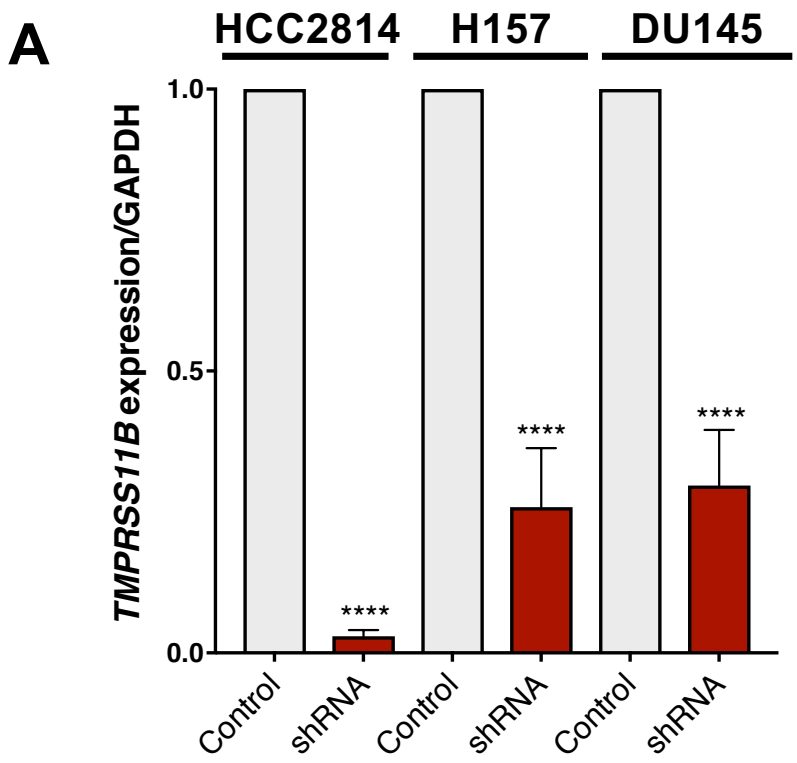

Figure 7: Doxycycline-inducible shRNAs deplete *TMPRSS11B* mRNA. **A**) qRT-PCR of *TMPRSS11B* mRNA normalized to *GAPDH* in LSCC lines HCC2814 and H157, and prostate cancer line DU145. shRNA was induced by treatment for 3 days in culture with doxycycline. Unpaired t-test; ****P<0.0001

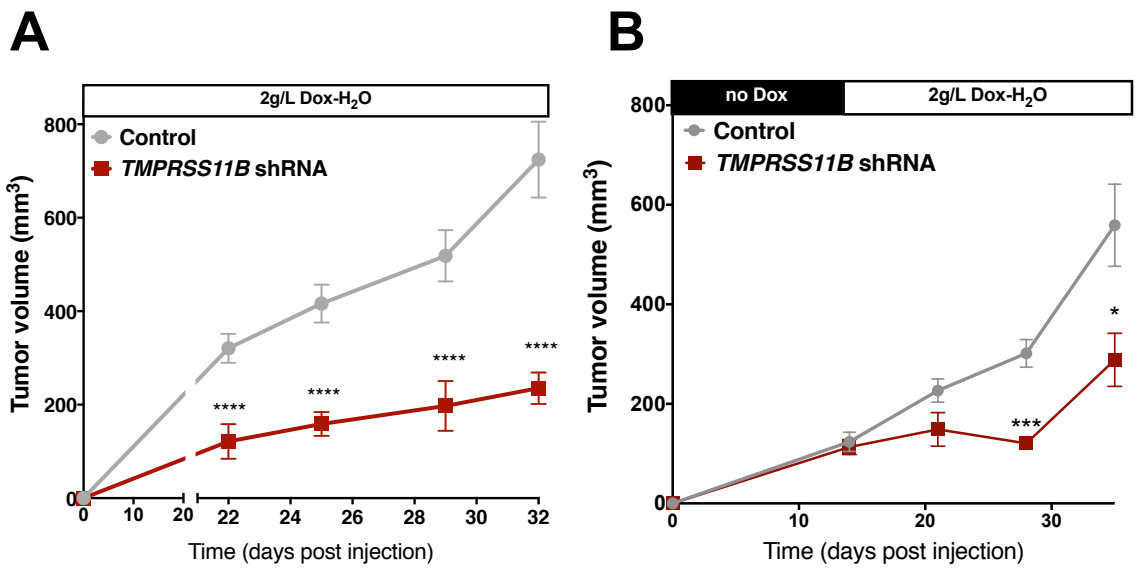

Figure 8: Depletion of TMPRSS11B slows tumor growth. **A**) Tumor volume over time of xenografted HCC2814 cells in NSG mice given doxycycline in drinking water on the day of engraftment. N=16 tumors each group **B**) Tumor volume over time of xenografted HCC2814 cells in NSG mice given doxycycline in drinking water following palpable tumor formation (~100mm^3). N=6 tumors each group. Unpaired t-test; *P<0.05, ***P<0.001, ****P<0.0001

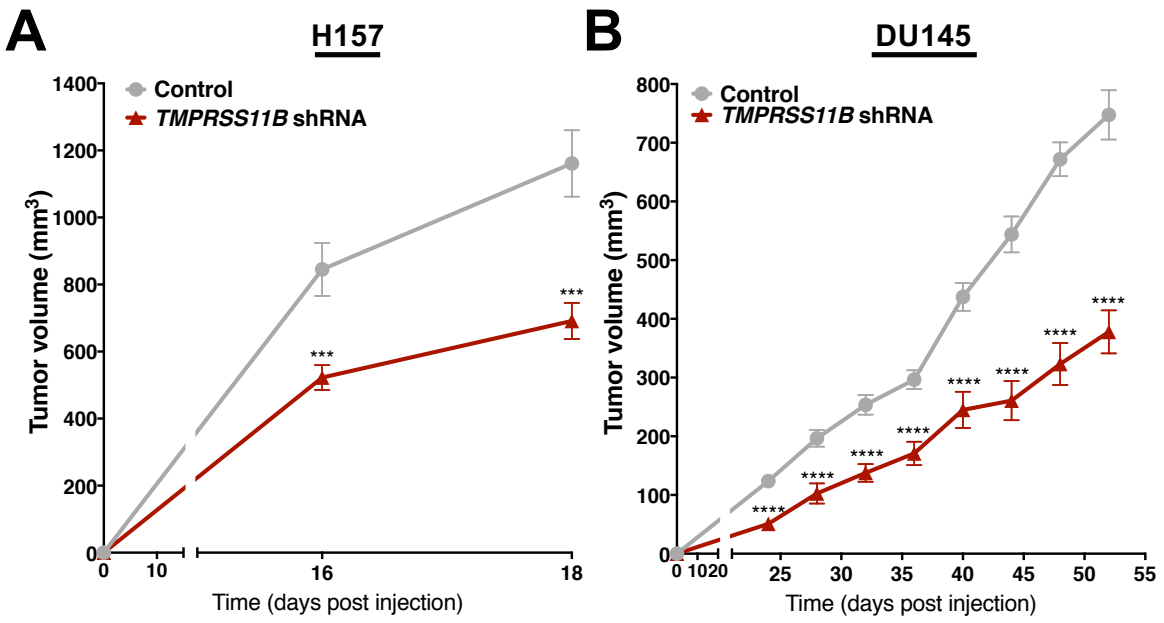

Figure 9: Depletion of TMPRSS11B slows tumor growth. A) Tumor volume over time of xenografted H157 (LSCC) cells in NSG mice given doxycycline in drinking water. **B**) Tumor volume over time of xenografted DU145 (prostate cancer) cells in NSG mice given doxycycline in drinking water. N=16 tumors each group. Unpaired t-test; ***P<0.001, ****P<0.0001

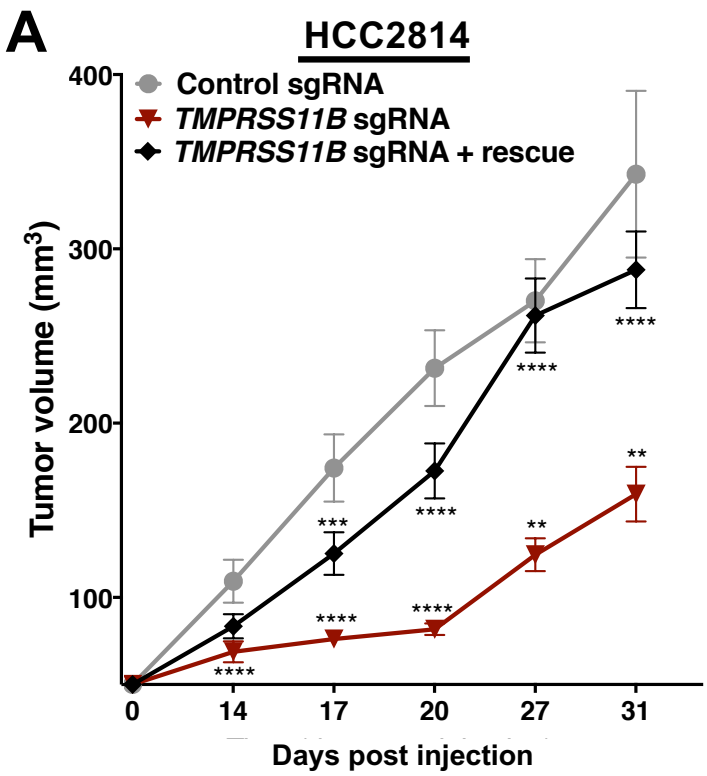

Figure 10: CRISPR/Cas9-mediated depletion of TMPRSS11B slows tumor growth that can be rescued by reintroduction of TMPRSS11B cDNA. **A**) Tumor volume of xenografted HCC2814 cells stably expressing CRISPR/Cas9 with non-targeting sgRNA control (grey), sgRNA targeting TMPRSS11B (red), or sgRNA targeting TMPRSS11B with stable reintroduction of TMPRSS11B (black). N=16 tumors each group. Unpaired t-test; **P< 0.01, ***P<0.001, ****P<0.0001

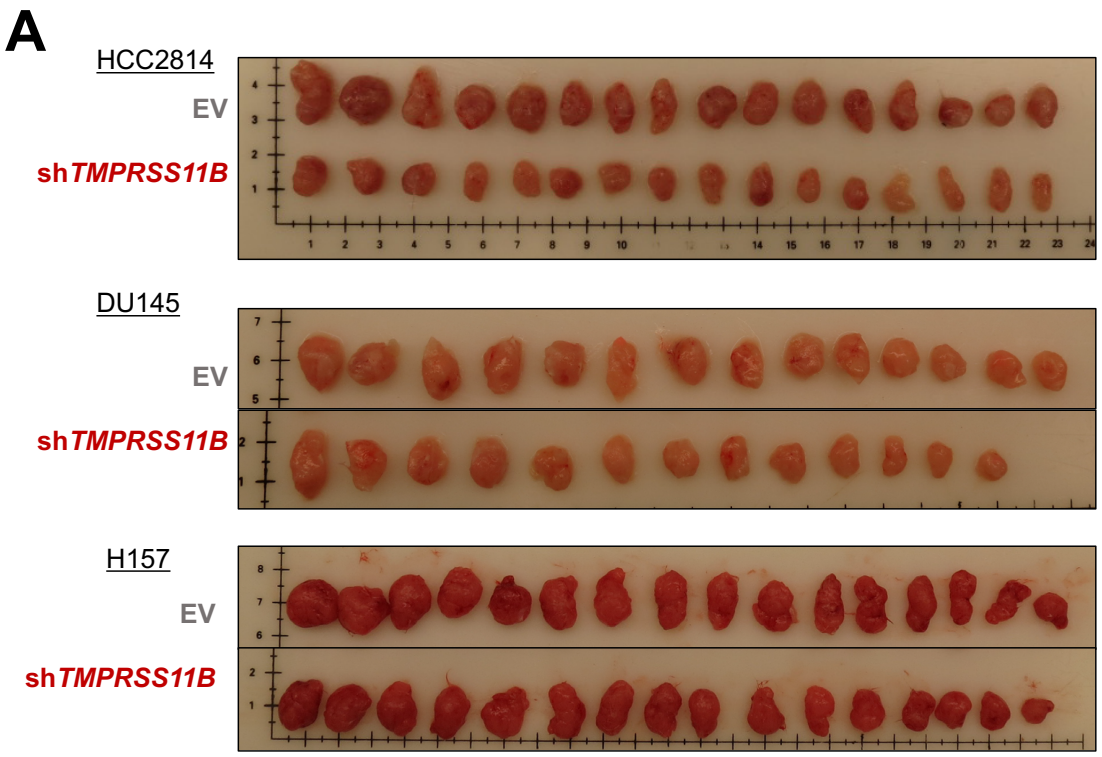

Figure 11: Depletion of TMPRSS11B slows tumor growth. **A**) Images of resected subcutaneously xenografted tumors from mice given doxycycline drinking water. EV: empty vector control.

TMPRSS11B promotes solubilization of Basigin

Given that TMPRSS11B harbors an extracellular (EC) protease domain, we hypothesized that proteolysis of a membrane bound substrate may underlie its transforming activity. To identify candidate substrates of TMPRSS11B, a set of soluble receptors was interrogated using proteome profiler arrays with conditioned media (CM) from HBEC-shp53 cells with or without TMPRSS11B overexpression. This revealed a ~10-fold enrichment in the levels of soluble Basigin/CD147 in CM from cells expressing TMPRSS11B (**Figure 12**). Through the analysis of HBEC-shp53 cells expressing wild-type TMPRSS11B or two catalytic mutants, we confirmed that expression of proteolytically active TMPRSS11B results in Basigin solubilization (**Figure 13**). Importantly, we assessed Basigin mRNA and protein expression in these cells to find no significant differences in levels of expression (**Figure 14**). TMPRSS11B overexpression in HCC95 and HCC1313 LSCC cells also stimulated Basigin release (**Figure 15**). TMPRSS11B expression had varying effects on Basigin mRNA and protein in these cells (**Figures 16 and 17**). Treatment of HBEC-shp53-TMPRSS11B cells with the irreversible serine protease inhibitor 4-(2-aminoethyl)benzenesulfonyl fluoride (AEBSF) significantly impaired Basigin membrane release (**Figure 19**). AEBSF treatment had varying effects on Basigin mRNA expression and protein levels (**Figure 20**). Interestingly, cellular Basigin protein was increased in a dose-dependent manner with increasing concentrations of AEBSF, suggesting enhanced retention or reduced membrane release of Basigin (**Figure 20B**). Doxycycline-inducible knock-down of TMPRSS11B resulted in modest, but not significant, reduction in Basigin release into

conditioned medium (**Figure 21**). Moreover, AEBSF treatment of LSCC and lung adenocarcinoma cells reduced Basigin release (**Figure 21**). Furthermore, similar levels of Basigin mRNA and protein were observed in LSCC cells with control mCherry or TMPRSS11B expression, or control and TMPRSS11B shRNA (**Figures 16-17, 19, and 22**). Overall, these data indicate that TMPRSS11B gain- or loss-of-function does not have a major influence on Basigin mRNA or protein levels.

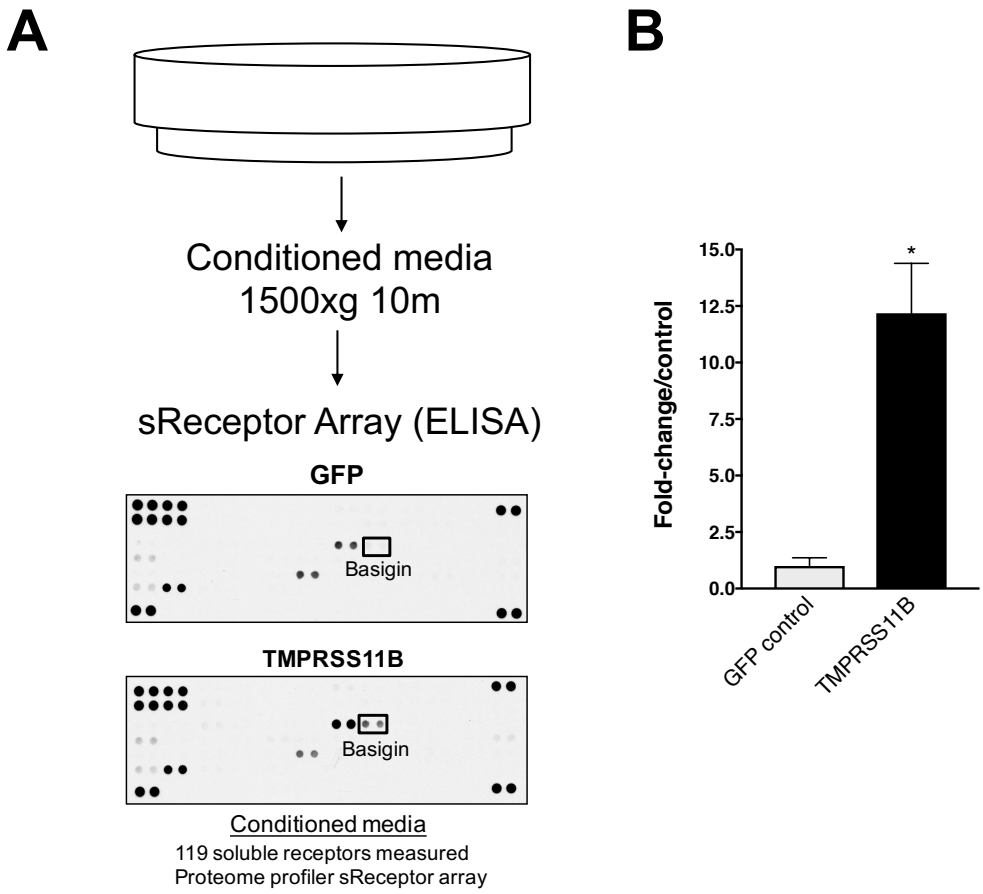

Figure 12: Basigin is enriched in conditioned media of HBEC-shp53 cells expressing TMPRSS11B. **A**) Conditioned media was purified from HBEC-shp53 cells expressing either control GFP or TMPRSS11B and incubated with an immobilized antibody array with antibodies to 119 soluble and transmembrane proteins. **B**) Pixel density quantitation of Basigin on the developed antibody array. Unpaired t-test; *P<0.05

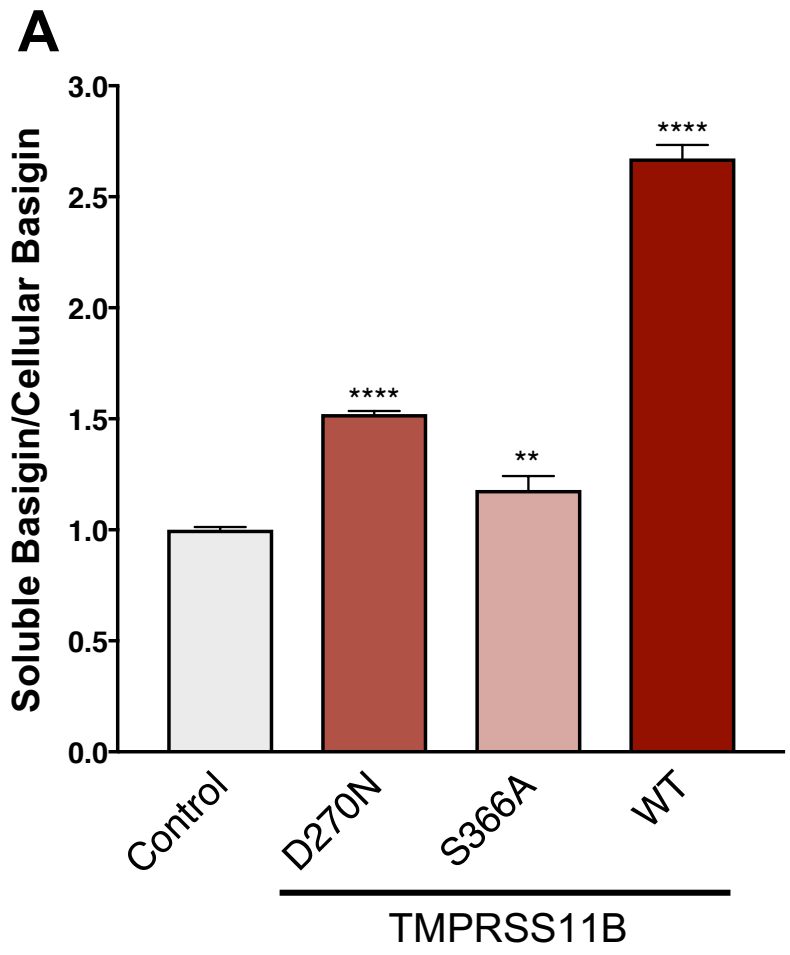

Figure 13: TMPRSS11B enhances membrane release of Basigin. **A**) ELISA assay of Basigin in conditioned media relative to cellular Basigin of HBEC-shp53 cells expressing either control GFP, TMPRSS11B^{D270N}, TMPRSS11B^{S366A}, or wild-type TMPRSS11B. Unpaired t-test; **P< 0.01, ****P<0.0001

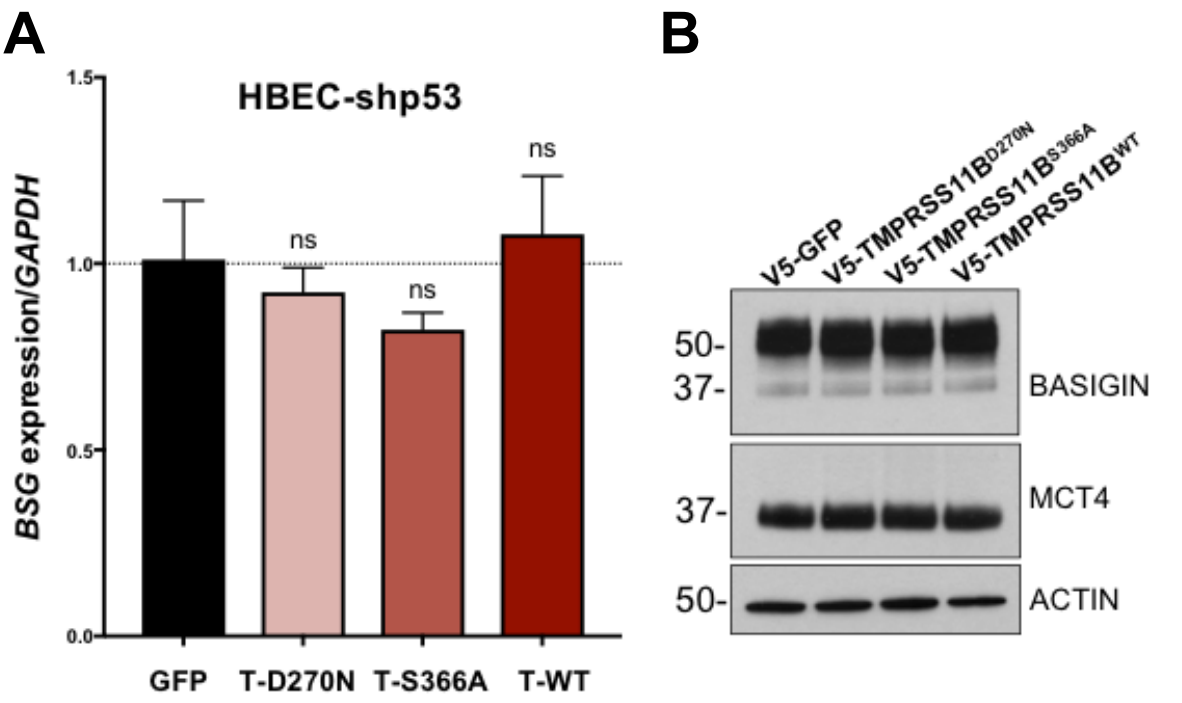

Figure 14: Basigin mRNA and protein expression is not affected by TMPRSS11B expression. A) qRT-PCR of *BSG* mRNA normalized to *GAPDH* in HBEC-shp53 cells expressing either control GFP, TMPRSS11B^{D270N}, TMPRSS11B^{S366A}, or wild-type TMPRSS11B. **B**) Western blot of HBEC-shp53 lysate probed with anti-Basigin, anti-MCT4, or anti-Actin antibodies. Actin serves as a loading control.

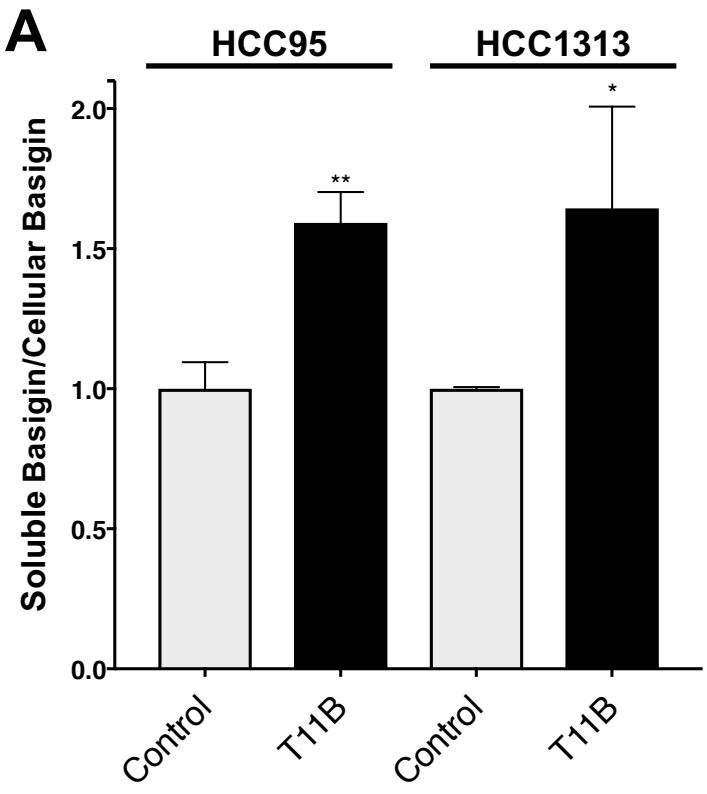

Figure 15: TMPRSS11B enhances membrane release of Basigin in LSCC cells. **A**) ELISA quantitation of Basigin in conditioned media relative to cellular Basigin from LSCC lines HCC95 or HCC1313 expressing either control mCherry or TMPRSS11B. Unpaired t-test; *P<0.05, **P< 0.01

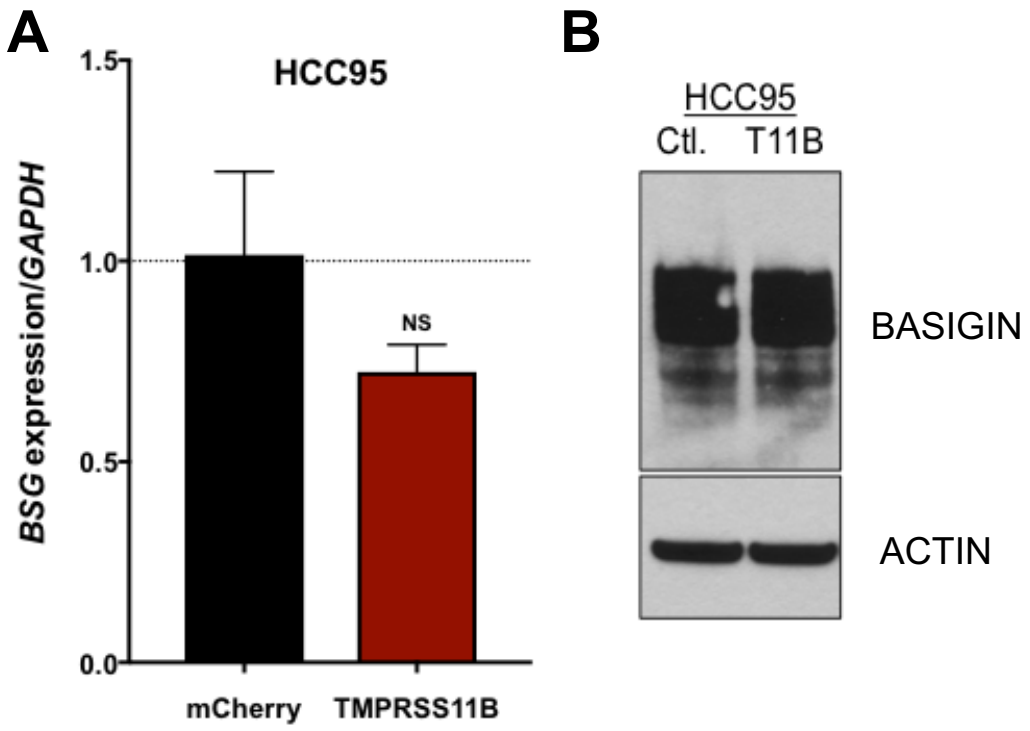

Figure 16: TMPRSS11B overexpression does not affect Basigin mRNA or protein in HCC95 cells. **A**) qRT-PCR quantitation of *BSG* mRNA normalized to *GAPDH.* **B**) Western blot of lysate from HCC95 cells using either anti-Basigin or anti-Actin antibodies. Actin serves as a loading control.

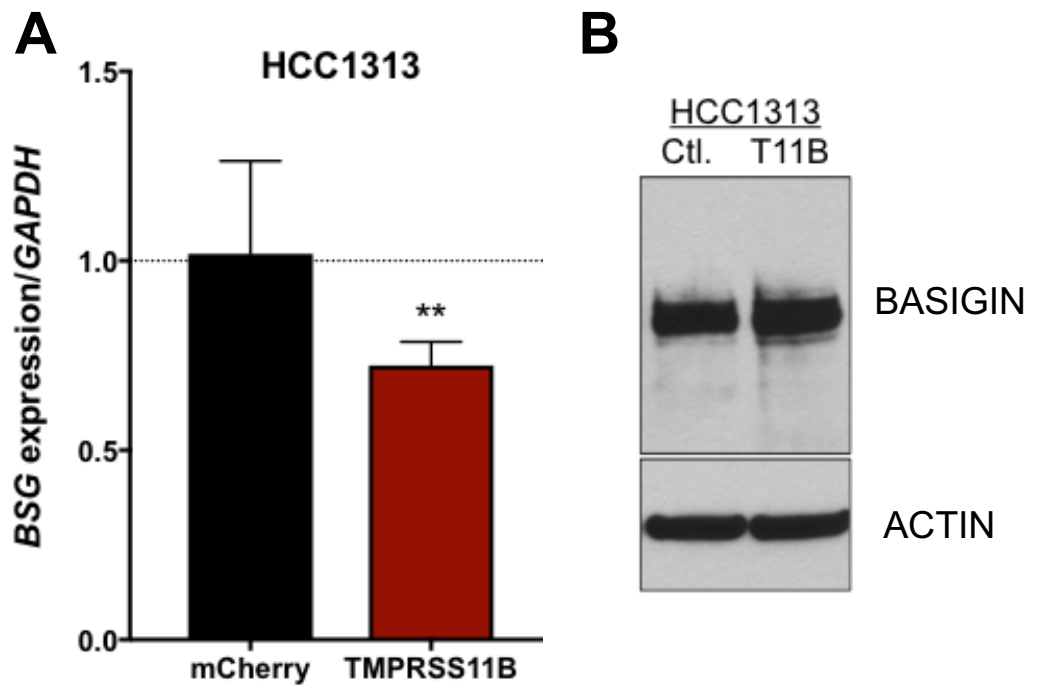

Figure 17: TMPRSS11B overexpression differentially effects Basigin mRNA and protein in HCC1313 cells. **A**) qRT-PCR quantitation of *BSG* mRNA normalized to *GAPDH.* **B**) Western blot of lysate from HCC1313 cells using either anti-Basigin or anti-Actin antibodies. Actin serves as a loading control. Unpaired t-test; **P< 0.01

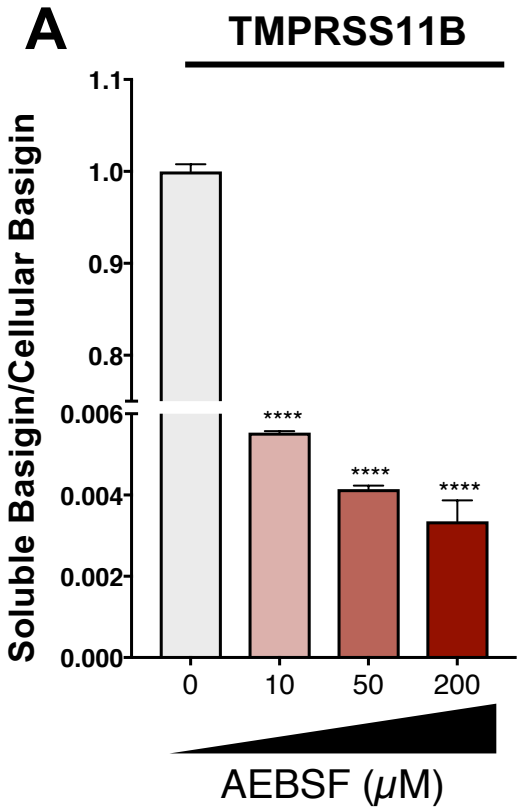

Figure 18: Chemical inhibition of serine proteases reduces Basigin membrane release. **A**) ELISA quantitation of Basigin in conditioned media relative to cellular Basigin in HBEC-shp53-TMPRSS11B cells treated with increasing concentrations of the serine protease inhibitor AEBSF. Unpaired t-test; ****P<0.0001

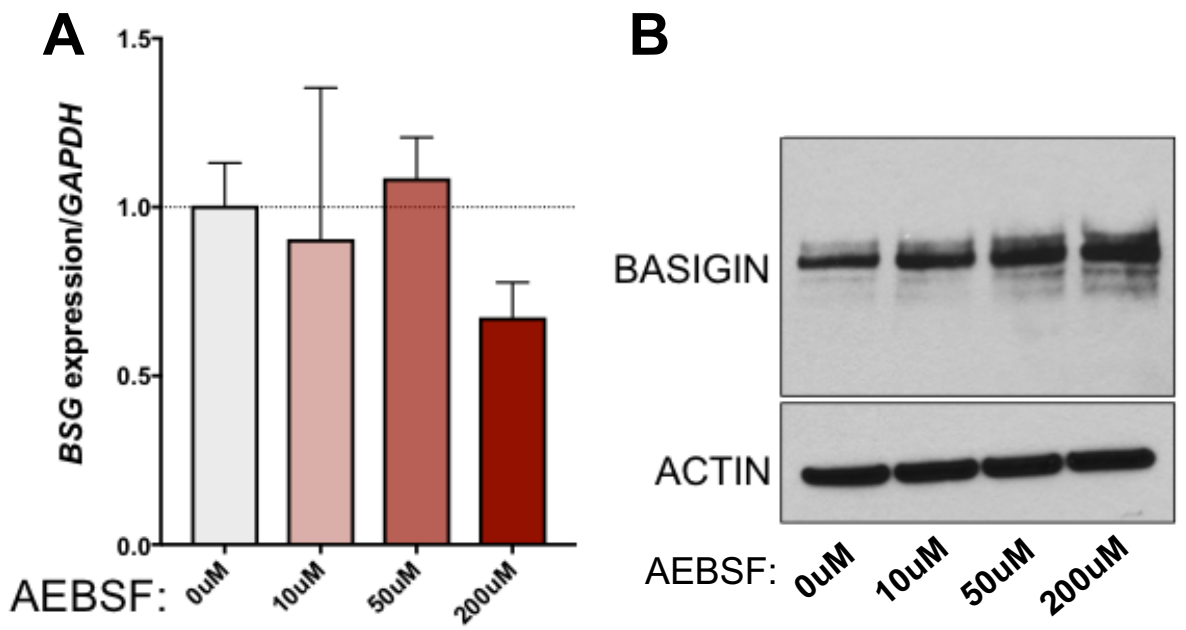

Figure 19: Chemical inhibition of serine proteases has varying effects on Basigin mRNA and protein. **A**) qRT-PCR of *BSG* mRNA normalized to *GAPDH* in HBEC-shp53-TMPRSS11B cells treated with serine protease inhibitor AEBSF. **B**) Western blot of HBEC-shp53-TMPRSS11B cellular lysate with anti-Basigin and anti-Actin antibodies. Actin serves as a loading control.

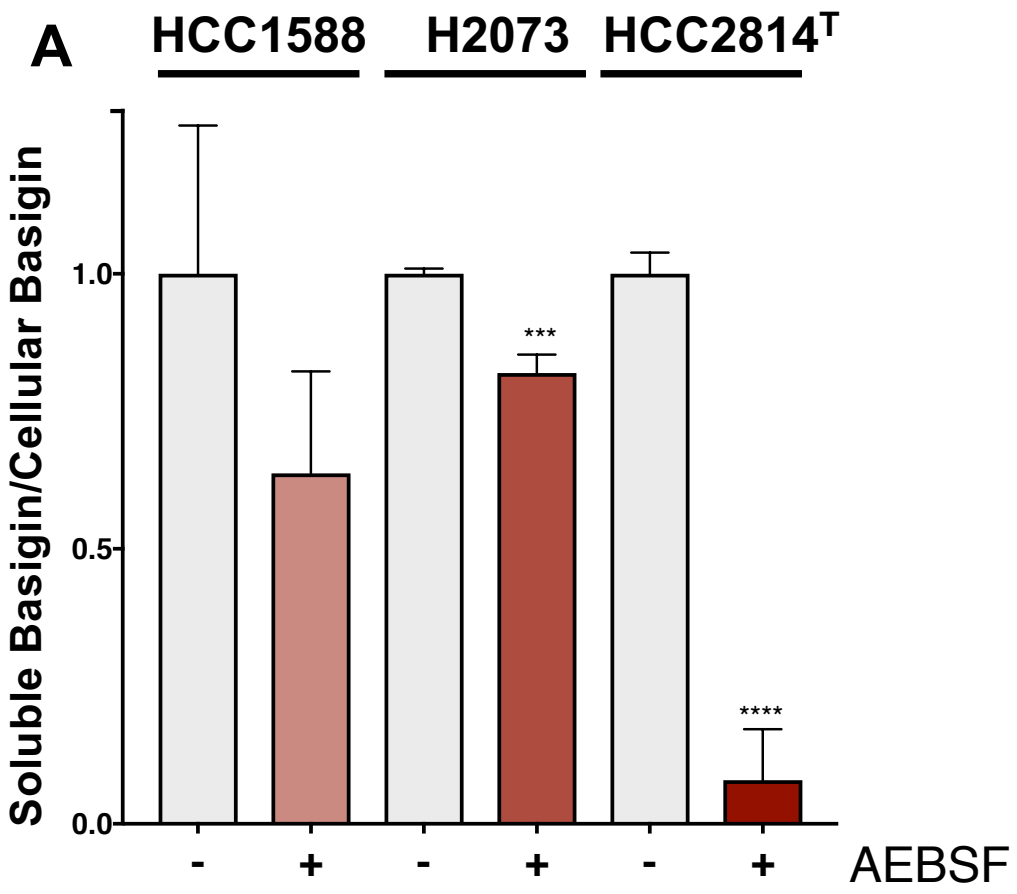

Figure 20: Chemical inhibition of serine proteases reduces Basigin membrane release. **A**) ELISA quantitation of Basigin in conditioned media relative to cellular Basigin in LSCC (HCC1588 and HCC2814) and lung adenocarcinoma cells (H2073) treated with serine protease inhibitor AEBSF. Unpaired t-test; ***P<0.001, ****P<0.0001

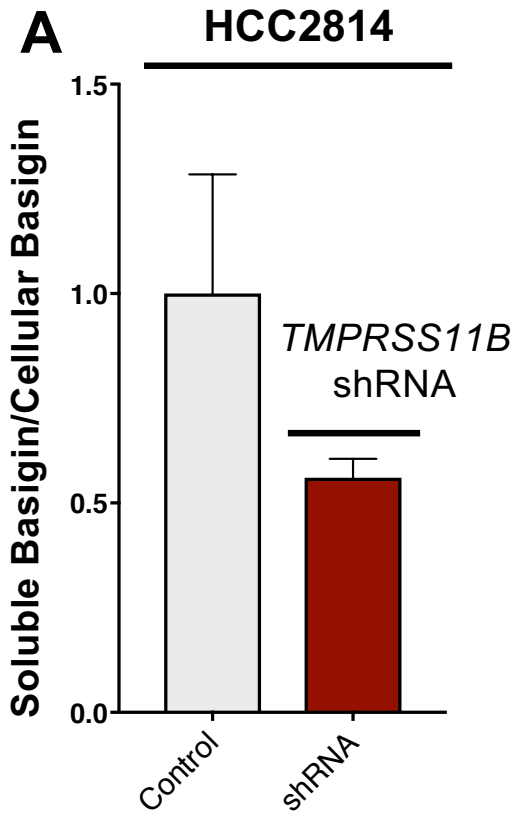

Figure 21: TMPRSS11B depletion modestly reduces Basigin membrane release. **A**) ELISA quantitation of Basigin in conditioned media normalized to cellular Basigin in HCC2814 cells harboring inducible control shRNA or shRNA targeting TMPRSS11B. Cells were treated for 3 days with doxycycline in culture media.

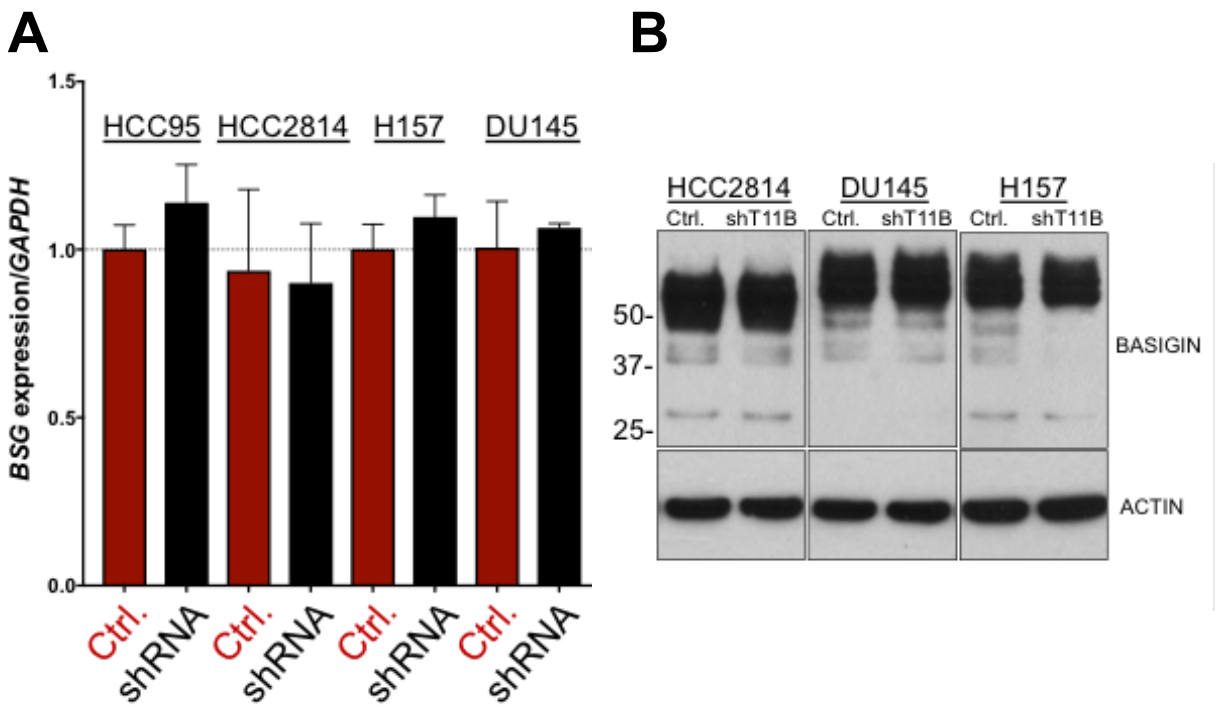

Figure 22: TMPRSS11B depletion does not alter Basigin mRNA or protein levels. A) qRT-PCR quantitation of *BSG* mRNA normalized to *GAPDH*. All groups were treated for 3 days with doxycycline in culture media. **B**) Western blot of cells from **(A**) probed with anti-Basigin or anti-Actin antibodies. Actin serves as a loading control.

Previous studies have shown that Basigin stimulates proliferation (Arendt et al., 2014, Su et al., 2009). We therefore assessed whether released Basigin could non-cell-autonomously enhance proliferation of HBEC-shp53 cells. Conditioned media from either HBEC-shp53-GFP, -TMPRSS11B^{S366A}, or -TMPRSS11B^{WT} expressing cells was transferred to HBEC-shp53 cells. No difference in proliferation was observed, suggesting that released Basigin in conditioned medium does not stimulate proliferation cell-non-autonomously in this system (**Figure 23**).

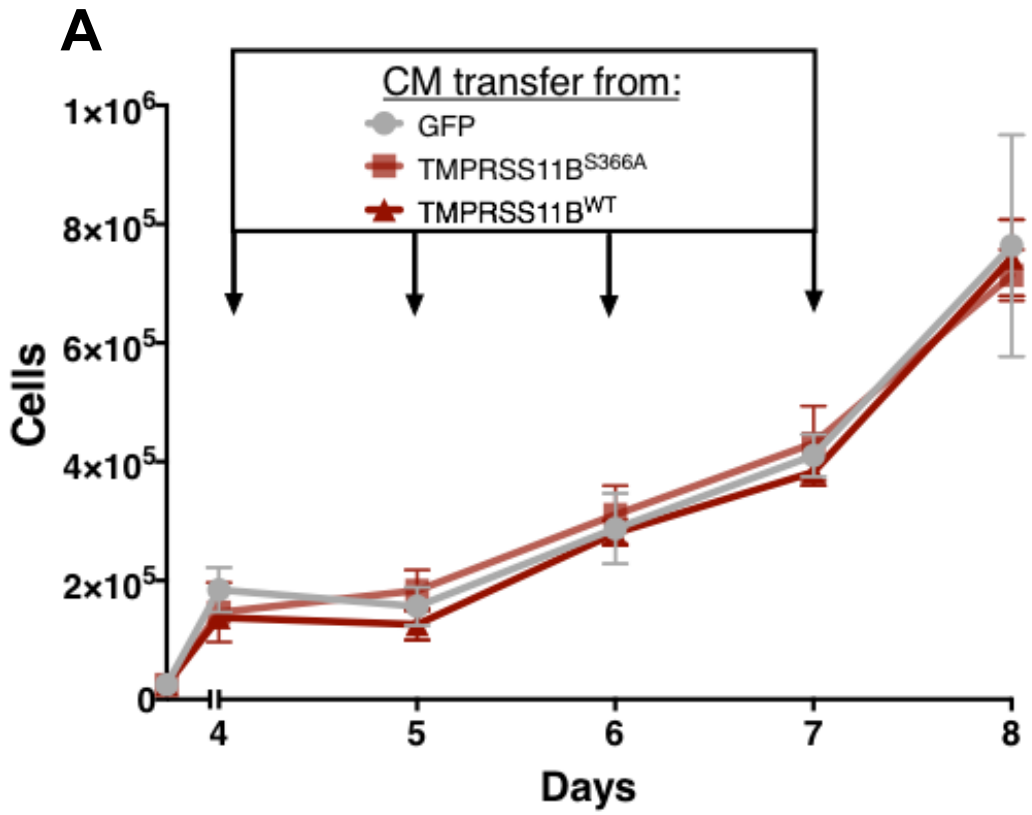

Figure 23: Conditioned media from cells expressing TMPRSS11B does not stimulate proliferation non-cell-autonomously. A) HBEC-shp53 cells were treated daily with fresh conditioned media from HBEC-shp53 cells expressing either control GFP, TMPRSS11B^{S366A}, or wild-type TMPRSS11B, and live cell numbers were measured.

TMPRSS11B interacts with Basigin and MCT4 at the plasma membrane

We next assessed interactions between TMPRSS11B, Basigin, and MCT4 by performing reciprocal co-immunoprecipitations in HBEC-shp53 and HCC2814 cells expressing tagged TMPRSS11B and Basigin constructs. Co-immunoprecipitation revealed interactions between HA-tagged TMPRSS11B and V5-tagged Basigin, and between V5-tagged TMPRSS11B and endogenous MCT4 (**Figure 24**). We further confirmed the interaction between V5-tagged TMPRSS11B and endogenous Basigin in HCC2814 cells by co-immunoprecipitation with three independent antibodies (**Figure 25)**. Immunofluorescence confocal microscopy revealed substantial co-localization of TMPRSS11B, MCT4, and Basigin at the plasma membrane of HBEC-shp53 cells (**Figures 26 and 27**). These data demonstrate that TMPRSS11B interacts with Basigin and MCT4 at the plasma membrane.

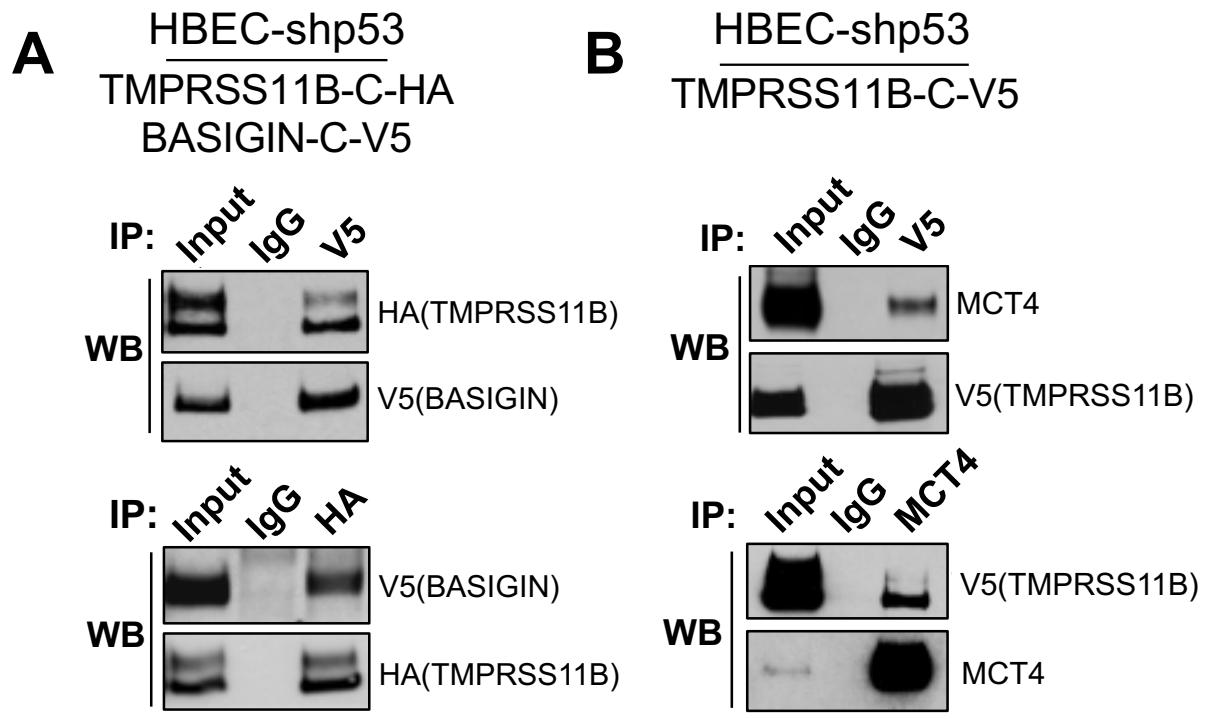

Figure 24: TMPRSS11B interacts with Basigin and MCT4. **A**) Reciprocal immunoprecipitation of HA-tagged TMPRSS11B and V5-tagged Basigin in HBEC-shp53 cells stably expressing TMPRSS11B-HA AND Basigin-V5. **B**) Reciprocal immunoprecipitation of V5-tagged TMPRSS11B and endogenous MCT4 in HBEC-shp53 cells stably expressing TMPRSS11B-V5.

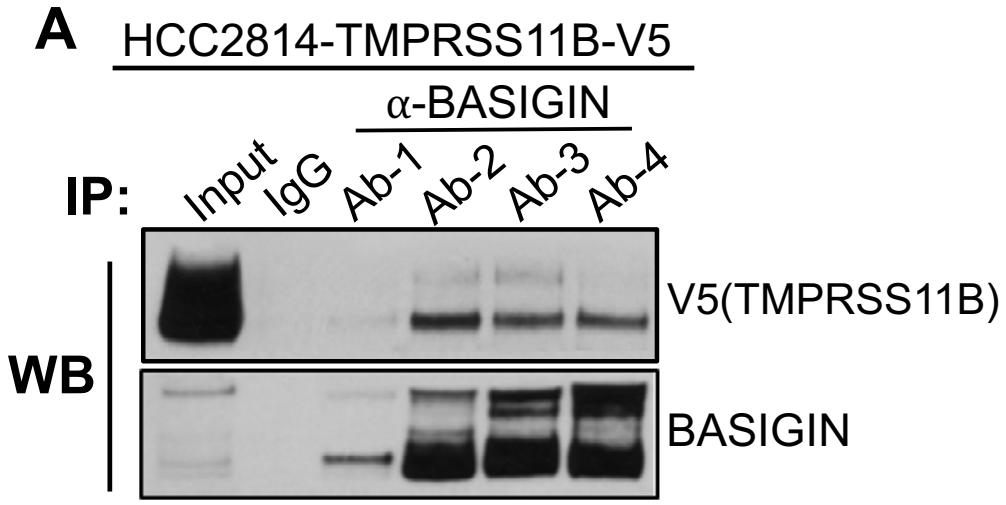

Figure 25: TMPRSS11B interacts with Basigin in LSCC cells.
A) Immunoprecipitation of V5-tagged TMPRSS11B in HCC2814 cells with multiple anti-Basigin antibodies. IgG serves as a negative control.

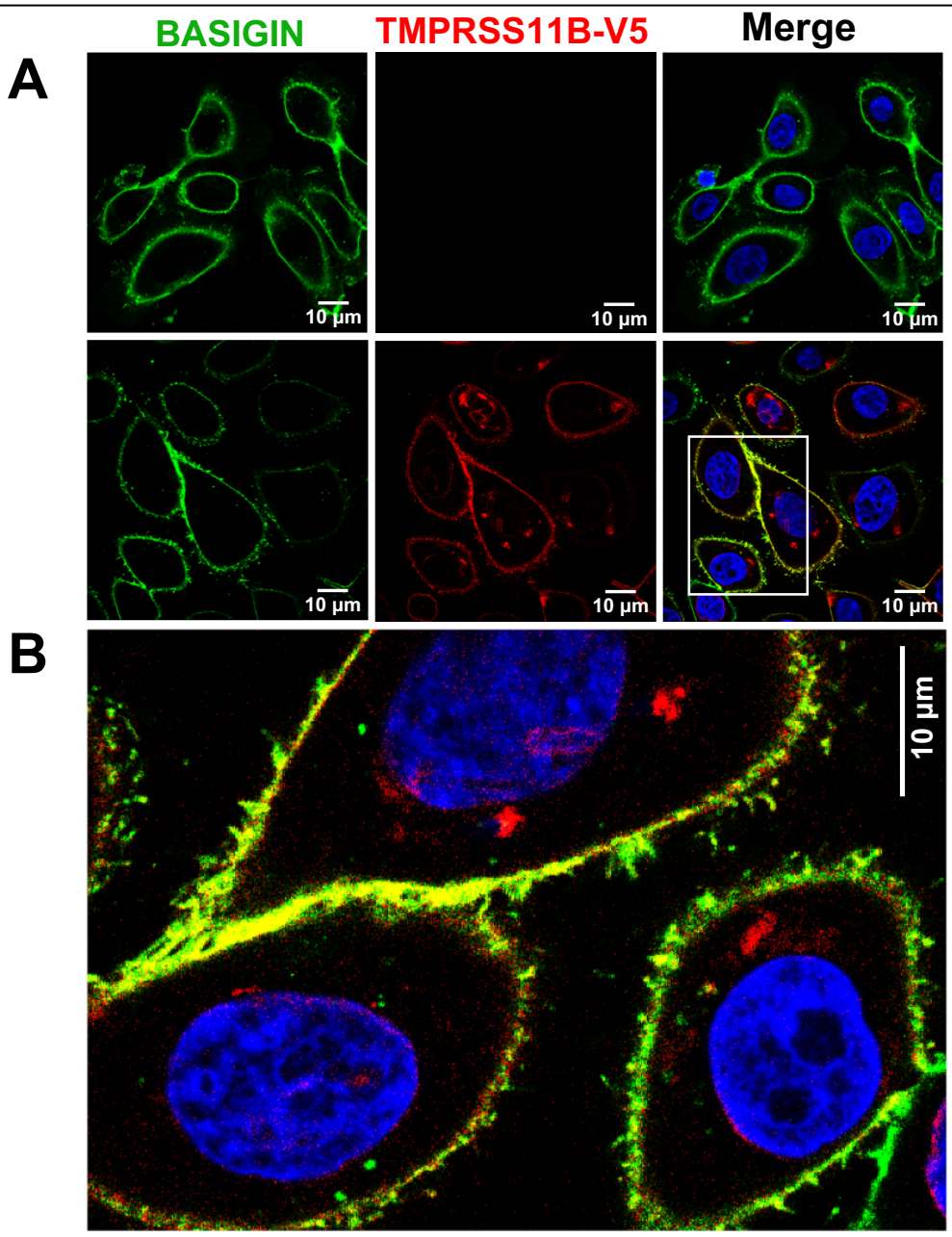

Figure 26: TMPRSS11B co-localizes with Basigin at the plasma membrane. **A**) HBEC-shp53-TMPRSS11B-V5 cells plated on cover slips and stained with anti-Basigin (green), anti-V5 (TMPRSS11B, red), and DAPI (blue). **B**) Inset of (**A**) merged image.

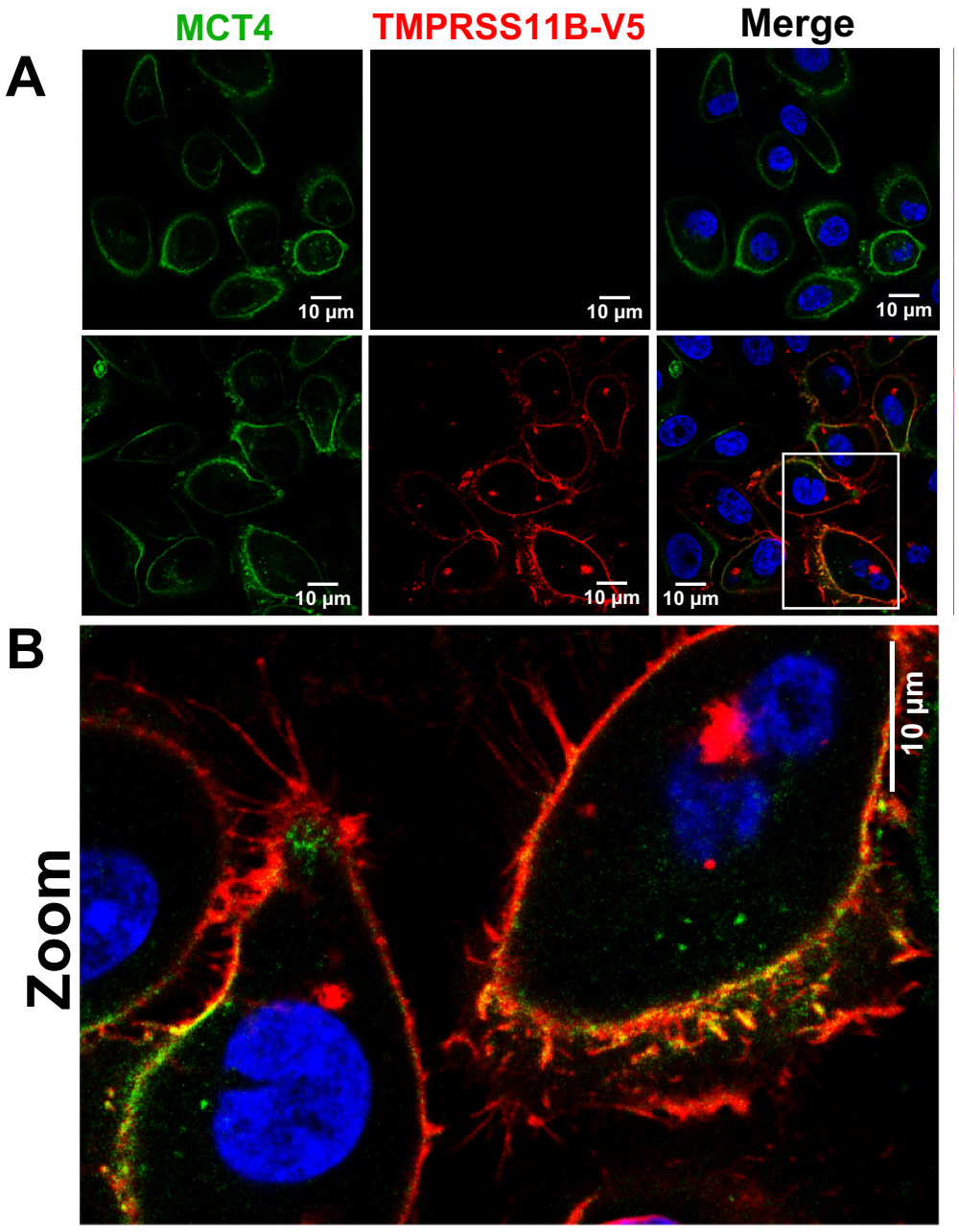

Figure 27: TMPRSS11B co-localizes with MCT4 at the plasma membrane. **A**) HBEC-shp53-TMPRSS11B-V5 cells plated on cover slips and stained with anti-MCT4 (green), anti-V5 (TMPRSS11B, red), and DAPI (blue). **B**) Inset of (**A**) merged image.

Immunofluorescence staining further showed modest alterations in Basigin localization upon TMPRSS11B loss-of-function. TMPRSS11B knockdown in HCC2814 cells resulted in less distinct membrane staining of Basigin relative to control cells (**Figure 28**). Total levels of cellular Basigin remained unchanged in these cells (**Figure 22**), suggesting that TMPRSS11B may have influenced trafficking of Basigin to the plasma membrane that was not appreciated in whole cell lysate.

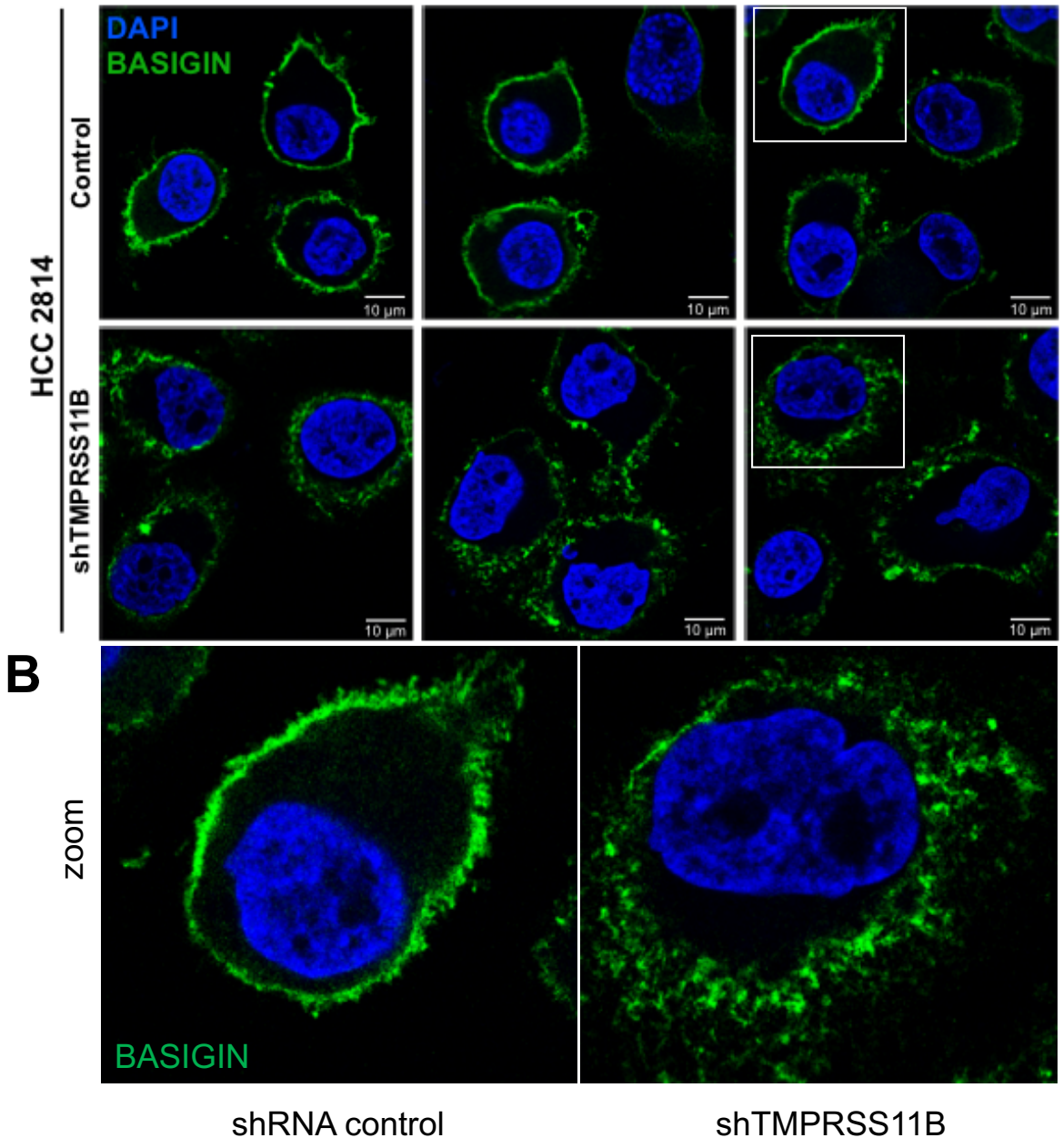

Figure 28: Depletion of TMPRSS11B results in more diffuse Basigin localization. A) HCC2814 cells with (bottom) and without (top) knock-down of TMPRSS11B stained with anti-Basigin antibodies and DAPI. **B**) Zoom of highlighted insets of **A.**

TMPRSS11B promotes lactate export

To investigate the role of Basigin downstream of TMPRSS11B, CRISPR/Cas9 was used to generate clonal HBEC-shp53-*TMPRSS11B* cells with Basigin (*BSG*) or MCT4 (*SLC16A3*) knock-out (**Figure 29**). Basigin deficiency led to decreased protein levels of MCT1 and MCT4, consistent with earlier reports demonstrating the essential chaperone function of Basigin for these lactate transporters (Philp et al., 2003) (**Figure 29A**). Moreover, Basigin and MCT4 were expressed similarly in control HBEC-shp53-GFP and HBEC-shp53-TMPRSS11B cells (**Figure 14B**), suggesting that membrane release of Basigin mediated by TMPRSS11B did not alter MCT4 expression. Next, we monitored the effects of Basigin depletion in HBEC-shp53 lacking TMPRSS11B by generating CRISPR/Cas9-edited clones (**Figure 30**). Basigin deficiency in these cells had no appreciable effect on proliferation (**Figure 31**). However, stable expression of TMPRSS11B failed to significantly stimulate proliferation in Basigin-deficient cells and TMPRSS11B-mediated anchorage-independent growth was reduced upon Basigin knock-out (**Figures 30 and 31**). These data demonstrate that Basigin knock-out is tolerated in HBEC-shp53 cells, and that TMPRSS11B-mediated proliferation and transformation is facilitated by Basigin in this system.

Given the critical role for Basigin in MCT1/MCT4 trafficking, we hypothesized that Basigin solubilization might serve to further regulate MCT1/MCT4-mediated lactate transport function. Consistent with this hypothesis, intracellular lactate quantification revealed a ~25% reduction in steady-state lactate content of HBEC-shp53-*TMPRSS11B* compared with HBEC-shp53-control GFP cells (**Figure 32**). Importantly, this reduction was reversed in independent *BSG* knockout clones, and partially in HBEC-sh53-

TMPRSS11B cells treated with AEBSF (**Figure 32**). To rule out the possibility that this reduction in steady state intracellular lactate levels was due to a defect in glucose uptake and therefore reduced glycolytic flux, we measured uptake of the fluorescent glucose analog 2-NBDG. No significant difference between HBEC-shp53-TMPRSS11B and HBEC-shp53 control cells was observed (**Figure 33**). Extracellular flux analysis further demonstrated that TMPRSS11B enhanced extracellular acidification rates (ECAR), a readout of glycolytic flux and a commonly used proxy for lactate secretion (**Figure 34**). Importantly, the enhanced export was reduced in independent Basigin deficient clones, and rescued in cells by reintroduction of a CRISPR/Cas9-resistant Basigin construct (**Figure 34)**. Moreover, in separate Basigin deficient cells lacking TMPRSS11B expression, we found only a modest (~10%) reduction in ECAR compared with control non-specific gRNA cells (sgNS), further suggesting that Basigin deficiency is tolerated in HBEC-shp53 cells (**Figure 35**). This may reflect a vulnerability of TMPRSS11B-expressing cells to Basigin deficiency that is not observed in syngeneic cells lacking TMPRSS11B. To distinguish between the roles of MCT1 and MCT4 in this system, we compared HBEC-shp53-TMPRSS11B cells with either MCT4 deletion or treatment with the chemical MCT1 inhibitor SR13800 and observed that ECAR was dramatically reduced in MCT4 KO cells, but minimally upon MCT1 inhibition (**Figure 36**). Taken together, these findings provide evidence that TMPRSS11B enhances the lactate transport efficiency of Basigin/MCT4 complexes in HBEC-shp53 cells.

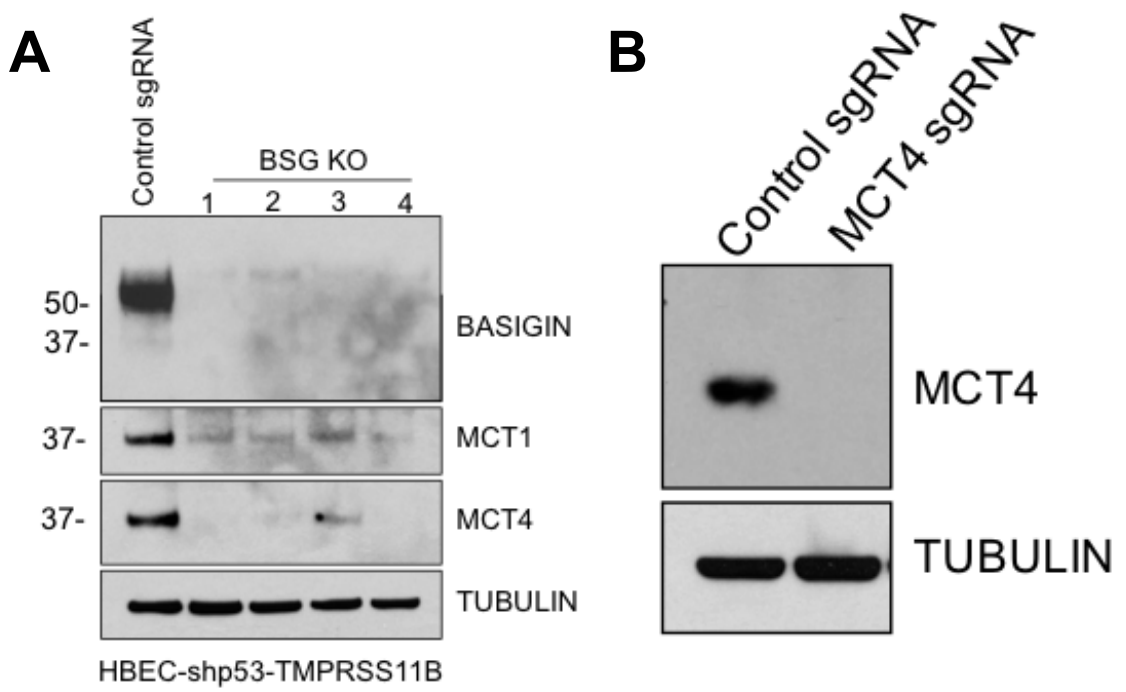

Figure 29: Basigin and MCT4 knock-out in HBEC-shp53-TMPRSS11B cells. A) Western blot of HBEC-shp53-TMPRSS11B cells with control non-targeting sgRNA or Basigin sgRNA. Antibodies recognizing Basigin, MCT1, MCT4, and tubulin were used. Each lane represents a clone and tubulin serves as a loading control. **B**) Western blot of HBEC-shp53-TMPRSS11B cells with control sgRNA or *SLC16A3* (MCT4) sgRNA. Tubulin serves as a loading control.

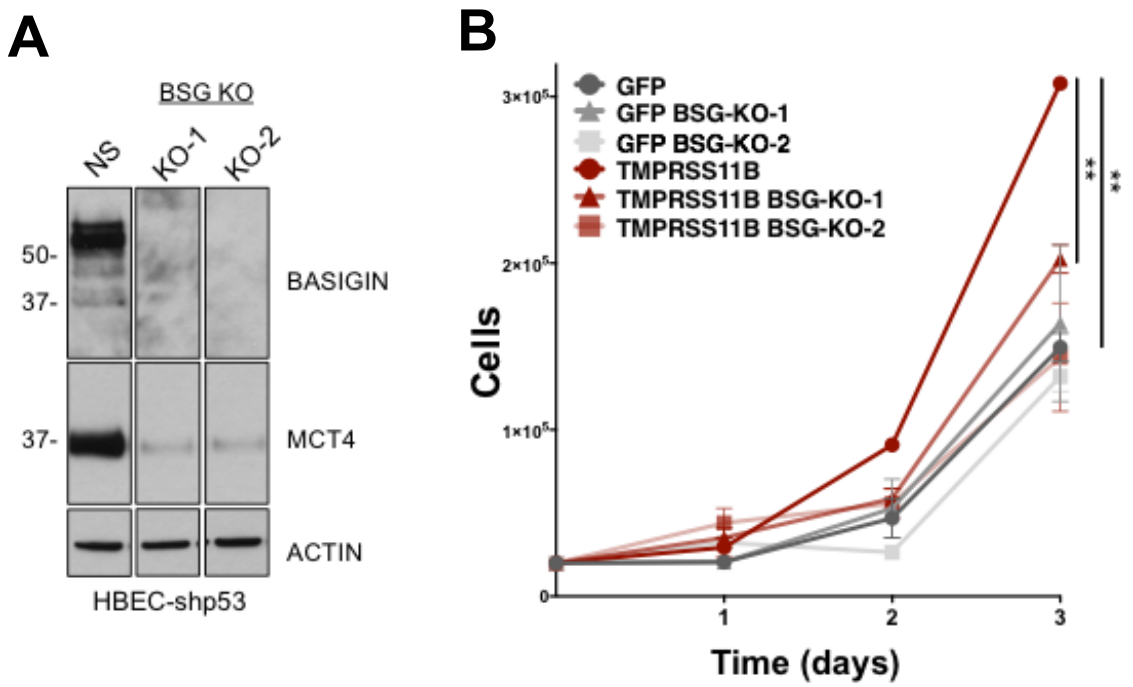

Figure 30: Depletion of Basigin impairs proliferation of HBEC-shp53 cells. A) Western blot of HBEC-shp53 cells edited with control sgRNA or sgRNA targeting *BSG.* Lanes represent independent clones **B**) Proliferation assay of HBEC-shp53 cells with CRISPR/Cas9-mediated depletion of Basigin or non-targeting control sgRNA, expressing either GFP control or TMPRSS11B. Asterisks represent significant differences between TMPRSS11B and GFP, and TMPRSS11B and TMPRSS11B-BSG-KO-1/KO-2. Unpaired t-test; **P< 0.01

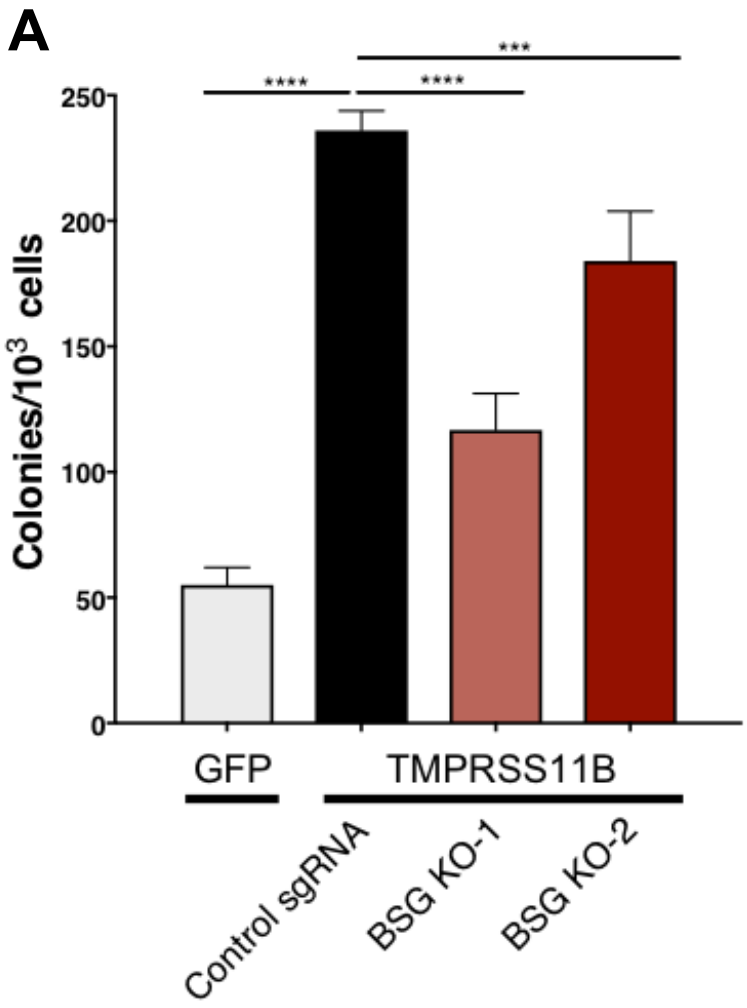

Figure 31: Depletion of Basigin impairs growth of HBEC-shp53 cells.
A) Soft agar colony formation assay of HBEC-shp53-TMPRSS11B Basigin knock-out, control sgRNA, or GFP control. Unpaired t-test; ***P<0.001, ****P<0.0001

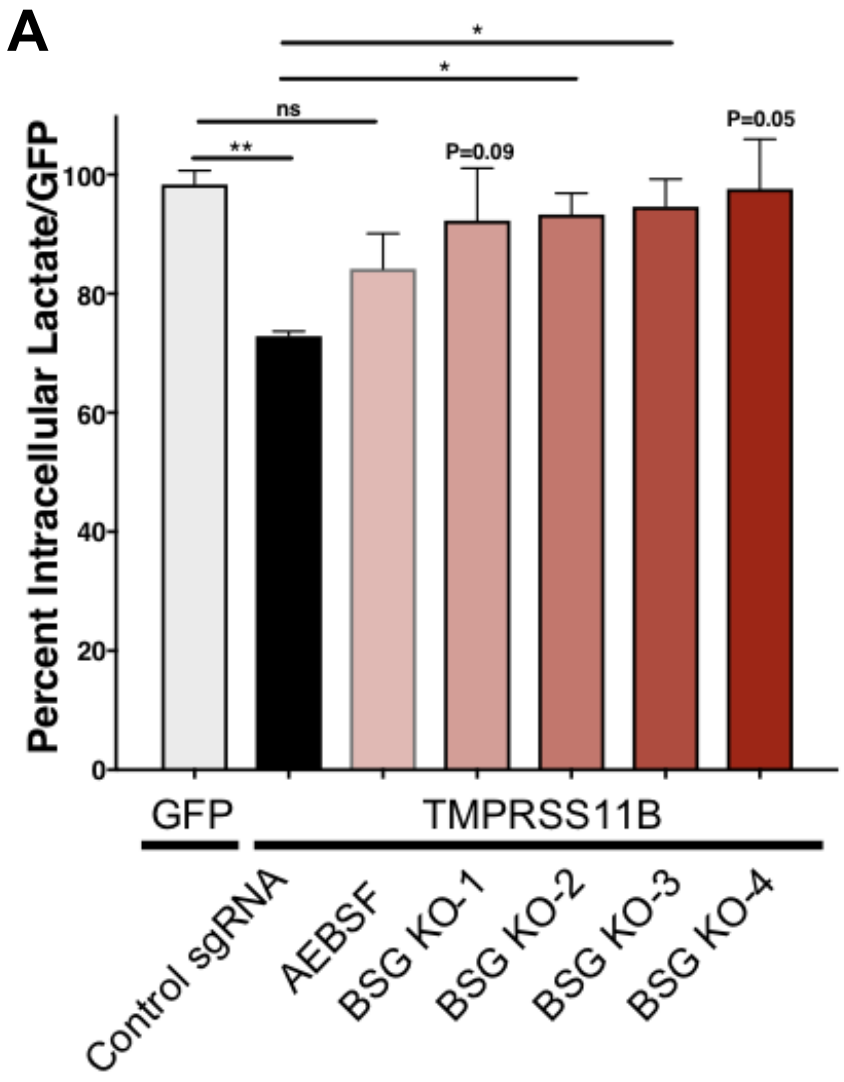

Figure 32: TMPRSS11B regulates cellular lactate levels. A) Intracellular lactate quantitation of HBEC-shp53 cells with either control GFP or TMPRSS11B expression. HBEC-shp53-TMPRSS11B cells were subjected to serine protease inhibitor treatment (AEBSF) or CRISPR/Cas9-mediated knock-out of Basigin. Unpaired t-test; *P<0.05, **P< 0.01

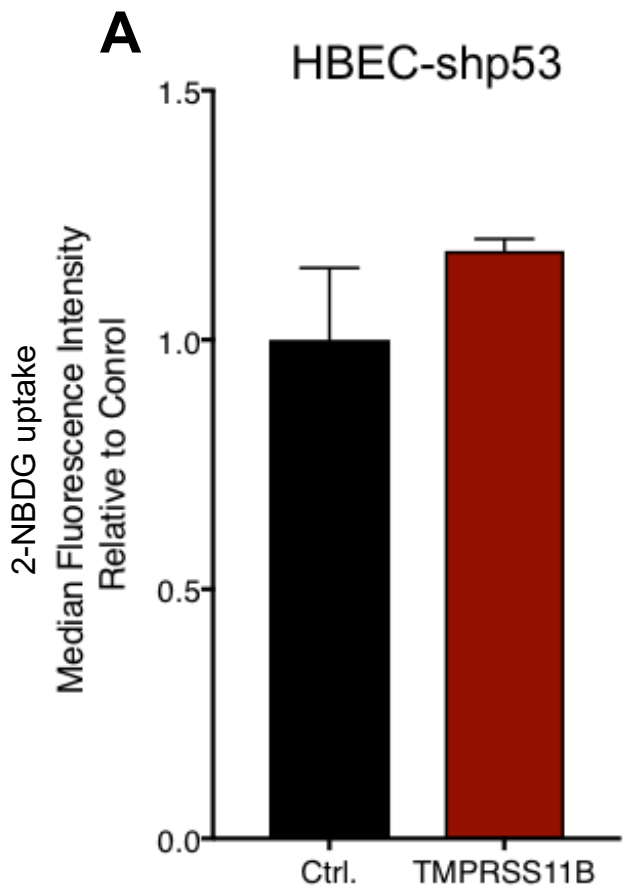

Figure 33: TMPRSS11B does not significantly alter glucose uptake. A) HBEC-shp53 cells with and without expression of TMPRSS11B were given the fluorescent glucose analog 2-NBDG and its accumulation in cells was monitored by flow cytometry.

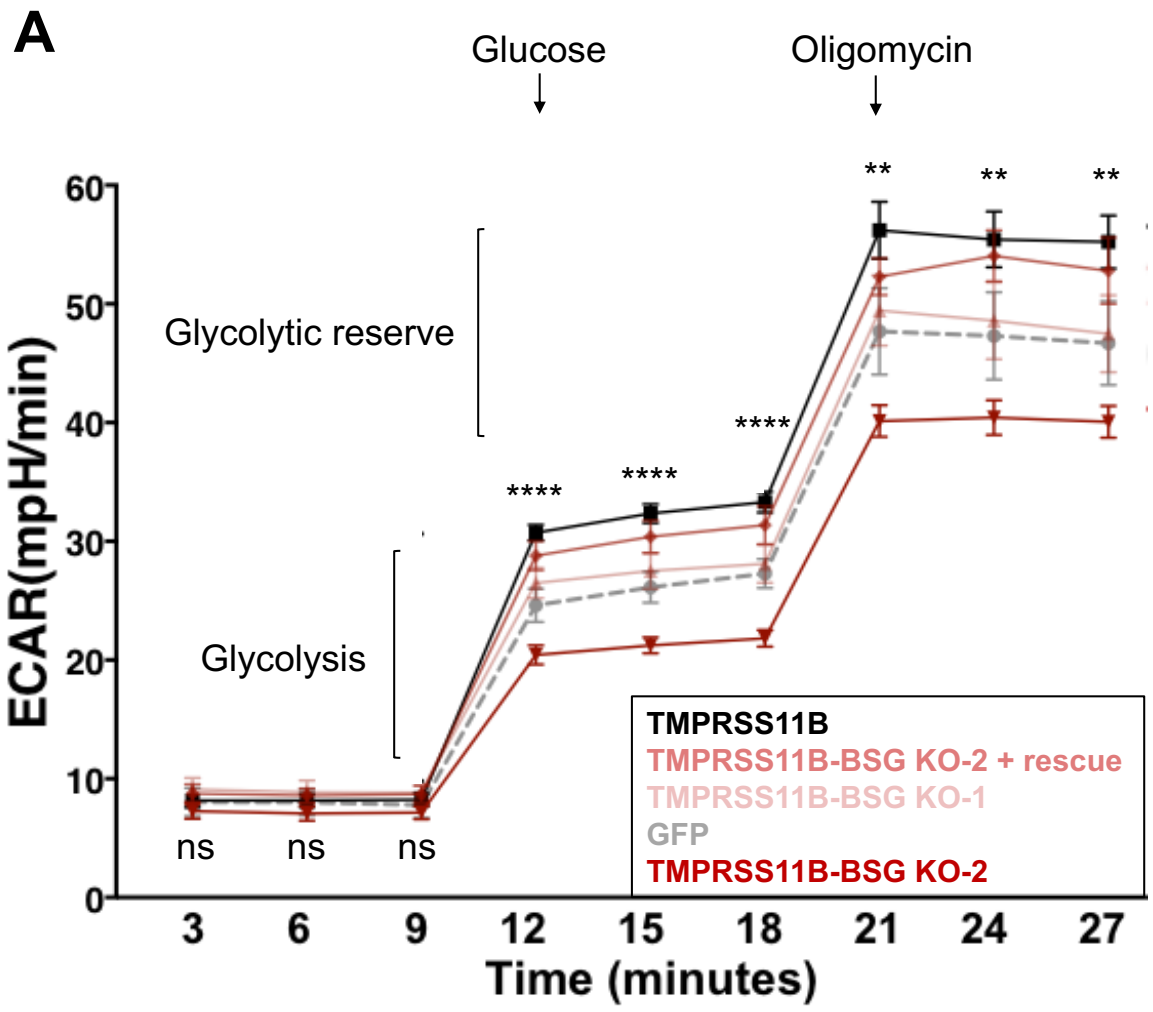

Figure 34: TMPRSS11B promotes Basigin-dependent lactate secretion. A) SeaHorse metabolic flux assay of HBEC-shp53 cells to assess extracellular acidification (ECAR) in response to glucose addition (glycolysis) and oligomycin treatment (glycolytic reserve). TMPRSS11B enhances ECAR compared to control GFP or HBEC-shp53-TMPRSS11B cells lacking Basigin. Cells lacking Basigin with reintroduction of CRISPR-resistant Basigin cDNA restored lactate export (ECAR). Asterisks represent the significant difference between GFP control and TMPRSS11B overexpressing cells. Unpaired t-test; ns: not significant, **P<0.01, ****P<0.0001

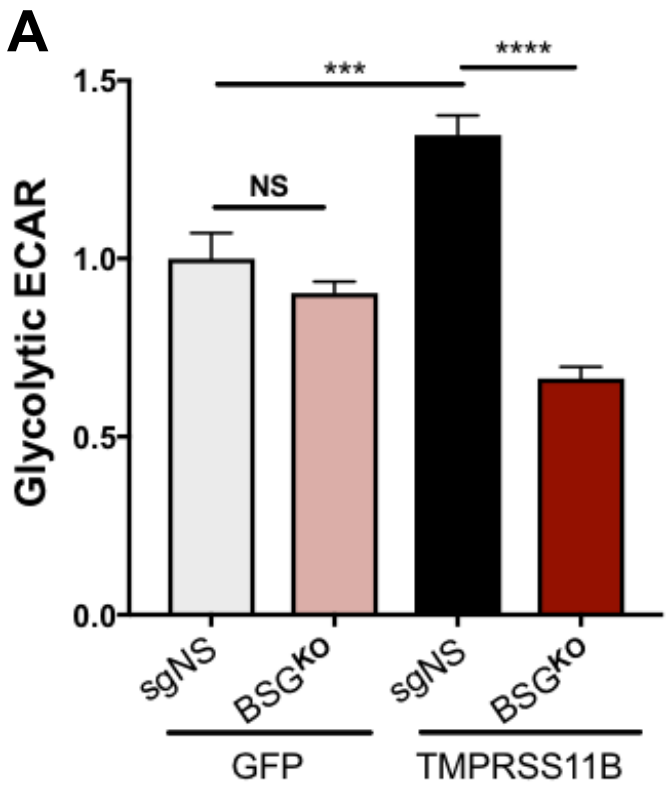

Figure 35: Basigin knock-out in HBEC-shp53 cells impairs lactate secretion only in the presence of TMPRSS11B. A) SeaHorse quantitation of glycolytic ECAR (ECAR post glucose addition – basal ECAR) in HBEC-shp53 cells that were edited with CRISPR/Cas9 with non-targeting sgRNA (sgNS) or sgRNA targeting *BSG* (Basigin). Basigin knock-out clones were expanded and then either control GFP or TMPRSS11B were stably introduced. Data represent 2 independent Basigin knock-out clones for each (GFP and TMPRSS11B). Unpaired t-test; ***P<0.001, ****P<0.0001

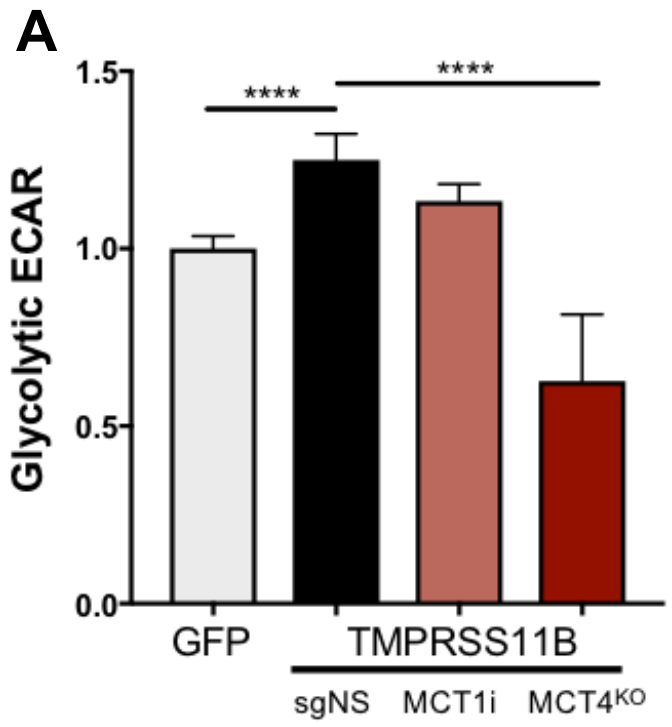

Figure 36: MCT4, and not MCT1, impairs lactate secretion in HBEC-shp53 cells expressing TMPRSS11B. A) SeaHorse quantitation of glycolytic ECAR (ECAR post glucose addition – basal ECAR) in HBEC-shp53 cells expressing control GFP or TMPRSS11B. HBEC-shp53-TMPRSS11B cells were treated with the MCT1-specific inhibitor SR13800 or were edited with CRISPR/Cas9 along with a non-targeting sgRNA or sgRNA targeting *SLC16A3* (MCT4). Unpaired t-test; ****P<0.0001

Depletion of TMPRSS11B reduces lactate export

To further test its role in promoting lactate export, TMPRSS11B was depleted using shRNA in the LSCC lines HCC2814, H157, and HCC95, and the prostate cancer line DU145 (**Figures 37 and 38**). CRISPR-mediated genome editing was used to edit the endogenous *TMPRSS11B* locus in polyclonal populations of the lung adenocarcinoma cell line H2073 and in clonal lines of HCC2814 cells (**Figures 39 and 40**). TMPRSS11B reduction in all of these cells resulted in ~1.3 to 3.5-fold intracellular lactate levels relative to control cells (**Figures 37-40)**. We performed qPCR analysis of *TMPRSS11B* mRNA in CRISPR/Cas9-edited clones to identify those with the most impaired TMPRSS11B expression to be used for rescue experiments (**Figure 41**) Increased intracellular lactate in *TMPRSS11B* knockout clones was specifically due to TMPRSS11B loss of function since restoring TMPRSS11B expression with cDNA harboring silent mutations in the sgRNA targeting site led to a significant reduction in intracellular lactate levels (**Figure 42**). We also confirmed that these cells consume similar amounts of 2-NBDG (**Figures 43-46**), ruling out the possibility that this lactate accumulation is caused by enhanced glucose uptake.

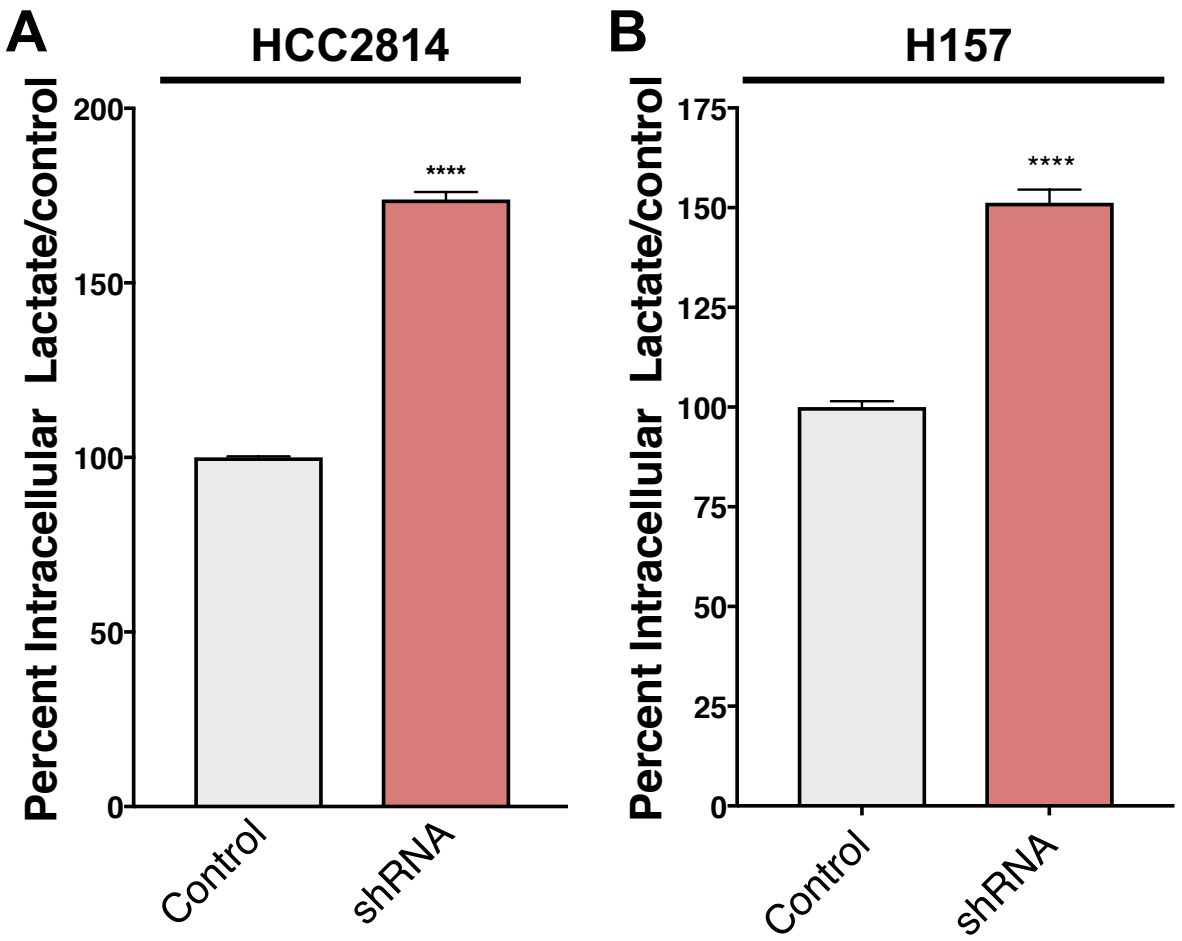

Figure 37: TMPRSS11B depletion results in cellular lactate accumulation in LSCC cells. A) Intracellular lactate quantitation of HCC2814 cells harboring doxycycline-inducible shRNA control, or shRNA targeting TMPRSS11B. Cells were treated for 3 days with doxycycline in culture media. **B**) Intracellular lactate quantitation of H157 cells harboring doxycycline-inducible shRNA control or shRNA targeting TMPRSS11B. Cells were treated for 3 days with doxycycline in culture media. Unpaired t-test; ****P<0.0001.

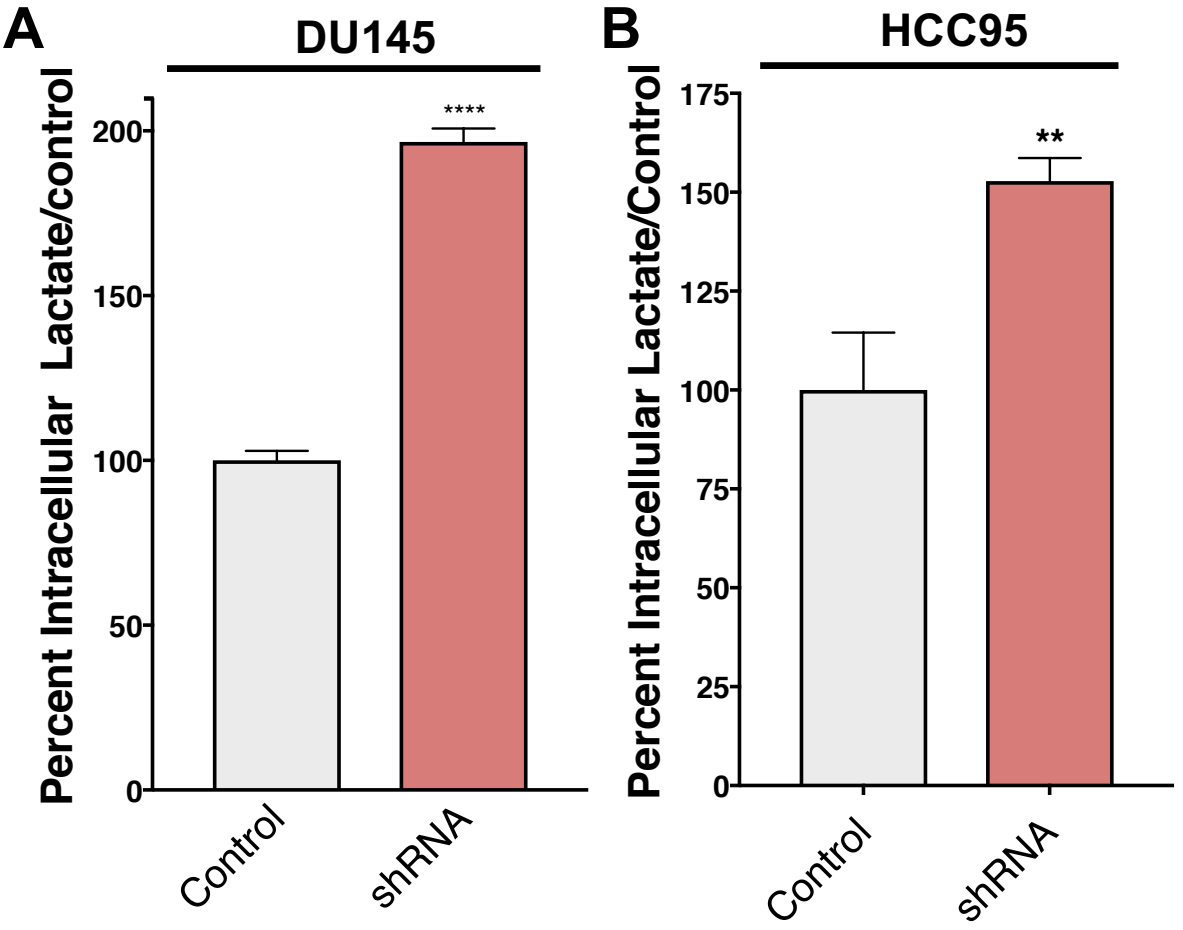

Figure 38: TMPRSS11B depletion results in cellular lactate accumulation in prostate cancer and LSCC cells. A) Intracellular lactate quantitation of DU145 cells harboring doxycycline-inducible shRNA control, or shRNA targeting TMPRSS11B. Cells were treated for 3 days with doxycycline in culture media. **B**) Intracellular lactate quantitation of HCC95 cells harboring doxycycline-inducible shRNA control or shRNA targeting TMPRSS11B. Cells were treated for 3 days with doxycycline in culture media. Unpaired t-test; **P<0.01, ****P<0.0001

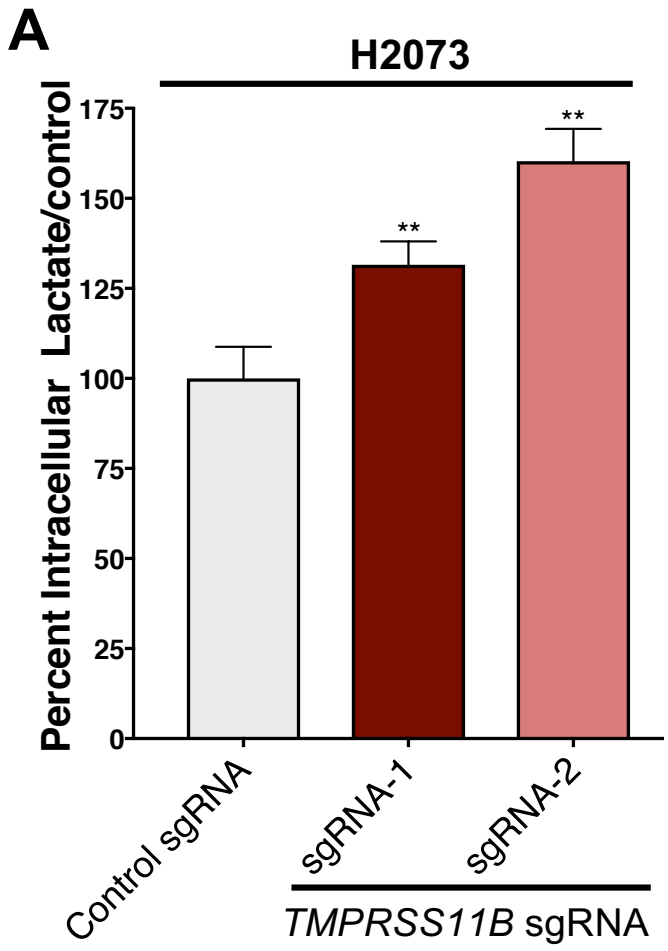

Figure 39: TMPRSS11B depletion results in lactate accumulation in LUAD cell line H2073. A) Intracellular lactate quantitation of lung adenocarcinoma cell line H2073 edited with CRISPR/Cas9 with control non-targeting sgRNA, or 2 independent sgRNA targeting *TMPRSS11B.* Groups represent pools of edited cells. Unpaired t-test; **P<0.01

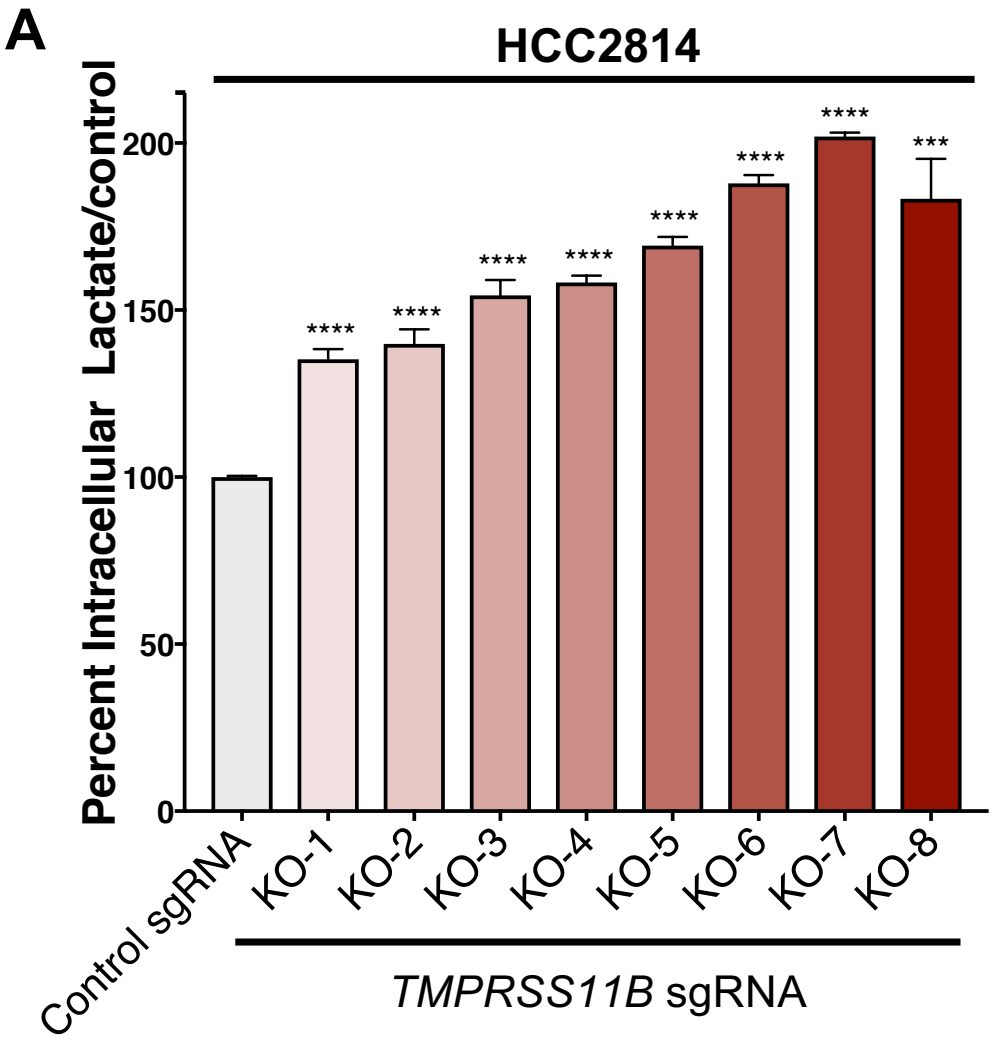

Figure 40: TMPRSS11B depletion results in lactate accumulation in LSCC line HCC2814. A) Intracellular lactate quantitation of HCC2814 cells edited with CRISPR/Cas9 with control non-targeting sgRNA or sgRNA targeting TMPRSS11B. Cells edited with TMPRSS11B sgRNA were clonally expanded and represent clones from 2 independent sgRNAs targeting *TMPRSS11B.* Unpaired t-test; ***P<0.001, ****P<0.0001

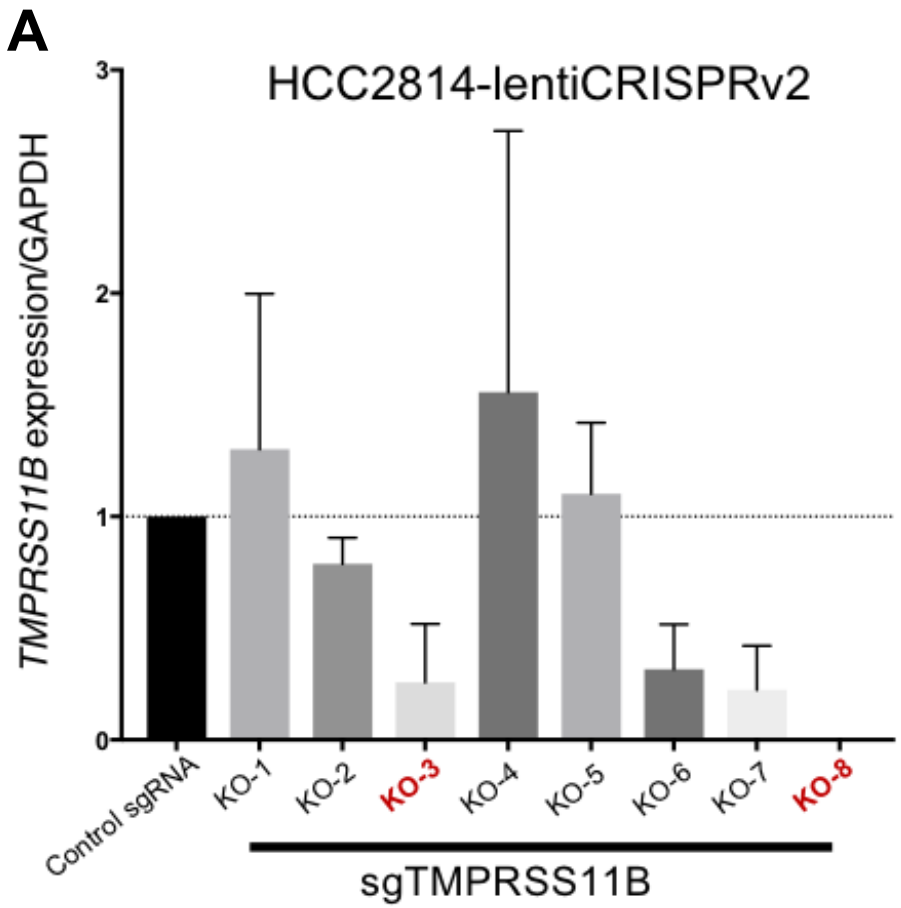

Figure 41: *TMPRSS11B* mRNA expression in CRISPR/Cas9-edited clones. A) qRT-PCR quantitation of *TMPRSS11B* mRNA normalized to *GAPDH* in HCC2814 cells edited with non-targeting sgRNA control or sgRNA targeting *TMPRSS11B.* Clones highlighted in red were used for rescue experiments.

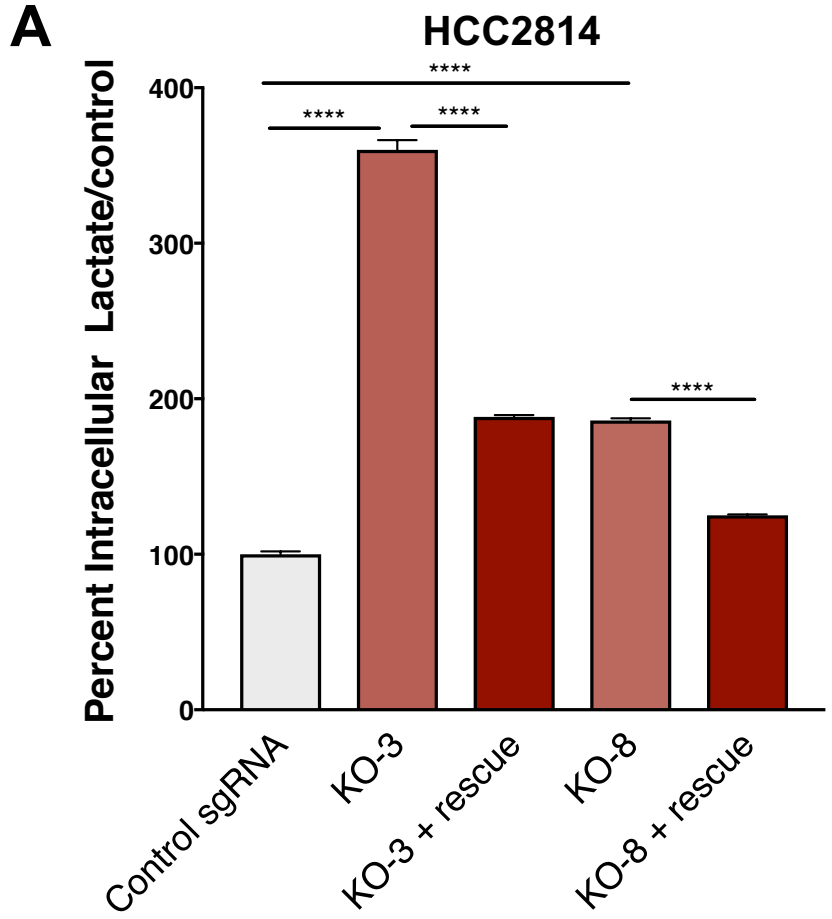

Figure 42: TMPRSS11B depletion results in lactate accumulation that can be restored upon reintroduction of TMPRSS11B. A) Intracellular lactate quantitation of HCC2814 cells edited with CRISPR/Cas9 with control non-targeting sgRNA or sgRNA targeting TMPRSS11B. Cells edited with TMPRSS11B sgRNA were clonally expanded and represent clones from 2 independent sgRNAs targeting *TMPRSS11B.* CRISPR/Cas9-resistant TMPRSS11B cDNA was stably reintroduced into edited clones. Unpaired t-test; ****P<0.0001

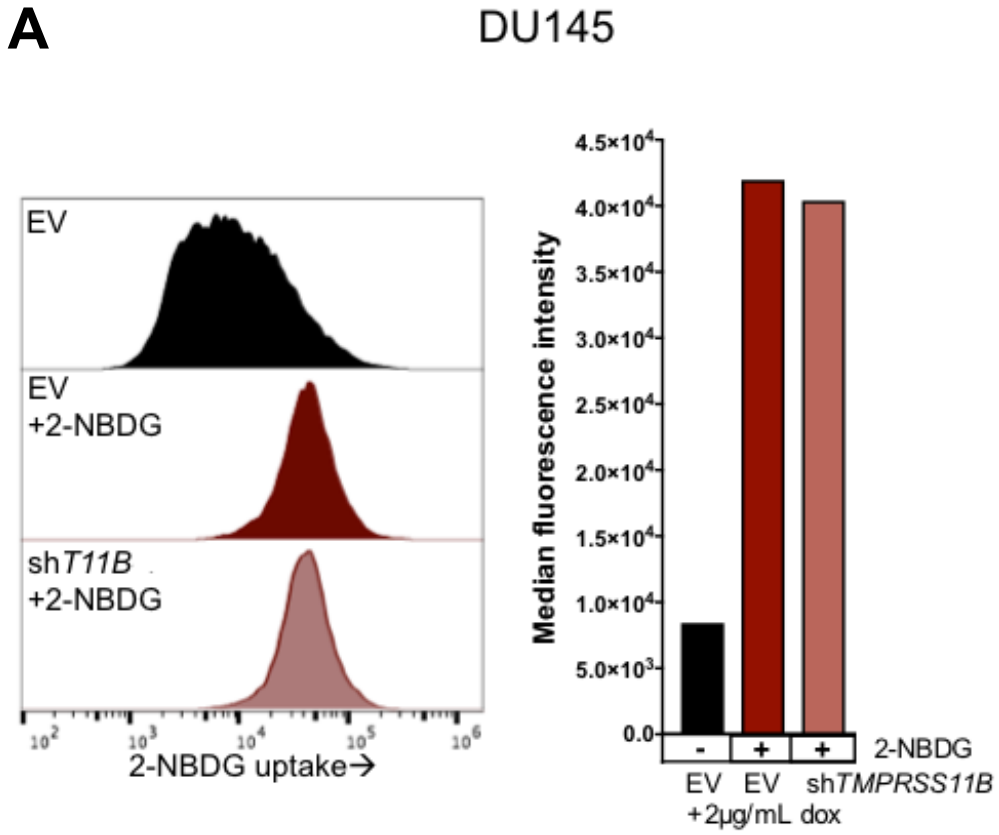

Figure 43: TMPRSS11B depletion does not affect glucose uptake in prostate cancer cell line DU145. A) Flow cytometry quantitation of 2-NBDG uptake in DU145 cells harboring doxycycline-inducible shRNA control or shRNA targeting TMPRSS11B treated for 3 days with doxycycline in culture media. EV: empty vector control.

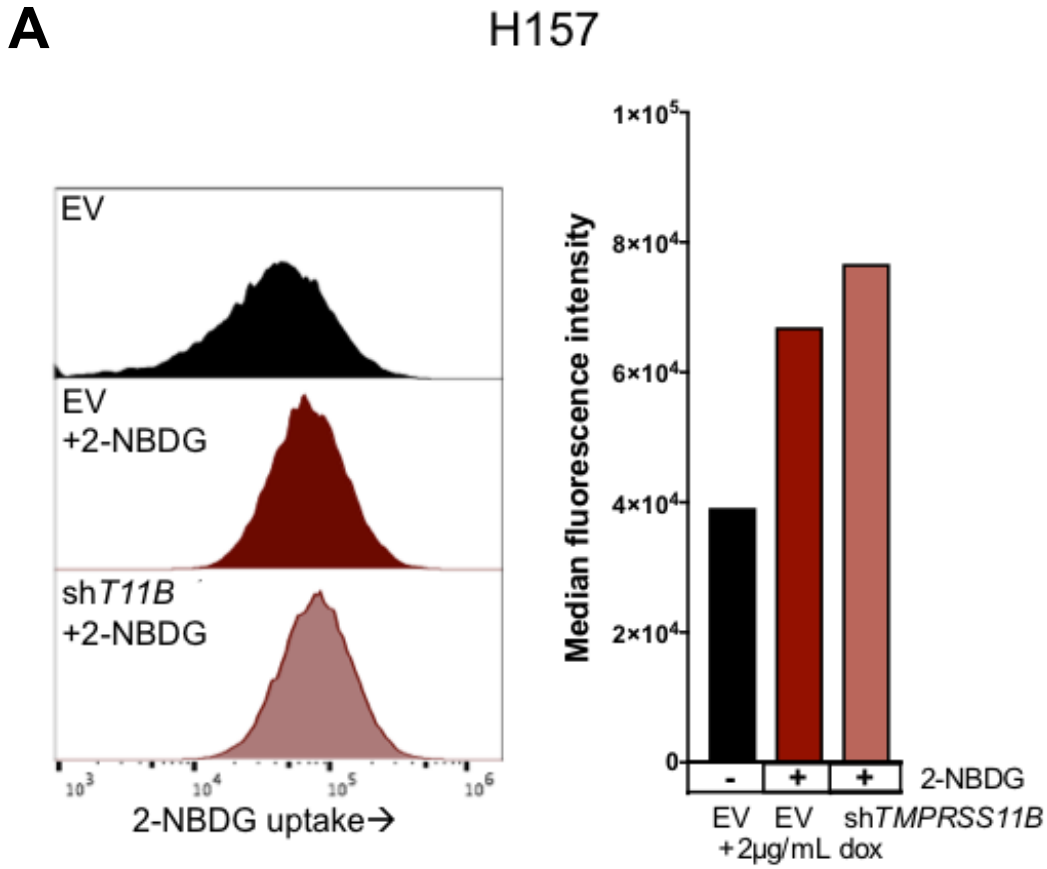

Figure 44: TMPRSS11B depletion does not affect glucose uptake in LSCC line H157. A) Flow cytometry quantitation of 2-NBDG uptake in H157 cells harboring doxycycline-inducible shRNA control or shRNA targeting TMPRSS11B treated for 3 days with doxycycline in culture media. EV: empty vector control.

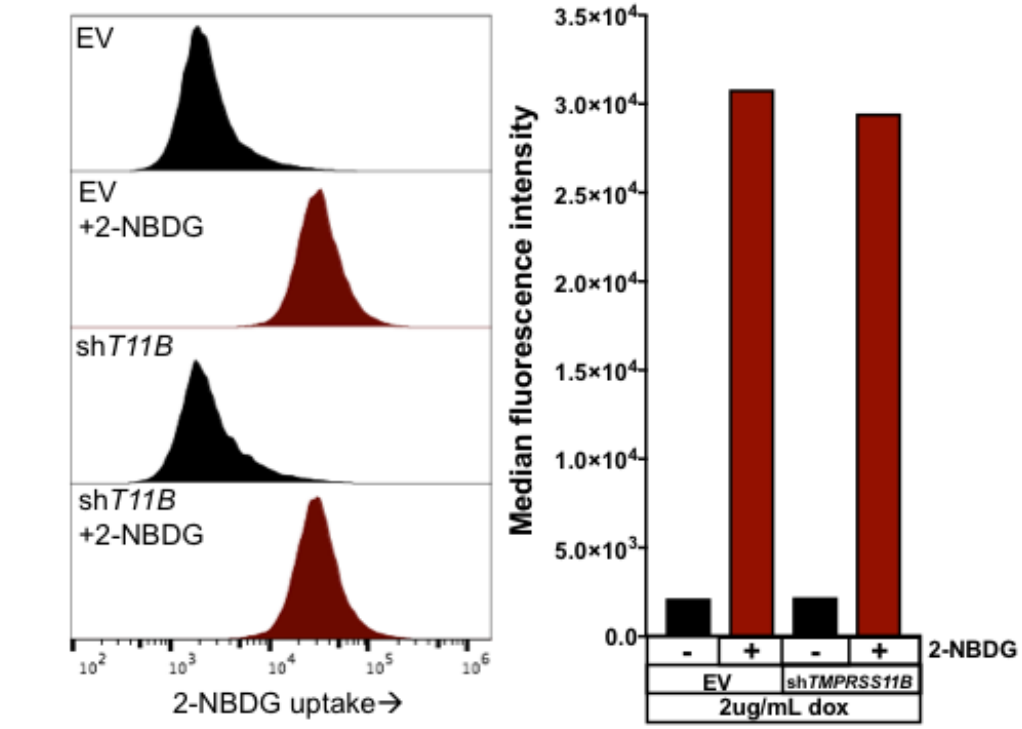

Figure 45: TMPRSS11B depletion does not affect glucose uptake in LSCC line HCC2814. A) Flow cytometry quantitation of 2-NBDG uptake in HCC2814 cells harboring doxycycline-inducible shRNA control or shRNA targeting TMPRSS11B treated for 3 days with doxycycline in culture media. EV: empty vector control.

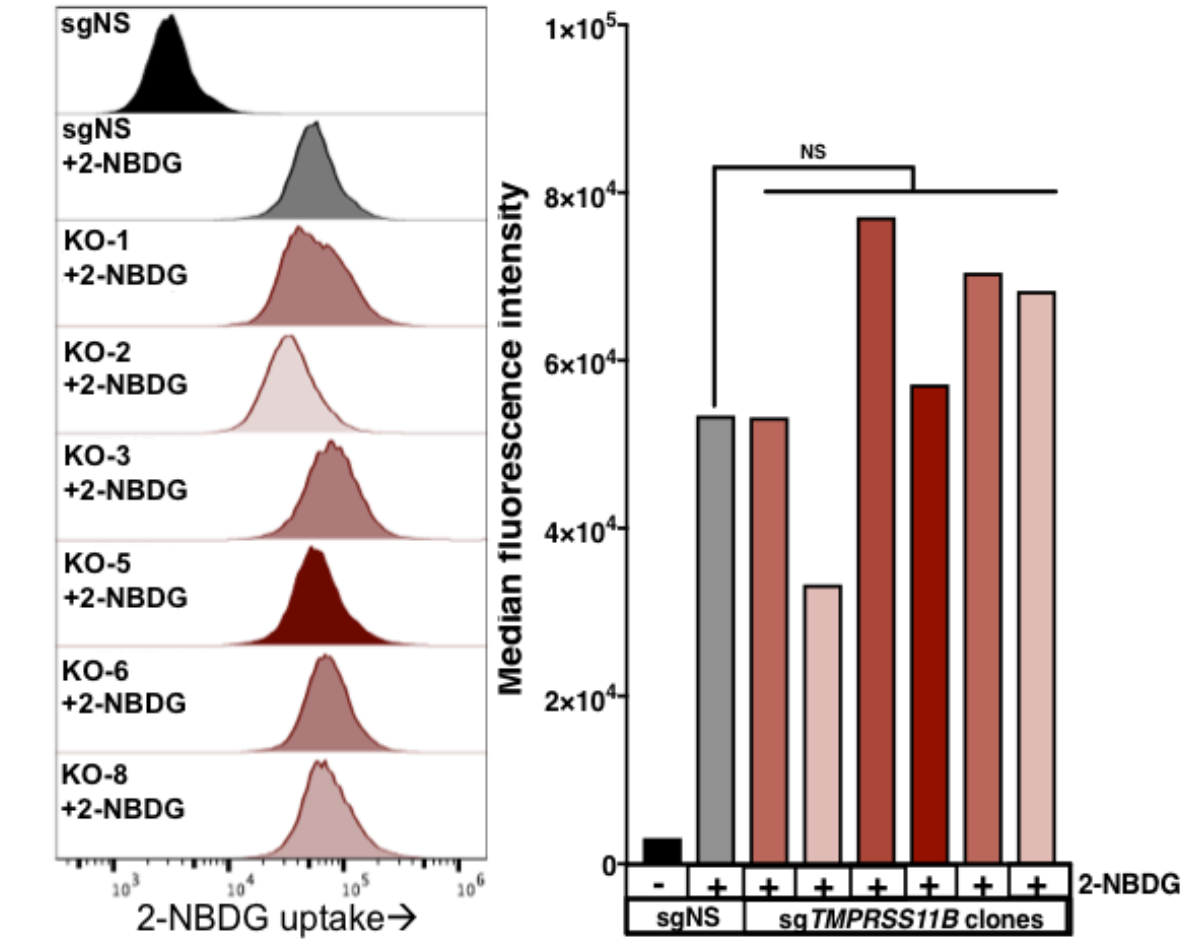

Figure 46: TMPRSS11B depletion does not affect glucose uptake in LSCC line HCC2814. A) Flow cytometry quantitation of 2-NBDG uptake in HCC2814 cells edited with CRISPR/Cas9 with control non-targeting sgRNA (sgNS) or sgRNA targeting *TMPRSS11B*. Values represent independent edited clones.

To further monitor the metabolic consequences of TMPRSS11B inhibition, we performed [1,6-^{13}C]glucose tracing in HCC2814 cells with shRNA-mediated TMPRSS11B knockdown and observed a modest reduction in lactate^{m+1} export (**Figure 47)** in the same cells in which we documented significant accumulation of steady state intracellular lactate (**Figure 37A**). Overall, our findings suggest that TMPRSS11B in LSCC enhances tumorigenesis by facilitating lactate export.

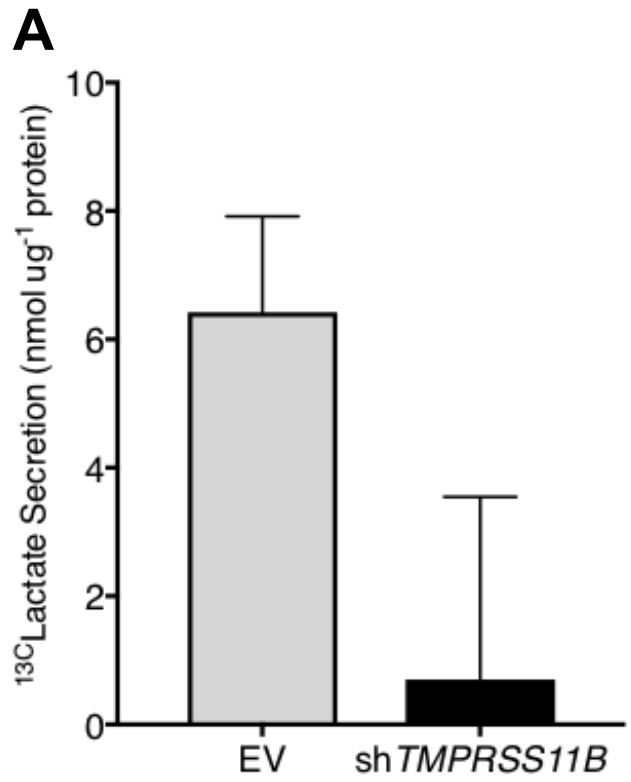

Figure 47: TMPRSS11B depletion modestly, but not significantly, results in reduced labeled lactate secretion. A) HCC2814 cells harboring doxycycline-inducible shRNA control or shRNA targeting TMPRSS11B were treated for 3 days with doxycycline in culture media. The morning of the experiment, cells were washed and exchanged into glucose-free media with [1,6-^{13}C]glucose added. Samples of culture media were taken at 15 minutes and labeled metabolites were assessed through GC-MS.

We determined whether expression of *TMPRSS11B* or its other family members correlated with lactate secretion in cultured human lung SCCs. Rates of lactate secretion were measured in a panel of non-small cell lung cancer cell lines, including 12 cell lines derived from LSCC. The lactate secretion rate was then correlated with transcript abundance for each of the TMPRSS11 family members. Interestingly, TMPRSS11B mRNA, but none of the other TMPRSS11 family members, positively correlated with lactate secretion (**Figure 48**), suggesting TMPRSS11B acts non-redundantly to enhance lactate secretion.

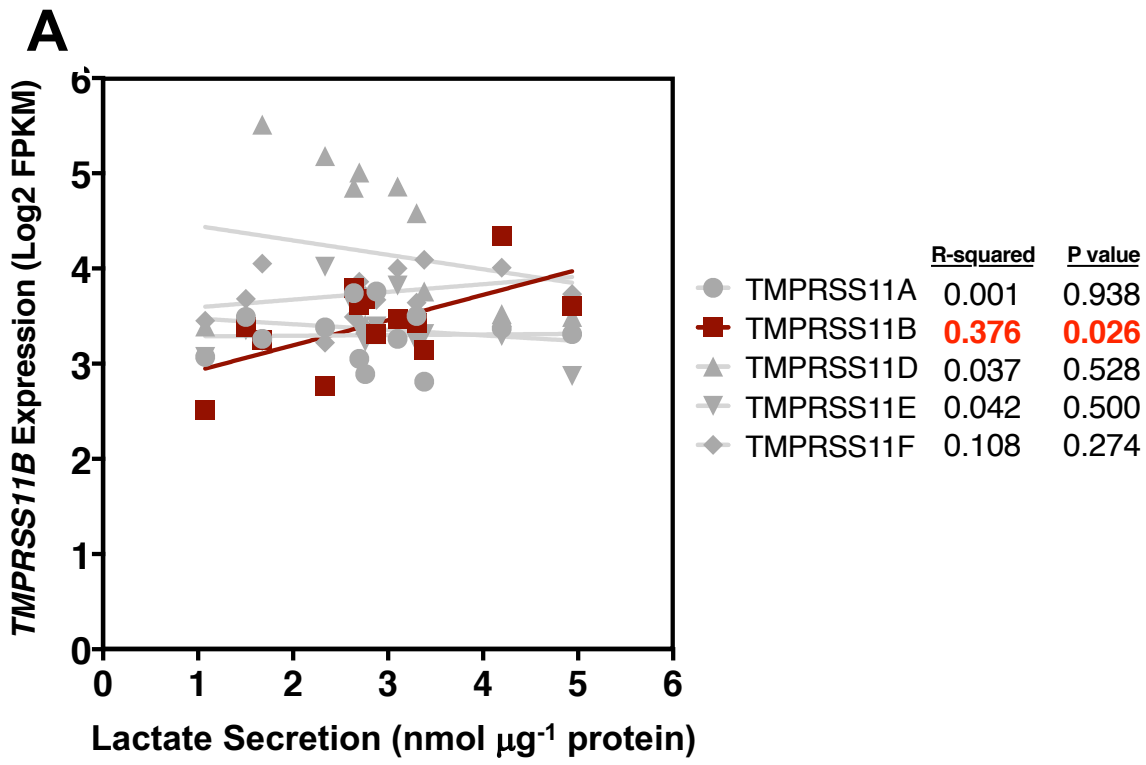

Figure 48: mRNA expression of *TMPRSS11B*, and not other TMPRSS11 family members, is positively correlated with lactate secretion in culture. A) TMPRSS11 mRNA expression curated from John Minna's lab (y-axis) was plotted against lactate secretion in culture (x-axis) of 12 LSCC cell lines. Human TMPRSS11 family members include TMPRSS11A, TMPRSS11B, TMPRSS11D, TMPRSS11E, and TMPRSS11F. mRNA of *TMPRSS11B*, but no other TMPRSS11 family members was significantly positively correlated with lactate secretion. Linear regression and goodness of fit analysis.

TMPRSS11B promotes expression of genes in glucose-handling pathways

RNA-sequencing (RNA-seq) was used to further assess the cellular consequences of TMPRSS11B gain-of-function (GOF, HBEC-shp53-GFP vs HBEC-shTP53-TMPRSS11B) and loss-of-function (LOF, HCC2814-EV and HCC2814-sh*TMPRSS11B*). In TMPRSS11B overexpressing cells, DAVID pathway analysis of significantly up-regulated genes retrieved metabolic pathways as the top hit ($P<0.05$, FDR<0.1, **Figure 49**). We also assessed levels of transcripts in pathways involved in glucose metabolism. This revealed subtle yet consistent up-regulation of genes involved in glucose uptake, glycolysis, Pentose phosphate pathway (PPP), and TCA cycle following TMPRSS11B overexpression, and down-regulation of these pathways following TMPRSS11B loss-of-function (**Figure 50**). This poses the intriguing possibility that enhanced lactate export also induces a transcriptional program favoring a metabolic shift towards aerobic glycolysis and that this may function to bolster the proliferative capacity of cells. This agrees with earlier studies demonstrating that depletion of MCT4, Basigin, or both induces lactate accumulation and slows glycolytic flux (Marchiq et al., 2015).

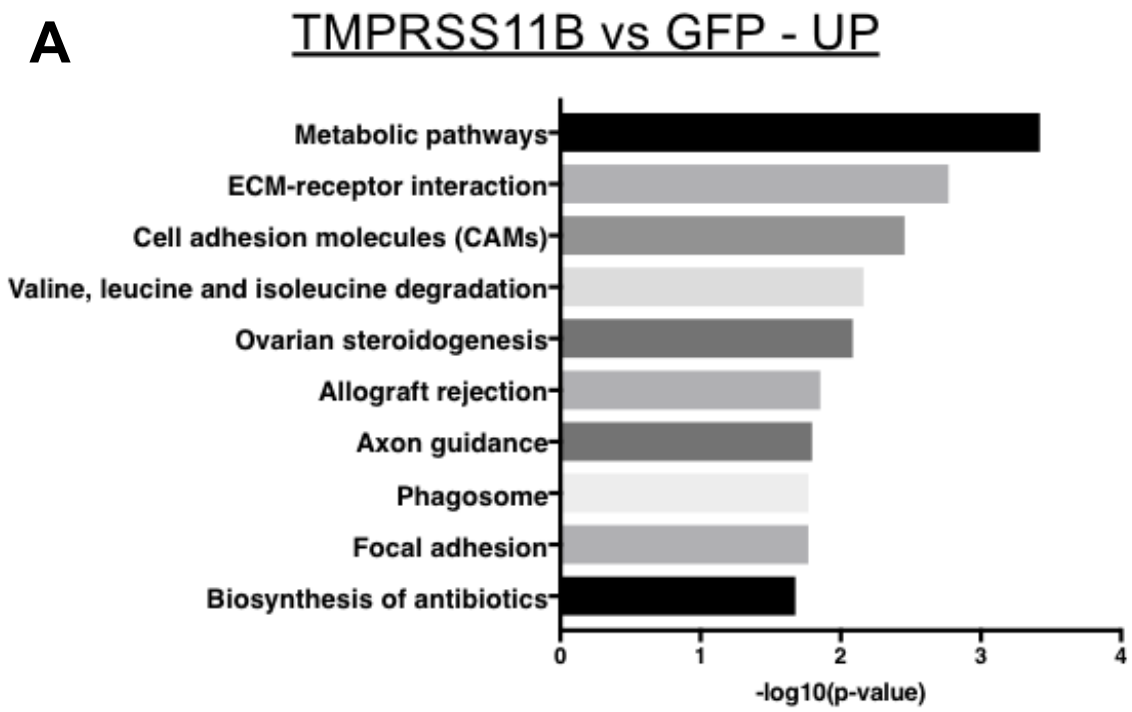

Figure 49: Overexpression of TMPRSS11B results in up-regulation of metabolic pathways. A) DAVID analysis of common pathways of differentially expressed (increased) genes from RNAseq of HBEC-shp53 cells stably expressing control GFP or TMPRSS11B. Differentially expressed genes were defined by $P<0.05$ and FDR <0.1.

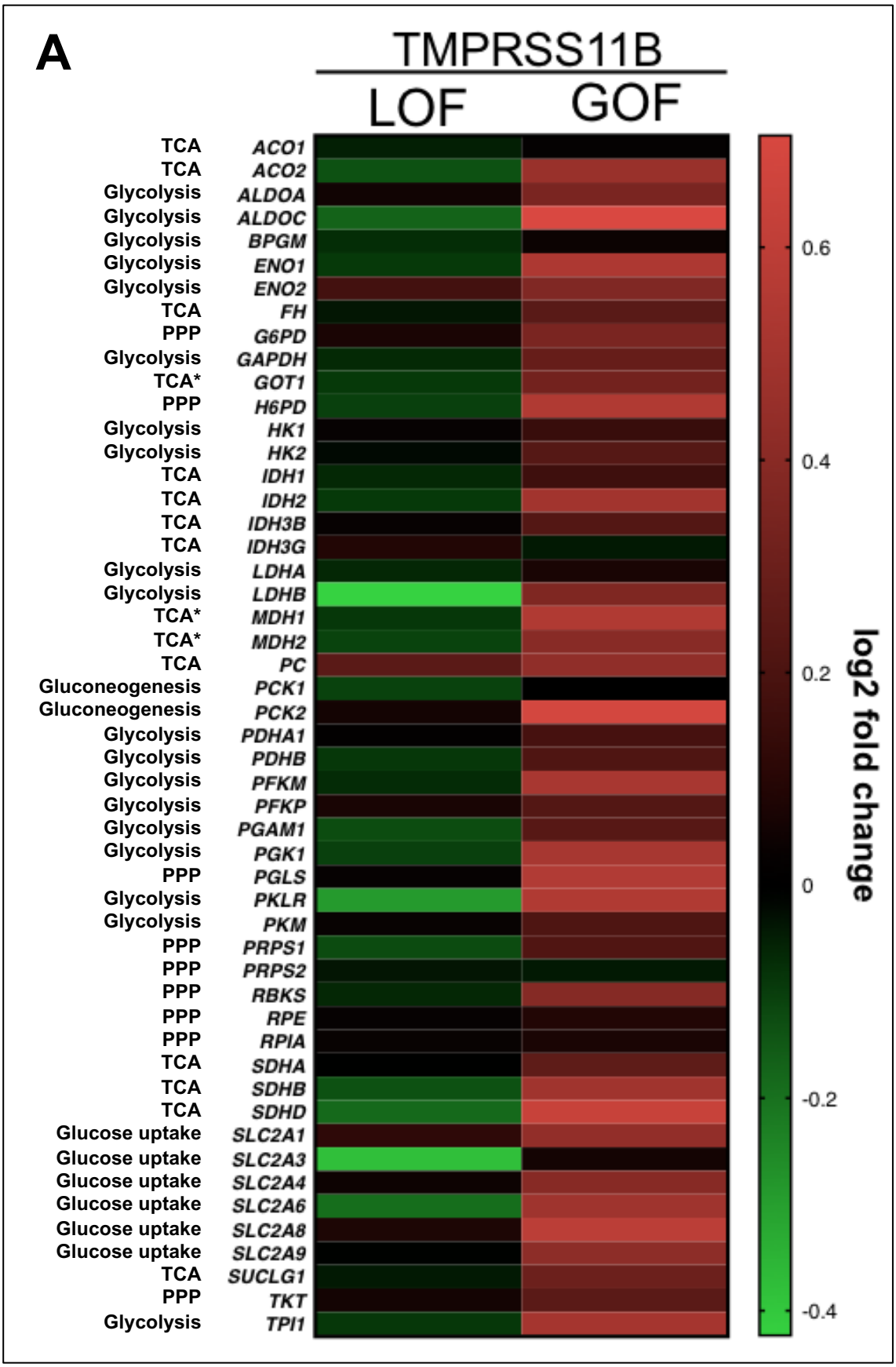
A
TMPRSS11B
LOF
GOF
TCA ACO1
TCA ACO2
Glycolysis ALDOA
Glycolysis ALDOC
Glycolysis BPGM
Glycolysis ENO1
Glycolysis ENO2
TCA FH
PPP G6PD
Glycolysis GAPDH
TCA* GOT1
PPP H6PD
Glycolysis HK1
Glycolysis HK2
TCA IDH1
TCA IDH2
TCA IDH3B
TCA IDH3G
Glycolysis LDHA
Glycolysis LDHB
TCA* MDH1
TCA* MDH2
TCA PC
Gluconeogenesis PCK1
Gluconeogenesis PCK2
Glycolysis PDHA1
Glycolysis PDHB
Glycolysis PFKM
Glycolysis PFKP
Glycolysis PGAM1
Glycolysis PGK1
PPP PGLS
Glycolysis PKLR
Glycolysis PKM
PPP PRPS1
PPP PRPS2
PPP RBKS
PPP RPE
PPP RPIA
TCA SDHA
TCA SDHB
TCA SDHD
Glucose uptake SLC2A1
Glucose uptake SLC2A3
Glucose uptake SLC2A4
Glucose uptake SLC2A6
Glucose uptake SLC2A8
Glucose uptake SLC2A9
TCA SUCLG1
PPP TKT
Glycolysis TPI1
0.6
0.4
0.2
0
-0.2
-0.4
log2 fold change

Figure 50: Modulation of TMPRSS11B expression affects transcripts involved in glucose handling. A) RNAseq differential expression analysis of LOF (left column, HCC2814 cells harboring shRNA control or shRNA targeting TMPRSS11B) and GOF (right column, HBEC-shp53 cells with either control GFP or TMPRSS11B expression). The metabolic pathways these transcripts belong to are in the far left text column.

Chapter VI: Discussion and future directions

Discussion

To identify new genes that promote transformation of human bronchial epithelial cells, we performed an unbiased forward genetic screen and identified putative oncogenes and tumor suppressors relevant to lung cancer pathogenesis. We were particularly interested in cell surface proteins since they may represent therapeutic targets that are accessible to antibody-based therapies. These efforts revealed that overexpression of the transmembrane serine protease TMPRSS11B promotes transformation in this system. TMPRSS11B is highly expressed in lung SCC tumors and is associated with poor clinical outcomes. TMPRSS11B overexpression induced cellular transformation *in vitro*, while depletion of TMPRSS11B reduced the tumor growth of LSCC and prostate cancer cells in mice, supporting an oncogenic function for this protein in tumorigenesis. Our mechanistic studies support a model whereby TMPRSS11B interacts with and promotes Basigin solubilization, resulting in enhanced MCT4-mediated lactate export. Consequently, this increased glycolytic flux and tumor growth (**Figure 51**). These results, coupled with the fact that TMPRSS11B is an enzyme localized to the cell membrane, raise the possibility that this protein may be targeted with novel therapeutic antibodies or small molecules in LSCC and other malignancies. Moreover, these findings further our understanding of the function and regulation of Basigin, a protein that is known to act as an essential chaperone for cell surface expression of the lactate transporters MCT1 and MCT4.

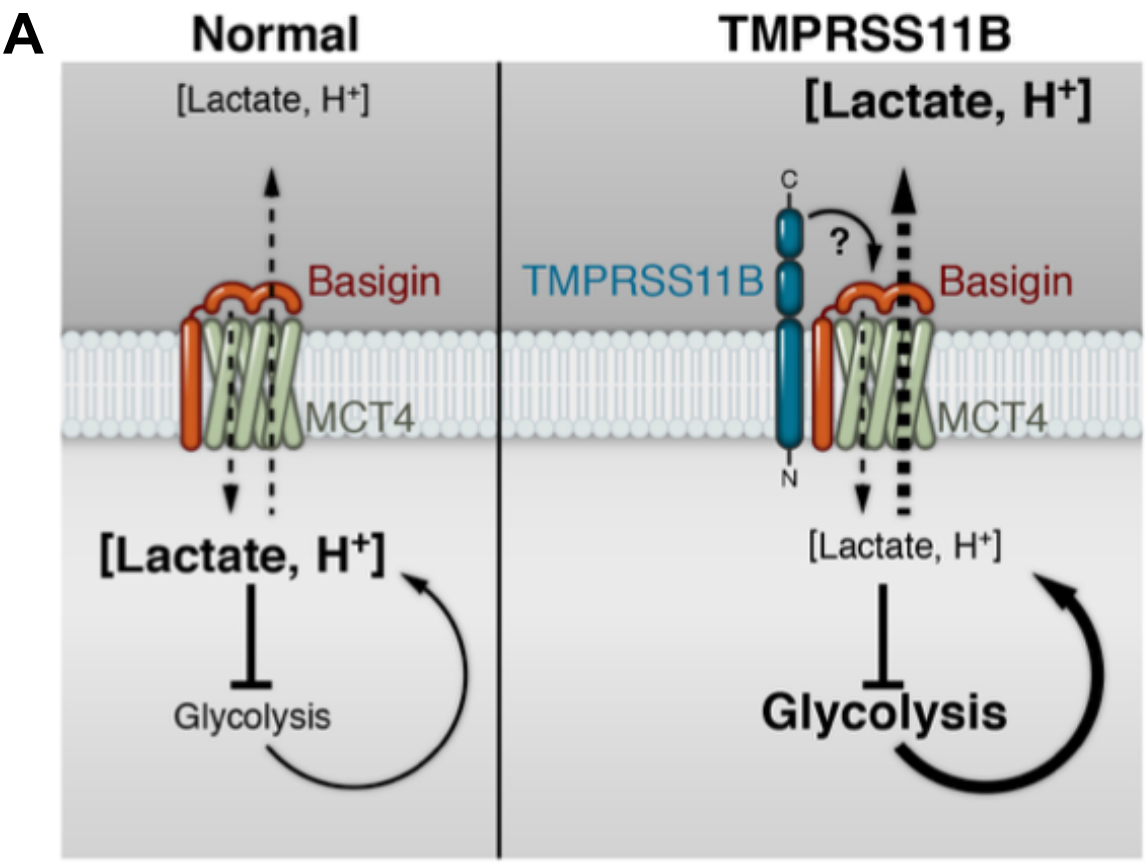

Figure 51: TMPRSS11B enhances lactate export and glycolysis. A) Schematic of potential mechanism of TMPRSS11B promoted lactate export through modulation of Basigin/MCT4.

Recent studies have demonstrated that human lung tumors as well as a majority of healthy tissues in the body utilize circulating lactate to fuel TCA cycle oxidation, suggesting that glycolytic flux is uncoupled from TCA cycle flux at the level of pyruvate reduction to lactate, and importantly that enhancing lactate secretion may fuel cellular respiration non-autonomously (Hui et al., 2017, Faubert et al., 2017). Moreover, clinical progression of post-operative NSCLC patients correlated with tumor lactate uptake and oxidation, in a manner dependent on MCT1 in experimental NSCLC tumors (Faubert et al., 2017). These findings underscore the importance of investigating mechanisms of lactate transport in order to develop novel therapies that target this process.

TMPRSS11B may regulate Basigin through multiple possible non-mutually-exclusive mechanisms including direct proteolytic cleavage as well as enhanced Basigin secretion. Consistent with the latter possibility, MCT4 and Basigin have been found in secreted vesicles purified from the sera of prostate cancer patients and in conditioned media of human ovarian and breast carcinoma cell lines (Gallagher et al., 2007, Millimaggi et al., 2007, Yoshioka et al., 2014). Interestingly, metabolic profiling of exosomal vesicles isolated from prostate cancer patients revealed higher concentrations of lactate than any other metabolite measured (Zhao et al., 2016). Additionally, flux analysis in cultured cells revealed substantial rates of labeled lactate secretion via exosomes and uptake of exosomal lactate by recipient cells (Achreja et al., 2017). This raises the intriguing possibility of vesicular export of lactate, where the pH gradient between cytosol and golgi secretory compartments, along with the topological orientation of Basigin and MCT4, would favor the import of lactate into vesicles (Achreja et al., 2017, Zhao et al., 2016). Moreover, Basigin-decorated vesicles are subject to

regulated endosomal recycling through clathrin-independent endocytosis (Maldonado-Baez et al., 2013). Our data demonstrating reduced plasma membrane localization of Basigin upon TMPRSS11B loss-of-function is also consistent with this hypothesis. Nevertheless, proteolysis is likely a key component of the relevant TMPRSS11B mechanism given our data demonstrating the reduced transforming activity and Basigin solubilization by TMPRSS11B catalytic mutants. Thus, while our findings have uncovered a previously unrecognized TMPRSS11B-Basigin regulatory interaction that is crucial for lactate metabolism and secretion in cancer cells, important mechanistic questions remain for future investigation.

Our study expands our understanding of the metabolic alterations that contribute to tumor progression in LSCC. Yet, the mechanism by which TMPRSS11B is upregulated in LSCC is currently unknown. In a mouse model of LSCC with homozygous deletion of *Pten* and *Stk11* (Lkb1), the mouse ortholog of *TMPRSS11B*, *Tmprss11bnl*, is among the top 20 up-regulated genes in tumors, hinting at a conserved mechanism of tumor metabolic regulation (Xu et al., 2014). Notably, physiologic TMPRSS11B expression is largely restricted to cervical and esophageal tissue (Consortium, 2013), but highly upregulated in LSCC and other squamous cell carcinomas (Gao et al., 2013), while Basigin and MCT4 are expressed highly throughout the body in tissues such as erythrocytes, brain, skeletal muscle, and activated immune populations. This suggests that therapies targeting TMPRSS11B may be more specific to tumor cells and result in fewer side effects and less toxicity compared to Basigin or MCT4 inhibitors (Halestrap and Price, 1999). Additional studies are warranted to identify substrates of TMPRSS11B in both physiologic and

pathophysiologic settings. Given that this cell surface protein is also an enzyme, small molecules or antibodies directed against the site of catalysis may be developed to inhibit TMPRSS11B function in future studies.

Future directions and perspectives

These studies leave many questions unanswered but warrant further investigation into lactate biology in LSCC. Interestingly, in addition to enhancing glycolytic ECAR, overexpression of TMPRSS11B significantly enhanced the oxygen consumption rate (OCR) in HBEC-shp53 cells (**Figure 52**), consistent with a recent report demonstrating that transported lactate contributes to the TCA cycle carbon pool more than pyruvate directly derived from glycolysis (Faubert et al., 2017). However, direct evidence supporting this mechanism in cultured cells is lacking.

We have conducted preliminary labeling studies *in vivo* in mice harboring xenografted HCC2814 LSCC cells with or without knockdown of TMPRSS11B. Infusion of [U-^{13}C]glucose in anaesthetized mice demonstrated that depletion of TMPRSS11B resulted modest, but not significant, increases in intratumoral labeled lactate relative to the upstream glycolytic metabolite 3PG (**Figure 53**). This result suggests that TMPRSS11B depletion either (i) results in accumulation of labeled lactate due to defects in lactate export, as we have documented in these cells in culture previously (**Figure 37A**), or (ii) there is enhanced import of labeled lactate in these tumors, which has been shown to rely on MCT1 in NSCLC. In future studies, we plan to perform labeling experiments to dissect these two distinct possibilities. Faubert *et al.* used a unique strategy of co-infusion of labeled lactate and glucose to dissect their contributions to the TCA cycle. By co-infusion of lactate and glucose labeled at distinct

carbons, such as [1,6-^{13}C]glucose and [U-^{13}C]lactate, the fate of these distinct carbon pools can be traced in LSCC tumors. Performing this experiment with or without TMPRSS11B depletion would yield insight into lactate handling *in vivo* and contribute to our knowledge of the role TMPRSS11B plays in regulating lactate metabolism.

Additional preliminary studies of lactate homeostasis suggest that MCT1 contributes significantly to basal lactate export in LSCC and is essential for lactate export upon loss of MCT4 (**Figure 54**). All LSCC lines tested tolerated the loss of MCT4, whereas combined inhibition of MCT1 in these cells resulted in massive accumulation of intracellular lactate. This suggests that although MCT1 is thought to mediate import of lactate, it also facilitates basal lactate export that is exacerbated upon MCT4 loss. The means through which MCT1 activity is enhanced upon MCT4 depletion are unknown, but total levels of MCT1 protein are unaffected by MCT4 depletion suggesting alternative modes of regulation (**Figure 55**). Interestingly, MCT4 depletion resulted in Basigin depletion in three of the four lines tested, consistent with previous reports of MCT4 regulating Basigin protein stability (Le Floch et al., 2011). Importantly, our study demonstrated that depletion of TMPRSS11B alone resulted in lactate accumulation, revealing a novel regulator of cellular lactate levels. These studies will support our understanding of lactate homeostasis in cancer and the therapeutic opportunities targeting this process.

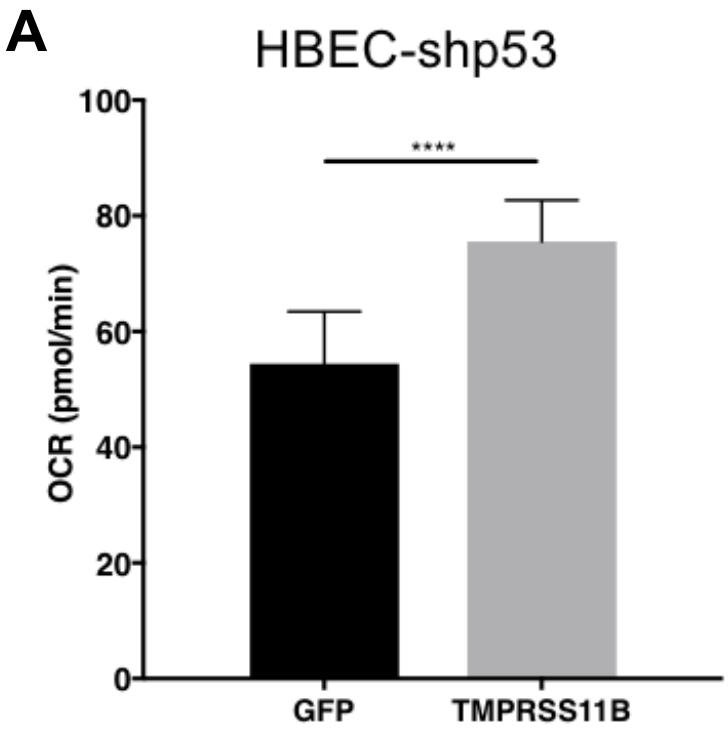

Figure 52: Overexpression of TMPRSS11B enhances oxygen consumption rate of cells in culture. A) SeaHorse OCR analysis of HBEC-shp53 cells expressing control GFP or TMPRSS11B. Unpaired t-test; ****P<0.0001.

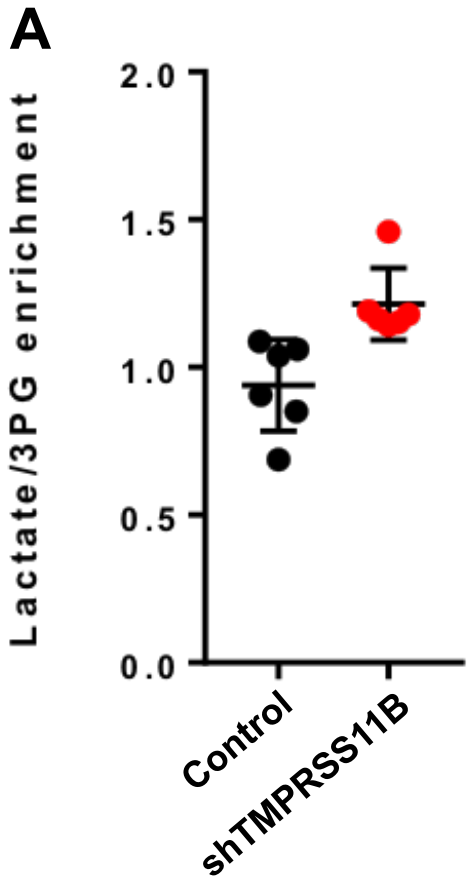

Figure 53: TMPRSS11B depletion in LSCC xenografts results in enhanced levels of intracellular labeled lactate relative to the upstream glycolytic metabolite 3PG. A) NSG mice xenografted with HCC2814 cells harboring inducible shRNA control or shRNA targeting TMPRSS11B were given doxycycline in drinking water when tumors reached ~100mm^3 (**Figure 8B**). Two weeks after the addition of doxycycline to drinking water, mice were infused with [U-^{13}C]glucose for 90 minutes and tumors excised. N= 6; 3 tumors per group with 2 slices of tumor each.

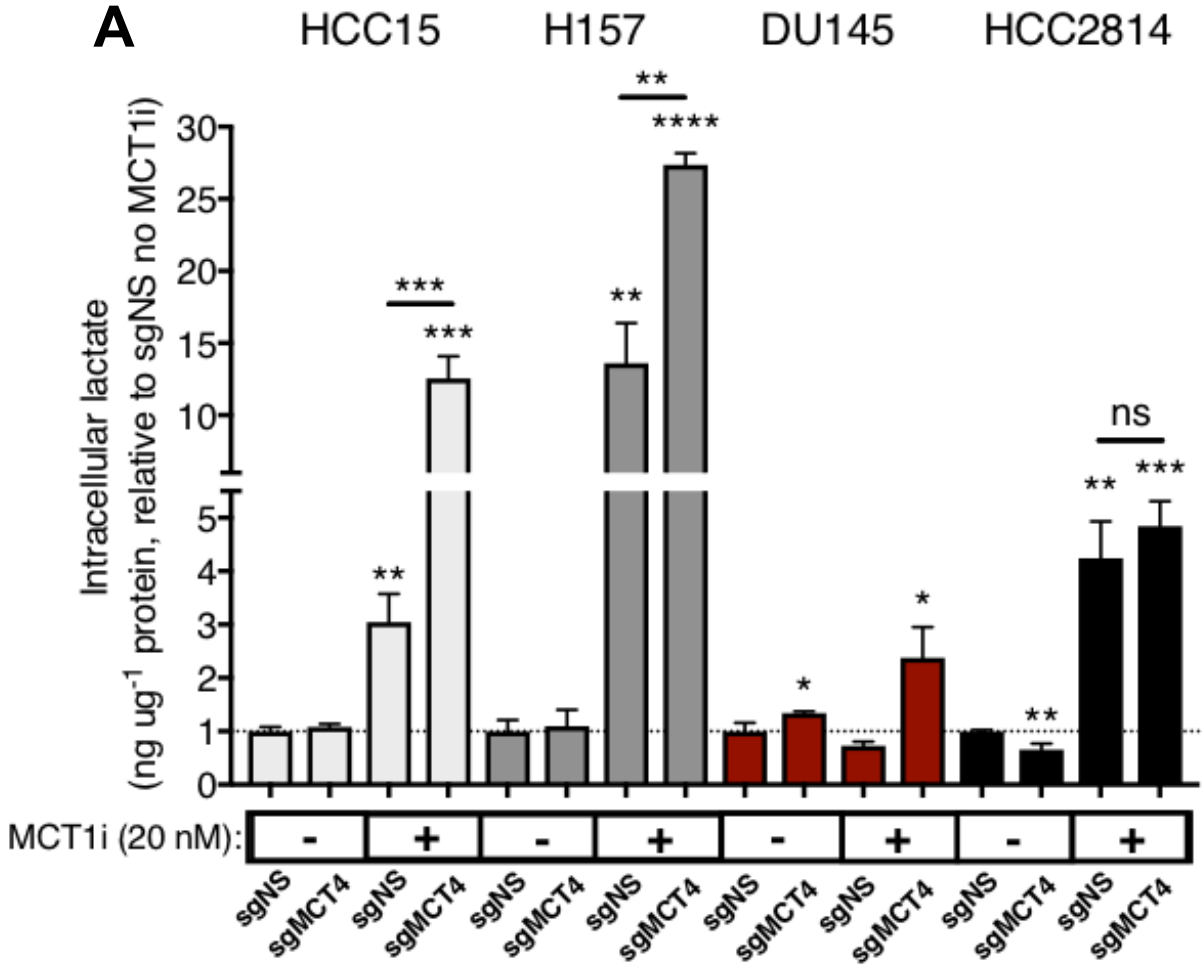

Figure 54: MCT1 and MCT4 differentially control intracellular lactate levels across cell lines. A) LSCC cell lines HCC15, H157, HCC2814, and the prostate cancer cell line DU145 were edited using CRISPR/Cas9 with control non-targeting sgRNA (sgNS) or sgRNA targeting *SLC16A3* (sgMCT4). Cells were cultured with or without the chemical MCT1-specific inhibitor SR13800 and intracellular lactate was measured. Unpaired t-test *P<0.05, **P< 0.01, ***P<0.001, ****P<0.0001.

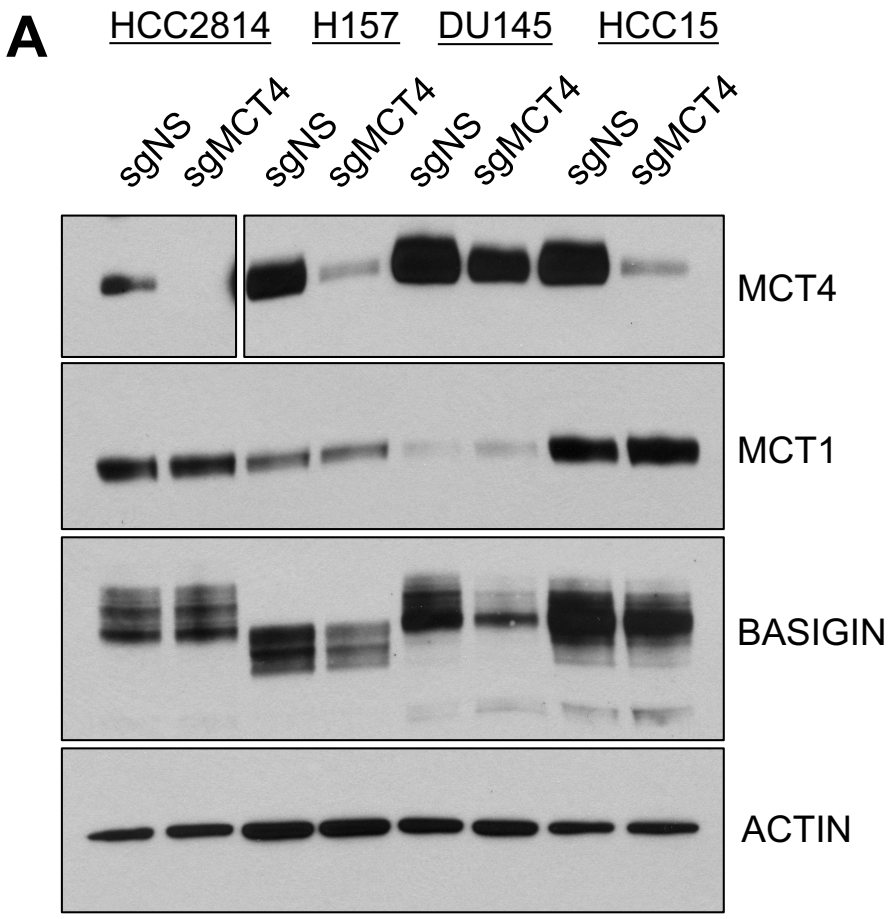

Figure 55: Depletion of MCT4 does not alter MCT1 protein levels. A) Western blot analysis of LSCC lines HCC2814, H157, and HCC15, and prostate cancer line DU145 edited with CRISPR/Cas9 with non-targeting sgRNA or sgRNA targeting *SLC16A3* (MCT4). Blots were probed with anti-MCT4, anti-MCT1, or anti-Basigin antibodies. Actin serves a loading control. MCT4 blot for HCC2814 was cropped to include a longer exposure, as these cells express low MCT4 levels compared to other cell lines.

A

Gene	CIS P value	Gene	CIS P value
EXOC6	8.45E-06	*CCNL1*	0.004069723
CYP26C1	8.45E-06	*SMIM15*	0.004248251
CYP26A1	8.45E-06	*ZSWIM6*	0.004248251
RGS18	0.000245546	*C5orf64*	0.004248251
RGS21	0.000245546	*ROCK1*	0.004387458
RGS1	0.000245546	*GREB1L*	0.004387458
RGS13	0.000245546	* *TMPRSS11B*	0.005900657
EMB	0.00054237	* *TMPRSS11GP*	0.005900657
BMP2K	0.000657361	* *TMPRSS11F*	0.005900657
PAQR3	0.000657361	*LOC550113*	0.005900657
LOC100505875	0.000657361	*SYT14L*	0.005900657
NAA11	0.000657361	*FTLP10*	0.005900657
GK2	0.000657361	* *TMPRSS11BNL*	0.005900657
LOC100506035	0.000657361	*SLITRK1*	0.006405077
NPR3	0.000692233	*DDX60*	0.007237188
LOC340113	0.000692233	*DDX60L*	0.007237188
CDC42SE2	0.001015549	*PALLD*	0.007237188
RAPGEF6	0.001015549	*TASP1*	0.007334725
FNIP1	0.001015549	*ESF1*	0.007334725
LOC100505718	0.00150855	*NDUFAF5*	0.007334725
ARHGEF38	0.001596982	*SEL1L2*	0.007334725
INTS12	0.001596982	*MACROD2*	0.007334725
GSTCD	0.001596982	*TEC*	0.007788812
NPNT	0.001596982	*SLAIN2*	0.007788812
TBCK	0.001596982	*SLC10A4*	0.007788812
AIMP1	0.001596982	*ZAR1*	0.007788812
HCN1	0.001846958	*FRYL*	0.007788812
LOC100270679	0.002760328	*OCIAD1*	0.007788812
GRIA1	0.002896929	*RNA5SP411*	0.007834733
CAPN14	0.002958095	*FLJ26245*	0.007834733
EHD3	0.002958095	*NXN*	0.0083968
XDH	0.002958095	*TIMM22*	0.0083968
SRD5A2	0.002958095	*LINC00861*	0.008636996
CDH6	0.003180157	*EYA1*	0.008826594
DGKB	0.00333133	*RAB28*	0.008903939
LOC389831	0.003894066	*LOC285547*	0.008903939
MRPS30	0.003968062	*NKX3-2*	0.008903939
SKP1P2	0.004007362	*LOC285548*	0.008903939
TIPARP-AS1	0.004069723	*BOD1L1*	0.008903939
TIPARP	0.004069723	*MIR5091*	0.008903939
LOC730091	0.004069723	*KCTD8*	0.00917654
PA2G4P4	0.004069723	*KCTD16*	0.009217926
LEKR1	0.004069723	*PELO*	0.009251797
LOC339894	0.004069723	*ITGA1*	0.009251797
LOC100498859	0.004069723	*ITGA2*	0.009251797

Appendix table 1: CIS genes identified through transposon mutagenesis. A) Common insertion site genes identified in an HBEC-shp53 *Sleeping Beauty* transposon mutagenesis screen. Asterisks represent TMPRSS11 family members.

Chapter 7: Materials and methods

Primers

Sequencing primers:

TMPRSS11B sgRNA-1 cut site

F: 5'-GATGACCTCAGATTTGACA-3'

R: 5'-AGGTATAAATGGATTATTTCT-3'

TMPRSS11B sgRNA-2 cut site

F: 5'- CCATGAGTTTAATGGAAGCAG-3'

R: 5'- AGCACATCTGAACTAGACG-3'

Mycoplasma testing

F: 5'-TGCACCATCTGTCACTCTGTTAACCTC-3'

R: 5'-GGGAGCAAACAGGATTAGATACCCT-3'

CRISPR/Cas9 sgRNA (PAM underlined)

TMPRSS11B sgRNA-1

gDNA: AAGCAAAGATATTGAGACTAAGG

TMPRSS11B sgRNA-2

gDNA: TAACTGCACATTTGAACCATTGG

SLC16A3 (MCT4) sgRNA

gDNA: CTCACCTGTCCCGTAGAGCATGG

BSG (Basigin) sgRNA-1

gDNA: GTCGTCAGAACACATCAACGAGG

BSG (Basigin) sgRNA-2

gDNA: AGAGTCAGTGATCTTGTACCAGG

shRNA

pTRIPZ shRNA

TMPRSS11B shRNA target: GGCAUCUUGUUGGAAUAGUAAG

RT-qPCR TaqMan probes

TMPRSS11B-1	Hs01113515_m1
TMPRSS11B-2	Hs00699337_m1
BSG	Hs00936295_m1
GAPDH	Hs03929097_g1

Tissue culture and cell lines

Lung squamous cell cancers (HCC95, HCC1313, HCC1588, HCC2814, and H157), lung adenocarcinoma (H2073), and prostate cancer (DU145) cells were cultured in ATCC-formulated RPMI-1640 with 5% FBS and antibiotic-antimycotic (Invitrogen). Human bronchial epithelial cells (HBEC-shp53) and all derivatives were cultured in keratinocyte serum-free media (KSFM) with antibiotic-antimycotic and supplied supplements (Ramirez et al., 2004). All cell lines used in this study were cultured in 5% CO_2 at 37C and tested negative for mycoplasma contamination.

[1,6-^{13}C]glucose tracing

3x10^5 HCC2814 cells with control or *TMPRSS11B* shRNA were plated in 6-well plates, cultured overnight, and exchanged into glucose- and bicarbonate-free RPMI-1640 with 4.5g/L [1,6-^{13}C]glucose and 2g/L $NaHCO_3$ added. Small aliquots of media were taken at t=0, 5m, 15m, 30m, and 60m after media exchange, clarified of debris, and stored at -80C. At the last time point, cells were washed on ice in cold saline

solution, scraped into 50% methanol, and transferred to -80C for subsequent analysis. We used a previously described GC-MS protocol (DeNicola et al., 2015) with the aforementioned culture conditions. Cells were lysed in RIPA to determine protein content, and lactate secretion rates were determined by normalizing the lactate abundance in the medium to cellular protein in each well. For *in vivo* labeling, anaesthetized mice harboring xenografted HCC2814 tumors expressing either shRNA control or shRNA targeting TMPRSSS11B were infused with [U-^{13}C]glucose for 90 minutes, animals were sacrificed, and tumors excised and snap-frozen in liquid nitrogen. Two independent tumor fragments were taken per tumor and homogenized. GC-MS prep was performed similarly to that of above.

Lentivirus and plasmids

TMPRSS11B^{D270N} and TMPRSS11B^{S366A} mutant constructs were generated with Phusion site-directed mutagenesis (ThermoFisher) of IOH35719 (pENTR221, Invitrogen Ultimate ORF collection). TMPRSS11B, GFP, or mCherry were cloned into pLX303 (25897 and 25890, Addgene) using Gateway LR clonase II (Invitrogen, Cat. No. 11791100). For *BSG* and *SLC16A3* knock-out, sgRNAs were cloned into pLentiCRISPRv2 modified to express GFP. Single GFP^{+} cells were sorted into 96-well plates and expanded for further study. For Basigin rescue experiments, Basigin (IOH3378, Invitrogen Ultimate ORF collection) was modified by site-directed mutagenesis to introduce synonymous mutations to sgRNA binding residues at +2, +6, and +9nt from the PAM and cloned into pLX308 (pLX304 modified to express mCherry instead of a Blast^{R} cassette) using Gateway LR clonase II. Following transduction mCherry+ cells were collected by FACS. For *TMPRSS11B* knock-out, sgRNAs were

cloned into pLentiCRISPRv2-Puro. TMPRSS11B-specific shRNA was cloned into pTRIPZ (Dharmacon, Cat. No. RHS4696**).**

All vectors were packaged in 293T by co-transfection with packaging plasmids pMD2 (Addgene,12259) and psPAX2 (Addgene,12260). Conditioned media was taken 48 and 72 hours post transfection, clarified of cells and debris, concentrated with Lenti-X following the manufacturer's protocol (Clontech, Cat. No. 631231), and resuspended in Hank's balanced salt solution (HBSS) (Invitrogen, Cat. No. 14175095). Recipient cells were transduced in the presence of 8μg/mL hexadimethrine bromide for ~5-8 hours. Transduced cells were selected with the following:

Lentiviral Construct	Selection
pLX303	Blasticidin (2-5 μg/mL)
pLX304	Blasticidin (2-5 μg/mL)
pLX308	mCherry^{+} FACS with Aria II
pLentiCRISPRv2-Puro	Puromycin (1.5-3 μg/mL)
pLentiCRISPRv2-GFP	GFP^{+} FACS in Aria II
pTRIPZ	Puromycin (1.5-3 μg/mL)

Lactate assays

Cells were washed twice in cold HBSS- and scraped on ice. Following centrifugation at 1,500 RPM for 5m at 4°C, cells were resuspended in 500μL Lactate Assay Buffer (Sigma, Cat. No. MAK064) and acoustically lysed in a BioRuptor for 20m of 1m on/off sonication on high at 4°C. Insoluble material was pelleted at 14,000xg for

5m and supernatant transferred to Amicon Ultra 0.5mL 10K MWCO columns and centrifuged at 14,000xg for 20m to remove endogenous lactate dehydrogenase. Undiluted filtrate was analyzed according to the manufacturer's protocol.

Seahorse XFe96 assays

$1.5*10^4$ HBEC cells were plated in a Seahorse XFe 96-well culture plate in KSFM. Glucose, oligomycin, and SR13800 (or DMSO) were loaded into injection wells of an XFe96 cartridge to achieve final concentrations of 10mM, 2μM, and 5nM, respectively. At the start of the experiment, cells were washed and exchanged into L-15 media without glucose or bicarbonate and run through 4 cycles of 3min mix / 3min measure per injectant, with the latter 3 measurements being used for data analysis and representation. Bicarbonate- and glucose-free Dulbecco's modified eagle media (DMEM) yielded similar results.

Xenograft assays

Cells were trypsinized, counted, resuspended in HBSS-, and injected subcutaneously at 4-5 x 10^6 cells per flank onto both flanks of 4-6-week-old female NOD/SCID Il2rγ$^-$ (NSG) mice. For inducible shRNA experiments, 2g/L doxycycline hyclate (Sigma, Cat. No. D9891) and 1.5% w/v sucrose was supplied in drinking water *ad libitum*. Tumors were measured every 3-4 days using digital calipers in two perpendicular directions with width measurements being the smaller of the two measurements. Tumor volume was calculated with the formula: volume (mm^3) = (length*(width^2))/2. At the end of the experiment, mice were euthanized and excised tumors photographed. Tumor fragments were stored in 10% neutral buffered formalin

or snap-frozen in liquid nitrogen. *TMPRSS11B* CRISPR clone 3 was used for tumorigenesis experiments shown in Figure 1H.

RT-qPCR

Cells with inducible shRNA were cultured in 2μg/mL dox for >3 days with fresh dox added every 2 days. Cells were washed in cold HBSS-, scraped on ice into HBSS-, and centrifuged at 1,500RPM for 5m at 4C. Cell pellets were resuspended in 600μL RLT buffer with fresh β-mercaptoethanol, vortexed, transferred to a QiaShredder column, and centrifuged at max speed for 2m at 4C. RNA was then extracted according to the RNeasy protocol (Qiagen) with on-column DNase digest and resuspended in 50μL nuclease-free H_2O. RNA (1μg) served as template for reverse transcription with SuperScript IV VILO (Invitrogen, Cat. No. 11756050). TaqMan probes (Invitrogen) corresponding to *TMPRSS11B* (Hs01113515 m1 and Hs00699337 m1), *BSG* (Hs00936295_m1), and *GAPDH* (Hs03929097) were used to detect transcripts in 384-well format, and expression calculating using the 2^{ddCt} method.

2-NBDG uptake assay

Cells were washed in warm HBSS- and exchanged into glucose- and bicarbonate-free RPMI1640 media with 5% FBS, antibiotic-antimycotic, 2g/L $NaHCO_3$, +/- 50μM 2-NBDG (Fisher, Cat. No. N13195). After incubation for 30m at 37C, cells were washed twice in warm HBSS-, trypsinized, resuspended in cold FACS buffer, and 2-NBDG uptake was assessed using a BD Accuri benchtop flow cytometer in the FL-1 channel.

sReceptor Proteome Profiler Array

Conditioned media was taken from 75% confluent HBEC-shp53-GFP and HBEC-shp53-TMPRSS11B cells, debris pellet at 1,500xg for 10m, and supernatant used as substrate for the immobilized antibody array following the manufacturer's protocol (119 factors, sReceptor Proteome Profiler, R&D Systems, Cat. No. ARY012). Developed arrays were scanned and pixel density was quantitated using ImageJ software.

Basigin ELISA

For quantitation of Basigin in conditioned media, media was taken and clarified of cells and debris by pelleting at 1,500xg for 10m. HALT protease and phosphatase inhibitor cocktail (ThermoFisher**,** Cat. No. 78443) was added to the supernatant and assayed immediately according to the manufacturer's protocol (R&D systems, Human EMMPRIN/CD147 Quantikine ELISA kit, Cat. No. DEMP00). For cellular Basigin quantitation, cells were washed in cold HBSS- after conditioned media collection, scraped on ice into HBSS-, and cells pelleted at 1,500RPM for 5m at 4C. Cell pellets were resuspended in non-denaturing lysis buffer (LB-17, R&D systems) with protease/phosphatase inhibitors and acoustically lysed using a BioRuptor Plus (Diagenode**)** at 1m on/off sonication cycle for 20m on high at 4°C. Insoluble material was pelleted at 14,000xg for 5m at 4°C and supernatant transferred to a clean tube for immediate analysis according to the manufacturer's protocol. Basigin solubilization was calculated as ([soluble Basigin] / [cellular Basigin]).

Western blotting

Cells were washed and scraped on ice into HBSS-, pelleted at 1,500 RPM for 5m at 4C, and resuspended in LB-17 with HALT protease and phosphatase inhibitor

cocktail (ThermoFisher, Cat. No. 78443) Cells were acoustically ruptured in a Bioruptor for 15m of 1m on/off on high, or in some instances lysed using a QiaShredder column. Insoluble material was pelleted at 14,000xg for 5m at 4C and supernatant was transferred to a clean tube. Protein concentration of samples was determined by BCA assay (23227, ThermoFisher). 10-30μg total protein was combined with 4X LDS loading buffer (NP0008, ThermoFisher) and 10X reducing agent (B0009, ThermoFisher), heated to 70C for 10m, and loaded into 4-12% or 10% polyacrylamide SDS gels. Electrophoresed protein was transferred to nitrocellulose membranes using semi-dry transfer (iBlot II, Invitrogen) then blocked and probed in TBST with 5% w/v milk. A detailed list of antibodies used in this study is found below.

Immunofluorescence and confocal microscopy

Cells were seeded in 6-well plates with UV-sterilized glass coverslips. Cells were washed in PBS and fixed with 4% paraformaldehyde in PBS for 20 min. at room temperature. Cells were washed 3x10 minutes in PBS, blocked with 2%BSA in PBS for 1 hour at room temperature, and then incubated with primary antibodies (1:100 dilution) at 4°C overnight. Cells were washed 3x10 minutes in PBS and incubated in Alexa Flour-conjugated secondary antibodies (CST, 1:500 dilution; Anti-Mouse Alexa Flour 488, Anti-Mouse Alexa Flour 594, Anti-Rabbit Alexa Flour 488, Anti-Rabbit Alexa Flour 594 and Anti-Rat Alexa Flour 647) in 2%BSA in PBS for 2 hours at room temperature. Coverslips with cells were mounted on Superfrost®Plus microscope slides (Fisher) with VECTASHIELD hard set mounting media with DAPI (Vector Labs). All images were captured using a ZEISS confocal microscope LSM-700.

Antibodies

Antibody Target	Catalog No.	Company	Use
Basigin/CD147	13287S	CST	WB
Basigin/CD147	MAB2623	Millipore	WB, IP
Basigin/CD147	ab119114	Abcam	IP, IF
Basigin/CD147	ab666	Abcam	IP
Basigin/CD147	MA1-10103	ThermoFisher	IP
beta-actin	4970S	CST	WB
HA	3724S	CST	WB
HA	H3663	Sigma	IP
MCT1	sc-365501	SCBT	WB
MCT4	HPA021451	Sigma	WB, IP, IF
MCT4	sc-376140	SCBT	WB
tubulin	ab7291	Abcam	WB
V5	R960-25	ThermoFisher	WB, IP
V5	13202S	CST	WB, IP

RNA sequencing

Cells were plated in triplicate in 15cm^2 dishes and allowed to reach 70% confluence. Cells were then washed in cold HBSS- twice and scraped on ice into HBSS-. Cells were pelleted at 1,500RPM for 5m at 4C and resuspended in 600μL RLT buffer with fresh β-mercaptoethanol, vortexed, transferred to a QiaShredder column, and centrifuged at max speed for 2m at 4C. RNA was then extracted according to the RNeasy protocol (Qiagen) with on-column DNase digest and resuspended in 50μL nuclease-free H_2O. Samples were run on the Agilent 2100 Bioanalyzer to evaluate RNA quality and were quantified by Qubit (Invitrogen) prior to staring library prep. Four micrograms of total DNAse treated RNA were prepared with the TruSeq Stranded Total

RNA LT Sample Prep Kit from Illumina. Poly-A RNA was purified and fragmented before strand specific cDNA synthesis. cDNA were A-tailed and indexed adapters were ligated. Samples were then PCR amplified and purified with AmpureXP beads, and validated again on the Agilent 2100 Bioanalyzer. Sequencing was performed on an Illumina NextSeq 500 to generate 76-bp single-ended reads.

RNA-seq analysis methods

Fastq files were checked for quality using fastqc (http://www.bioinformatics.babraham.ac.uk/projects/fastqc) and fastq screen (http://www.bioinformatics.babraham.ac.uk/projects/fastq_screen) and were quality trimmed using fastq-mcf (Aronesty, 2013). Trimmed fastq files were mapped to hg19 (UCSC version from igenomes) using TopHat (Kim and Salzberg, 2011), duplicates were marked using picard-tools (https://broadinstitute.github.io/picard/), read counts were generated using featureCounts (Liao et al., 2014) and differential expression analysis was performed using edgeR (Robinson et al., 2010). RNAseq data has been deposited to the National Center for Biotechnology Information (NCBI) GEO repository, http://www.ncbi.nlm.nih.gov/geo/ (Accession #GSE114850).

Acknowledgments

We thank the co-authors of the submitted manuscript described in this dissertation: Xiaorong Zhou, Yabin Guo, Mahesh S. Padanad, Pei-Hsuan Chen, Chendong Yang, Jessica Sudderth, Carla Rodriguez-Tirado, Luc Girard, John D. Minna, Prashant Mishra, Ralph J. DeBerardinis, and Kathryn A. O'Donnell. We also thank the McDermott Center Sequencing and Bioinformatics Cores for sequencing and analysis, Jose Cabrera for assistance with the model schematic in **Figure 51**, and Joshua Mendell and members of the O'Donnell laboratory for critical reading of the manuscript submitted to Cell Reports. Brandon Faubert assisted with the *in vivo* glucose labeling. We thank a summer undergraduate research fellow, Helena Hopson, for her help with experiments involving MCT4 knock-out in LSCC and prostate cancer lines. B.L.U. was supported by CPRIT (RP140110) and NIH Award (T32GM008203).

References

ACHREJA, A., ZHAO, H., YANG, L., YUN, T. H., MARINI, J. & NAGRATH, D. 2017. Exo-MFA - A 13C metabolic flux analysis framework to dissect tumor microenvironment-secreted exosome contributions towards cancer cell metabolism. *Metab Eng,* 43**,** 156-172.

ALTAMURA, S., D'ALESSIO, F., SELLE, B. & MUCKENTHALER, M. U. 2010. A novel TMPRSS6 mutation that prevents protease auto-activation causes IRIDA. *Biochem J,* 431**,** 363-71.

ARENDT, B. K., WALTERS, D. K., WU, X., TSCHUMPER, R. C. & JELINEK, D. F. 2014. Multiple myeloma dell-derived microvesicles are enriched in CD147 expression and enhance tumor cell proliferation. *Oncotarget,* 5**,** 5686-99.

ARONESTY, E. 2013. Comparison of Sequencing Utility Programs. *The Open Bioinformatics Journal,* 7**,** 1-8.

BABITT, J. L., HUANG, F. W., WRIGHTING, D. M., XIA, Y., SIDIS, Y., SAMAD, T. A., CAMPAGNA, J. A., CHUNG, R. T., SCHNEYER, A. L., WOOLF, C. J., ANDREWS, N. C. & LIN, H. Y. 2006. Bone morphogenetic protein signaling by hemojuvelin regulates hepcidin expression. *Nat Genet,* 38**,** 531-9.

BALABAN, R. S. 1990. Regulation of oxidative phosphorylation in the mammalian cell. *Am J Physiol,* 258**,** C377-89.

BANKS, R. D., BLAKE, C. C., EVANS, P. R., HASER, R., RICE, D. W., HARDY, G. W., MERRETT, M. & PHILLIPS, A. W. 1979. Sequence, structure and activity of phosphoglycerate kinase: a possible hinge-bending enzyme. *Nature,* 279**,** 773-7.

BARRETINA, J., CAPONIGRO, G., STRANSKY, N., VENKATESAN, K., MARGOLIN, A. A., KIM, S., WILSON, C. J., LEHAR, J., KRYUKOV, G. V., SONKIN, D., REDDY, A., LIU, M., MURRAY, L., BERGER, M. F., MONAHAN, J. E., MORAIS, P., MELTZER, J., KOREJWA, A., JANE-VALBUENA, J., MAPA, F. A., THIBAULT, J., BRIC-FURLONG, E., RAMAN, P., SHIPWAY, A., ENGELS, I. H., CHENG, J., YU, G. K., YU, J., ASPESI, P., JR., DE SILVA, M., JAGTAP, K., JONES, M. D., WANG, L., HATTON, C., PALESCANDOLO, E., GUPTA, S., MAHAN, S., SOUGNEZ, C., ONOFRIO, R. C., LIEFELD, T., MACCONAILL, L., WINCKLER, W., REICH, M., LI, N., MESIROV, J. P., GABRIEL, S. B., GETZ, G., ARDLIE, K., CHAN, V., MYER, V. E., WEBER, B. L., PORTER, J., WARMUTH, M., FINAN, P., HARRIS, J. L., MEYERSON, M., GOLUB, T. R., MORRISSEY, M. P., SELLERS, W. R., SCHLEGEL, R. & GARRAWAY, L. A. 2012. The Cancer Cell Line Encyclopedia enables predictive modelling of anticancer drug sensitivity. *Nature,* 483**,** 603-7.

BASS, A. J., WATANABE, H., MERMEL, C. H., YU, S., PERNER, S., VERHAAK, R. G., KIM, S. Y., WARDWELL, L., TAMAYO, P., GAT-VIKS, I., RAMOS, A. H., WOO, M. S., WEIR, B. A., GETZ, G., BEROUKHIM, R., O'KELLY, M., DUTT, A., ROZENBLATT-ROSEN, O., DZIUNYCZ, P., KOMISAROF, J., CHIRIEAC, L. R., LAFARGUE, C. J., SCHEBLE, V., WILBERTZ, T., MA, C., RAO, S., NAKAGAWA, H., STAIRS, D. B., LIN, L., GIORDANO, T. J., WAGNER, P., MINNA, J. D., GAZDAR, A. F., ZHU, C. Q., BROSE, M. S., CECCONELLO, I., RIBEIRO, U., JR., MARIE, S. K., DAHL, O., SHIVDASANI, R. A., TSAO, M. S., RUBIN, M. A., WONG, K. K., REGEV, A., HAHN, W. C., BEER, D. G., RUSTGI, A. K. & MEYERSON, M.

2009. SOX2 is an amplified lineage-survival oncogene in lung and esophageal squamous cell carcinomas. *Nat Genet,* 41**,** 1238-42.

BAUER, D. E., HATZIVASSILIOU, G., ZHAO, F., ANDREADIS, C. & THOMPSON, C. B. 2005. ATP citrate lyase is an important component of cell growth and transformation. *Oncogene,* 24**,** 6314-22.

BEAUFORT, N., LEDUC, D., EGUCHI, H., MENGELE, K., HELLMANN, D., MASEGI, T., KAMIMURA, T., YASUOKA, S., FEND, F., CHIGNARD, M. & PIDARD, D. 2007. The human airway trypsin-like protease modulates the urokinase receptor (uPAR, CD87) structure and functions. *Am J Physiol Lung Cell Mol Physiol,* 292**,** L1263-72.

BENSAAD, K., TSURUTA, A., SELAK, M. A., VIDAL, M. N., NAKANO, K., BARTRONS, R., GOTTLIEB, E. & VOUSDEN, K. H. 2006. TIGAR, a p53-inducible regulator of glycolysis and apoptosis. *Cell,* 126**,** 107-20.

BIRSOY, K., WANG, T., CHEN, W. W., FREINKMAN, E., ABU-REMAILEH, M. & SABATINI, D. M. 2015. An Essential Role of the Mitochondrial Electron Transport Chain in Cell Proliferation Is to Enable Aspartate Synthesis. *Cell,* 162**,** 540-51.

BISWAS, B., BATISTA, F., SUNDARAM, S. & STANLEY, P. 2018. MGAT1 and Complex N-Glycans Regulate ERK Signaling During Spermatogenesis. *Sci Rep,* 8**,** 2022.

BLOW, D. 2000. So do we understand how enzymes work? *Structure,* 8**,** R77-81.

BONEN, A. 2001. The expression of lactate transporters (MCT1 and MCT4) in heart and muscle. *Eur J Appl Physiol,* 86**,** 6-11.

BRISSON, L., BANSKI, P., SBOARINA, M., DETHIER, C., DANHIER, P., FONTENILLE, M. J., VAN HEE, V. F., VAZEILLE, T., TARDY, M., FALCES, J., BOUZIN, C.,

PORPORATO, P. E., FREDERICK, R., MICHIELS, C., COPETTI, T. & SONVEAUX, P. 2016. Lactate Dehydrogenase B Controls Lysosome Activity and Autophagy in Cancer. *Cancer Cell,* 30**,** 418-431.

BROER, S., SCHNEIDER, H. P., BROER, A., RAHMAN, B., HAMPRECHT, B. & DEITMER, J. W. 1998. Characterization of the monocarboxylate transporter 1 expressed in Xenopus laevis oocytes by changes in cytosolic pH. *Biochem J,* 333 (Pt 1)**,** 167-74.

BROSNAN, J. T. 2000. Glutamate, at the interface between amino acid and carbohydrate metabolism. *J Nutr,* 130**,** 988S-90S.

BRUNS, J. B., CARATTINO, M. D., SHENG, S., MAAROUF, A. B., WEISZ, O. A., PILEWSKI, J. M., HUGHEY, R. P. & KLEYMAN, T. R. 2007. Epithelial Na+ channels are fully activated by furin- and prostasin-dependent release of an inhibitory peptide from the gamma-subunit. *J Biol Chem,* 282**,** 6153-60.

BUGGE, T. H., ANTALIS, T. M. & WU, Q. 2009. Type II transmembrane serine proteases. *J Biol Chem,* 284**,** 23177-81.

CAHILL, G. F., JR., ASHMORE, J., EARLE, A. S. & ZOTTU, S. 1958. Glucose penetration into liver. *Am J Physiol,* 192**,** 491-6.

CAMERER, E., BARKER, A., DUONG, D. N., GANESAN, R., KATAOKA, H., CORNELISSEN, I., DARRAGH, M. R., HUSSAIN, A., ZHENG, Y. W., SRINIVASAN, Y., BROWN, C., XU, S. M., REGARD, J. B., LIN, C. Y., CRAIK, C. S., KIRCHHOFER, D. & COUGHLIN, S. R. 2010. Local protease signaling contributes to neural tube closure in the mouse embryo. *Dev Cell,* 18**,** 25-38.

CANCER GENOME ATLAS RESEARCH, N. 2012. Comprehensive genomic characterization of squamous cell lung cancers. *Nature,* 489**,** 519-25.

CARLING, D., CLARKE, P. R., ZAMMIT, V. A. & HARDIE, D. G. 1989. Purification and characterization of the AMP-activated protein kinase. Copurification of acetyl-CoA carboxylase kinase and 3-hydroxy-3-methylglutaryl-CoA reductase kinase activities. *Eur J Biochem,* 186**,** 129-36.

CHECCONI, P., SALZANO, S., BOWLER, L., MULLEN, L., MENGOZZI, M., HANSCHMANN, E. M., LILLIG, C. H., SGARBANTI, R., PANELLA, S., NENCIONI, L., PALAMARA, A. T. & GHEZZI, P. 2015. Redox proteomics of the inflammatory secretome identifies a common set of redoxins and other glutathionylated proteins released in inflammation, influenza virus infection and oxidative stress. *PLoS One,* 10**,** e0127086.

CHEN, Y. J., MAHIEU, N. G., HUANG, X., SINGH, M., CRAWFORD, P. A., JOHNSON, S. L., GROSS, R. W., SCHAEFER, J. & PATTI, G. J. 2016. Lactate metabolism is associated with mammalian mitochondria. *Nat Chem Biol,* 12**,** 937-943.

CHIARUGI, A., DOLLE, C., FELICI, R. & ZIEGLER, M. 2012. The NAD metabolome--a key determinant of cancer cell biology. *Nat Rev Cancer,* 12**,** 741-52.

CHRISTOFK, H. R., VANDER HEIDEN, M. G., HARRIS, M. H., RAMANATHAN, A., GERSZTEN, R. E., WEI, R., FLEMING, M. D., SCHREIBER, S. L. & CANTLEY, L. C. 2008. The M2 splice isoform of pyruvate kinase is important for cancer metabolism and tumour growth. *Nature,* 452**,** 230-3.

CLEMENTS, J., HOOPER, J., DONG, Y. & HARVEY, T. 2001. The expanded human kallikrein (KLK) gene family: genomic organisation, tissue-specific expression and potential functions. *Biol Chem,* 382**,** 5-14.

COMMISSO, C., DAVIDSON, S. M., SOYDANER-AZELOGLU, R. G., PARKER, S. J., KAMPHORST, J. J., HACKETT, S., GRABOCKA, E., NOFAL, M., DREBIN, J. A., THOMPSON, C. B., RABINOWITZ, J. D., METALLO, C. M., VANDER HEIDEN, M. G. & BAR-SAGI, D. 2013. Macropinocytosis of protein is an amino acid supply route in Ras-transformed cells. *Nature,* 497**,** 633-7.

CONSORTIUM, G. T. 2013. The Genotype-Tissue Expression (GTEx) project. *Nat Genet,* 45**,** 580-5.

CORI, G. T., SLEIN, M. W. & CORI, C. F. 1948. Crystalline d-glyceraldehyde-3-phosphate dehydrogenase from rabbit muscle. *J Biol Chem,* 173**,** 605-18.

CURRIE, E., SCHULZE, A., ZECHNER, R., WALTHER, T. C. & FARESE, R. V., JR. 2013. Cellular fatty acid metabolism and cancer. *Cell Metab,* 18**,** 153-61.

DANG, C. V. & SEMENZA, G. L. 1999. Oncogenic alterations of metabolism. *Trends Biochem Sci,* 24**,** 68-72.

DAVIES, S. P., CARLING, D. & HARDIE, D. G. 1989. Tissue distribution of the AMP-activated protein kinase, and lack of activation by cyclic-AMP-dependent protein kinase, studied using a specific and sensitive peptide assay. *Eur J Biochem,* 186**,** 123-8.

DAWSON, D. M., GOODFRIEND, T. L. & KAPLAN, N. O. 1964. Lactic Dehydrogenases: Functions of the Two Types Rates of Synthesis of the Two Major Forms Can Be Correlated with Metabolic Differentiation. *Science,* 143**,** 929-33.

DEBERARDINIS, R. J. 2011. Serine metabolism: some tumors take the road less traveled. *Cell Metab,* 14**,** 285-6.

DEBERARDINIS, R. J. & CHANDEL, N. S. 2016. Fundamentals of cancer metabolism. *Sci Adv,* 2**,** e1600200.

DEBERARDINIS, R. J., LUM, J. J., HATZIVASSILIOU, G. & THOMPSON, C. B. 2008. The biology of cancer: metabolic reprogramming fuels cell growth and proliferation. *Cell Metab,* 7**,** 11-20.

DEBERARDINIS, R. J., MANCUSO, A., DAIKHIN, E., NISSIM, I., YUDKOFF, M., WEHRLI, S. & THOMPSON, C. B. 2007. Beyond aerobic glycolysis: transformed cells can engage in glutamine metabolism that exceeds the requirement for protein and nucleotide synthesis. *Proc Natl Acad Sci U S A,* 104**,** 19345-50.

DENDEN, S., KHELIL, A. H., KNANI, J., LAKHDAR, R., PERRIN, P., LEFRANC, G. & CHIBANI, J. B. 2010. Alpha-1 antitrypsin gene polymorphism in Chronic Obstructive Pulmonary Disease (COPD). *Genet Mol Biol,* 33**,** 23-6.

DENICOLA, G. M., CHEN, P. H., MULLARKY, E., SUDDERTH, J. A., HU, Z., WU, D., TANG, H., XIE, Y., ASARA, J. M., HUFFMAN, K. E., WISTUBA, II, MINNA, J. D., DEBERARDINIS, R. J. & CANTLEY, L. C. 2015. NRF2 regulates serine biosynthesis in non-small cell lung cancer. *Nat Genet,* 47**,** 1475-81.

DENICOLA, G. M., KARRETH, F. A., HUMPTON, T. J., GOPINATHAN, A., WEI, C., FRESE, K., MANGAL, D., YU, K. H., YEO, C. J., CALHOUN, E. S., SCRIMIERI, F., WINTER, J. M., HRUBAN, R. H., IACOBUZIO-DONAHUE, C., KERN, S. E., BLAIR, I. A. & TUVESON, D. A. 2011. Oncogene-induced Nrf2 transcription promotes ROS detoxification and tumorigenesis. *Nature,* 475**,** 106-9.

DEPREZ, J., VERTOMMEN, D., ALESSI, D. R., HUE, L. & RIDER, M. H. 1997. Phosphorylation and activation of heart 6-phosphofructo-2-kinase by protein kinase B and other protein kinases of the insulin signaling cascades. *J Biol Chem,* 272**,** 17269-75.

DIETL, K., RENNER, K., DETTMER, K., TIMISCHL, B., EBERHART, K., DORN, C., HELLERBRAND, C., KASTENBERGER, M., KUNZ-SCHUGHART, L. A., OEFNER, P. J., ANDREESEN, R., GOTTFRIED, E. & KREUTZ, M. P. 2010. Lactic acid and acidification inhibit TNF secretion and glycolysis of human monocytes. *J Immunol,* 184**,** 1200-9.

DIMMER, K. S., FRIEDRICH, B., LANG, F., DEITMER, J. W. & BROER, S. 2000. The low-affinity monocarboxylate transporter MCT4 is adapted to the export of lactate in highly glycolytic cells. *Biochem J,* 350 Pt 1**,** 219-27.

DOGRULUK, T., TSANG, Y. H., ESPITIA, M., CHEN, F., CHEN, T., CHONG, Z., APPADURAI, V., DOGRULUK, A., ETEROVIC, A. K., BONNEN, P. E., CREIGHTON, C. J., CHEN, K., MILLS, G. B. & SCOTT, K. L. 2015. Identification of Variant-Specific Functions of PIK3CA by Rapid Phenotyping of Rare Mutations. *Cancer Res,* 75**,** 5341-54.

DOHERTY, J. R., YANG, C., SCOTT, K. E., CAMERON, M. D., FALLAHI, M., LI, W., HALL, M. A., AMELIO, A. L., MISHRA, J. K., LI, F., TORTOSA, M., GENAU, H. M., ROUNBEHLER, R. J., LU, Y., DANG, C. V., KUMAR, K. G., BUTLER, A. A., BANNISTER, T. D., HOOPER, A. T., UNSAL-KACMAZ, K., ROUSH, W. R. & CLEVELAND, J. L. 2014. Blocking lactate export by inhibiting the Myc target MCT1 Disables glycolysis and glutathione synthesis. *Cancer Res,* 74**,** 908-20.

DU, S., GUAN, Z., HAO, L., SONG, Y., WANG, L., GONG, L., LIU, L., QI, X., HOU, Z. & SHAO, S. 2014. Fructose-bisphosphate aldolase a is a potential metastasis-associated marker of lung squamous cell carcinoma and promotes lung cell tumorigenesis and migration. *PLoS One,* 9**,** e85804.

DU, X., SHE, E., GELBART, T., TRUKSA, J., LEE, P., XIA, Y., KHOVANANTH, K., MUDD, S., MANN, N., MORESCO, E. M., BEUTLER, E. & BEUTLER, B. 2008. The serine protease TMPRSS6 is required to sense iron deficiency. *Science,* 320**,** 1088-92.

DUPAGE, M., DOOLEY, A. L. & JACKS, T. 2009. Conditional mouse lung cancer models using adenoviral or lentiviral delivery of Cre recombinase. *Nat Protoc,* 4**,** 1064-72.

EAGLE, H. 1959. Amino acid metabolism in mammalian cell cultures. *Science,* 130**,** 432-7.

EICHNER, R., HEIDER, M., FERNANDEZ-SAIZ, V., VAN BEBBER, F., GARZ, A. K., LEMEER, S., RUDELIUS, M., TARGOSZ, B. S., JACOBS, L., KNORN, A. M., SLAWSKA, J., PLATZBECKER, U., GERMING, U., LANGER, C., KNOP, S., EINSELE, H., PESCHEL, C., HAASS, C., KELLER, U., SCHMID, B., GOTZE, K. S., KUSTER, B. & BASSERMANN, F. 2016. Immunomodulatory drugs disrupt the cereblon-CD147-MCT1 axis to exert antitumor activity and teratogenicity. *Nat Med,* 22**,** 735-43.

ELSTROM, R. L., BAUER, D. E., BUZZAI, M., KARNAUSKAS, R., HARRIS, M. H., PLAS, D. R., ZHUANG, H., CINALLI, R. M., ALAVI, A., RUDIN, C. M. & THOMPSON, C. B. 2004. Akt stimulates aerobic glycolysis in cancer cells. *Cancer Res,* 64**,** 3892-9.

FAN, J., HITOSUGI, T., CHUNG, T. W., XIE, J., GE, Q., GU, T. L., POLAKIEWICZ, R. D., CHEN, G. Z., BOGGON, T. J., LONIAL, S., KHURI, F. R., KANG, S. & CHEN, J. 2011. Tyrosine phosphorylation of lactate dehydrogenase A is important for NADH/NAD(+) redox homeostasis in cancer cells. *Mol Cell Biol,* 31**,** 4938-50.

FANTIN, V. R., ST-PIERRE, J. & LEDER, P. 2006. Attenuation of LDH-A expression uncovers a link between glycolysis, mitochondrial physiology, and tumor maintenance. *Cancer Cell,* 9**,** 425-34.

FAUBERT, B., BOILY, G., IZREIG, S., GRISS, T., SAMBORSKA, B., DONG, Z., DUPUY, F., CHAMBERS, C., FUERTH, B. J., VIOLLET, B., MAMER, O. A., AVIZONIS, D., DEBERARDINIS, R. J., SIEGEL, P. M. & JONES, R. G. 2013. AMPK is a negative regulator of the Warburg effect and suppresses tumor growth in vivo. *Cell Metab,* 17**,** 113-24.

FAUBERT, B., LI, K. Y., CAI, L., HENSLEY, C. T., KIM, J., ZACHARIAS, L. G., YANG, C., DO, Q. N., DOUCETTE, S., BURGUETE, D., LI, H., HUET, G., YUAN, Q., WIGAL, T., BUTT, Y., NI, M., TORREALBA, J., OLIVER, D., LENKINSKI, R. E., MALLOY, C. R., WACHSMANN, J. W., YOUNG, J. D., KERNSTINE, K. & DEBERARDINIS, R. J. 2017. Lactate Metabolism in Human Lung Tumors. *Cell,* 171**,** 358-371 e9.

FENG, J., YANG, H., ZHANG, Y., WEI, H., ZHU, Z., ZHU, B., YANG, M., CAO, W., WANG, L. & WU, Z. 2017. Tumor cell-derived lactate induces TAZ-dependent upregulation of PD-L1 through GPR81 in human lung cancer cells. *Oncogene*.

FISCHER, K., HOFFMANN, P., VOELKL, S., MEIDENBAUER, N., AMMER, J., EDINGER, M., GOTTFRIED, E., SCHWARZ, S., ROTHE, G., HOVES, S.,

RENNER, K., TIMISCHL, B., MACKENSEN, A., KUNZ-SCHUGHART, L., ANDREESEN, R., KRAUSE, S. W. & KREUTZ, M. 2007. Inhibitory effect of tumor cell-derived lactic acid on human T cells. *Blood,* 109**,** 3812-9.

GALLAGHER, S. M., CASTORINO, J. J., WANG, D. & PHILP, N. J. 2007. Monocarboxylate transporter 4 regulates maturation and trafficking of CD147 to the plasma membrane in the metastatic breast cancer cell line MDA-MB-231. *Cancer Res,* 67**,** 4182-9.

GAO, J., AKSOY, B. A., DOGRUSOZ, U., DRESDNER, G., GROSS, B., SUMER, S. O., SUN, Y., JACOBSEN, A., SINHA, R., LARSSON, E., CERAMI, E., SANDER, C. & SCHULTZ, N. 2013. Integrative analysis of complex cancer genomics and clinical profiles using the cBioPortal. *Sci Signal,* 6**,** pl1.

GOODWIN, J., NEUGENT, M. L., LEE, S. Y., CHOE, J. H., CHOI, H., JENKINS, D. M. R., RUTHENBORG, R. J., ROBINSON, M. W., JEONG, J. Y., WAKE, M., ABE, H., TAKEDA, N., ENDO, H., INOUE, M., XUAN, Z., YOO, H., CHEN, M., AHN, J. M., MINNA, J. D., HELKE, K. L., SINGH, P. K., SHACKELFORD, D. B. & KIM, J. W. 2017. The distinct metabolic phenotype of lung squamous cell carcinoma defines selective vulnerability to glycolytic inhibition. *Nat Commun,* 8**,** 15503.

GORDAN, J. D., THOMPSON, C. B. & SIMON, M. C. 2007. HIF and c-Myc: sibling rivals for control of cancer cell metabolism and proliferation. *Cancer Cell,* 12**,** 108-13.

GORRINI, C., HARRIS, I. S. & MAK, T. W. 2013. Modulation of oxidative stress as an anticancer strategy. *Nat Rev Drug Discov,* 12**,** 931-47.

GOTO, T., SUGAWARA, K., NAKAMURA, S., KIDOKORO, S. I., WAKUI, H. & NUNOMURA, W. 2016. Enzymatic and thermodynamic profiles of a

heterotetramer lactate dehydrogenase isozyme in swine. *Biochem Biophys Res Commun,* 479**,** 860-867.

GOTTFRIED, E., KUNZ-SCHUGHART, L. A., EBNER, S., MUELLER-KLIESER, W., HOVES, S., ANDREESEN, R., MACKENSEN, A. & KREUTZ, M. 2006. Tumor-derived lactic acid modulates dendritic cell activation and antigen expression. *Blood,* 107**,** 2013-21.

GOTTLOB, K., MAJEWSKI, N., KENNEDY, S., KANDEL, E., ROBEY, R. B. & HAY, N. 2001. Inhibition of early apoptotic events by Akt/PKB is dependent on the first committed step of glycolysis and mitochondrial hexokinase. *Genes Dev,* 15**,** 1406-18.

GREEN, D. E. 1936. The malic dehydrogenase of animal tissues. *Biochem J,* 30**,** 2095-110.

GREINER, E. F., GUPPY, M. & BRAND, K. 1994. Glucose is essential for proliferation and the glycolytic enzyme induction that provokes a transition to glycolytic energy production. *J Biol Chem,* 269**,** 31484-90.

GUMAA, K. A. & MCLEAN, P. 1969. The pentose phosphate pathway of glucose metabolism. Enzyme profiles and transient and steady-state content of intermediates of alternative pathways of glucose metabolism in Krebs ascites cells. *Biochem J,* 115**,** 1009-29.

GUO, Y., UPDEGRAFF, B. L., PARK, S., DURAKOGLUGIL, D., CRUZ, V. H., MADDUX, S., HWANG, T. H. & O'DONNELL, K. A. 2016. Comprehensive Ex Vivo Transposon Mutagenesis Identifies Genes That Promote Growth Factor Independence and Leukemogenesis. *Cancer Res,* 76**,** 773-86.

GURDA, G. T., ZHANG, L., WANG, Y., CHEN, L., GEDDES, S., CHO, W. C., ASKIN, F., GABRIELSON, E. & LI, Q. K. 2015. Utility of five commonly used immunohistochemical markers TTF-1, Napsin A, CK7, CK5/6 and P63 in primary and metastatic adenocarcinoma and squamous cell carcinoma of the lung: a retrospective study of 246 fine needle aspiration cases. *Clin Transl Med,* 4**,** 16.

GWINN, D. M., SHACKELFORD, D. B., EGAN, D. F., MIHAYLOVA, M. M., MERY, A., VASQUEZ, D. S., TURK, B. E. & SHAW, R. J. 2008. AMPK phosphorylation of raptor mediates a metabolic checkpoint. *Mol Cell,* 30**,** 214-26.

HALESTRAP, A. P. 2012. The monocarboxylate transporter family--Structure and functional characterization. *IUBMB Life,* 64**,** 1-9.

HALESTRAP, A. P. & PRICE, N. T. 1999. The proton-linked monocarboxylate transporter (MCT) family: structure, function and regulation. *Biochem J,* 343 Pt 2**,** 281-99.

HANAHAN, D. & WEINBERG, R. A. 2011. Hallmarks of cancer: the next generation. *Cell,* 144**,** 646-74.

HARDIE, D. G. 2007. AMP-activated/SNF1 protein kinases: conserved guardians of cellular energy. *Nat Rev Mol Cell Biol,* 8**,** 774-85.

HARRIS, I. S., TRELOAR, A. E., INOUE, S., SASAKI, M., GORRINI, C., LEE, K. C., YUNG, K. Y., BRENNER, D., KNOBBE-THOMSEN, C. B., COX, M. A., ELIA, A., BERGER, T., CESCON, D. W., ADEOYE, A., BRUSTLE, A., MOLYNEUX, S. D., MASON, J. M., LI, W. Y., YAMAMOTO, K., WAKEHAM, A., BERMAN, H. K., KHOKHA, R., DONE, S. J., KAVANAGH, T. J., LAM, C. W. & MAK, T. W. 2015. Glutathione and thioredoxin antioxidant pathways synergize to drive cancer initiation and progression. *Cancer Cell,* 27**,** 211-22.

HATZIVASSILIOU, G., ZHAO, F., BAUER, D. E., ANDREADIS, C., SHAW, A. N., DHANAK, D., HINGORANI, S. R., TUVESON, D. A. & THOMPSON, C. B. 2005. ATP citrate lyase inhibition can suppress tumor cell growth. *Cancer Cell,* 8**,** 311-21.

HEDESKOV, C. J. 1968. Early effects of phytohaemagglutinin on glucose metabolism of normal human lymphocytes. *Biochem J,* 110**,** 373-80.

HEDSTROM, L. 2002. Serine protease mechanism and specificity. *Chem Rev,* 102**,** 4501-24.

HENSLEY, C. T., FAUBERT, B., YUAN, Q., LEV-COHAIN, N., JIN, E., KIM, J., JIANG, L., KO, B., SKELTON, R., LOUDAT, L., WODZAK, M., KLIMKO, C., MCMILLAN, E., BUTT, Y., NI, M., OLIVER, D., TORREALBA, J., MALLOY, C. R., KERNSTINE, K., LENKINSKI, R. E. & DEBERARDINIS, R. J. 2016. Metabolic Heterogeneity in Human Lung Tumors. *Cell,* 164**,** 681-94.

HITOSUGI, T., ZHOU, L., ELF, S., FAN, J., KANG, H. B., SEO, J. H., SHAN, C., DAI, Q., ZHANG, L., XIE, J., GU, T. L., JIN, P., ALECKOVIC, M., LEROY, G., KANG, Y., SUDDERTH, J. A., DEBERARDINIS, R. J., LUAN, C. H., CHEN, G. Z., MULLER, S., SHIN, D. M., OWONIKOKO, T. K., LONIAL, S., ARELLANO, M. L., KHOURY, H. J., KHURI, F. R., LEE, B. H., YE, K., BOGGON, T. J., KANG, S., HE, C. & CHEN, J. 2012. Phosphoglycerate mutase 1 coordinates glycolysis and biosynthesis to promote tumor growth. *Cancer Cell,* 22**,** 585-600.

HOMMA, S., ISHII, Y., MORISHIMA, Y., YAMADORI, T., MATSUNO, Y., HARAGUCHI, N., KIKUCHI, N., SATOH, H., SAKAMOTO, T., HIZAWA, N., ITOH, K. &

YAMAMOTO, M. 2009. Nrf2 enhances cell proliferation and resistance to anticancer drugs in human lung cancer. *Clin Cancer Res,* 15**,** 3423-32.

HORI, K., KATAYAMA, N., KACHI, S., KONDO, M., KADOMATSU, K., USUKURA, J., MURAMATSU, T., MORI, S. & MIYAKE, Y. 2000. Retinal dysfunction in basigin deficiency. *Invest Ophthalmol Vis Sci,* 41**,** 3128-33.

HU, H., JUVEKAR, A., LYSSIOTIS, C. A., LIEN, E. C., ALBECK, J. G., OH, D., VARMA, G., HUNG, Y. P., ULLAS, S., LAURING, J., SETH, P., LUNDQUIST, M. R., TOLAN, D. R., GRANT, A. K., NEEDLEMAN, D. J., ASARA, J. M., CANTLEY, L. C. & WULF, G. M. 2016. Phosphoinositide 3-Kinase Regulates Glycolysis through Mobilization of Aldolase from the Actin Cytoskeleton. *Cell,* 164**,** 433-46.

HU, S., BALAKRISHNAN, A., BOK, R. A., ANDERTON, B., LARSON, P. E., NELSON, S. J., KURHANEWICZ, J., VIGNERON, D. B. & GOGA, A. 2011. 13C-pyruvate imaging reveals alterations in glycolysis that precede c-Myc-induced tumor formation and regression. *Cell Metab,* 14**,** 131-42.

HUANG, F., NI, M., CHALISHAZAR, M. D., HUFFMAN, K. E., KIM, J., CAI, L., SHI, X., CAI, F., ZACHARIAS, L. G., IRELAND, A. S., LI, K., GU, W., KAUSHIK, A. K., LIU, X., GAZDAR, A. F., OLIVER, T. G., MINNA, J. D., HU, Z. & DEBERARDINIS, R. J. 2018. Inosine Monophosphate Dehydrogenase Dependence in a Subset of Small Cell Lung Cancers. *Cell Metab,* 28**,** 369-382 e5.

HUBBARD, A. L., BARTLES, J. R. & BRAITERMAN, L. T. 1985. Identification of rat hepatocyte plasma membrane proteins using monoclonal antibodies. *J Cell Biol,* 100**,** 1115-25.

HUI, S., GHERGUROVICH, J. M., MORSCHER, R. J., JANG, C., TENG, X., LU, W., ESPARZA, L. A., REYA, T., LE, Z., YANXIANG GUO, J., WHITE, E. & RABINOWITZ, J. D. 2017. Glucose feeds the TCA cycle via circulating lactate. *Nature,* 551**,** 115-118.

HUI, S. T., ANDRES, A. M., MILLER, A. K., SPANN, N. J., POTTER, D. W., POST, N. M., CHEN, A. Z., SACHITHANANTHAM, S., JUNG, D. Y., KIM, J. K. & DAVIS, R. A. 2008. Txnip balances metabolic and growth signaling via PTEN disulfide reduction. *Proc Natl Acad Sci U S A,* 105**,** 3921-6.

HUME, D. A., RADIK, J. L., FERBER, E. & WEIDEMANN, M. J. 1978. Aerobic glycolysis and lymphocyte transformation. *Biochem J,* 174**,** 703-9.

IGAKURA, T., KADOMATSU, K., KANAME, T., MURAMATSU, H., FAN, Q. W., MIYAUCHI, T., TOYAMA, Y., KUNO, N., YUASA, S., TAKAHASHI, M., SENDA, T., TAGUCHI, O., YAMAMURA, K., ARIMURA, K. & MURAMATSU, T. 1998. A null mutation in basigin, an immunoglobulin superfamily member, indicates its important roles in peri-implantation development and spermatogenesis. *Dev Biol,* 194**,** 152-65.

INOKI, K., LI, Y., ZHU, T., WU, J. & GUAN, K. L. 2002. TSC2 is phosphorylated and inhibited by Akt and suppresses mTOR signalling. *Nat Cell Biol,* 4**,** 648-57.

INOUE, T., KIM, E. E., KOMAKI, R., WONG, F. C., BASSA, P., WONG, W. H., YANG, D. J., ENDO, K. & PODOLOFF, D. A. 1995. Detecting recurrent or residual lung cancer with FDG-PET. *J Nucl Med,* 36**,** 788-93.

IZUMI, H., TORIGOE, T., ISHIGUCHI, H., URAMOTO, H., YOSHIDA, Y., TANABE, M., ISE, T., MURAKAMI, T., YOSHIDA, T., NOMOTO, M. & KOHNO, K. 2003. Cellular

pH regulators: potentially promising molecular targets for cancer chemotherapy. *Cancer Treat Rev,* 29**,** 541-9.

JAIN, M., NILSSON, R., SHARMA, S., MADHUSUDHAN, N., KITAMI, T., SOUZA, A. L., KAFRI, R., KIRSCHNER, M. W., CLISH, C. B. & MOOTHA, V. K. 2012. Metabolite profiling identifies a key role for glycine in rapid cancer cell proliferation. *Science,* 336**,** 1040-4.

JANG, C., CHEN, L. & RABINOWITZ, J. D. 2018. Metabolomics and Isotope Tracing. *Cell,* 173**,** 822-837.

JI, H., RAMSEY, M. R., HAYES, D. N., FAN, C., MCNAMARA, K., KOZLOWSKI, P., TORRICE, C., WU, M. C., SHIMAMURA, T., PERERA, S. A., LIANG, M. C., CAI, D., NAUMOV, G. N., BAO, L., CONTRERAS, C. M., LI, D., CHEN, L., KRISHNAMURTHY, J., KOIVUNEN, J., CHIRIEAC, L. R., PADERA, R. F., BRONSON, R. T., LINDEMAN, N. I., CHRISTIANI, D. C., LIN, X., SHAPIRO, G. I., JANNE, P. A., JOHNSON, B. E., MEYERSON, M., KWIATKOWSKI, D. J., CASTRILLON, D. H., BARDEESY, N., SHARPLESS, N. E. & WONG, K. K. 2007. LKB1 modulates lung cancer differentiation and metastasis. *Nature,* 448**,** 807-10.

JIANG, P., DU, W., WANG, X., MANCUSO, A., GAO, X., WU, M. & YANG, X. 2011. p53 regulates biosynthesis through direct inactivation of glucose-6-phosphate dehydrogenase. *Nat Cell Biol,* 13**,** 310-6.

JOHNSON, L., MERCER, K., GREENBAUM, D., BRONSON, R. T., CROWLEY, D., TUVESON, D. A. & JACKS, T. 2001. Somatic activation of the K-ras oncogene causes early onset lung cancer in mice. *Nature,* 410**,** 1111-6.

KAM, Y. W., OKUMURA, Y., KIDO, H., NG, L. F., BRUZZONE, R. & ALTMEYER, R. 2009. Cleavage of the SARS coronavirus spike glycoprotein by airway proteases enhances virus entry into human bronchial epithelial cells in vitro. *PLoS One,* 4**,** e7870.

KANEKURA, T., CHEN, X. & KANZAKI, T. 2002. Basigin (CD147) is expressed on melanoma cells and induces tumor cell invasion by stimulating production of matrix metalloproteinases by fibroblasts. *Int J Cancer,* 99**,** 520-8.

KARAKAS, B., BACHMAN, K. E. & PARK, B. H. 2006. Mutation of the PIK3CA oncogene in human cancers. *Br J Cancer,* 94**,** 455-9.

KARPUSAS, M., BRANCHAUD, B. & REMINGTON, S. J. 1990. Proposed mechanism for the condensation reaction of citrate synthase: 1.9-A structure of the ternary complex with oxaloacetate and carboxymethyl coenzyme A. *Biochemistry,* 29**,** 2213-9.

KIM, D. & SALZBERG, S. L. 2011. TopHat-Fusion: an algorithm for discovery of novel fusion transcripts. *Genome Biol,* 12**,** R72.

KIM, J. W., TCHERNYSHYOV, I., SEMENZA, G. L. & DANG, C. V. 2006. HIF-1-mediated expression of pyruvate dehydrogenase kinase: a metabolic switch required for cellular adaptation to hypoxia. *Cell Metab,* 3**,** 177-85.

KIM, J. W., ZELLER, K. I., WANG, Y., JEGGA, A. G., ARONOW, B. J., O'DONNELL, K. A. & DANG, C. V. 2004. Evaluation of myc E-box phylogenetic footprints in glycolytic genes by chromatin immunoprecipitation assays. *Mol Cell Biol,* 24**,** 5923-36.

KIRK, P., WILSON, M. C., HEDDLE, C., BROWN, M. H., BARCLAY, A. N. & HALESTRAP, A. P. 2000. CD147 is tightly associated with lactate transporters MCT1 and MCT4 and facilitates their cell surface expression. *EMBO J,* 19**,** 3896-904.

KNAPPE, S., WU, F., MADLANSACAY, M. R. & WU, Q. 2004. Identification of domain structures in the propeptide of corin essential for the processing of proatrial natriuretic peptide. *J Biol Chem,* 279**,** 34464-71.

KONDOH, H., LLEONART, M. E., GIL, J., WANG, J., DEGAN, P., PETERS, G., MARTINEZ, D., CARNERO, A. & BEACH, D. 2005. Glycolytic enzymes can modulate cellular life span. *Cancer Res,* 65**,** 177-85.

KOUKOURAKIS, M. I., GIATROMANOLAKI, A., WINTER, S., LEEK, R., SIVRIDIS, E. & HARRIS, A. L. 2009. Lactate dehydrogenase 5 expression in squamous cell head and neck cancer relates to prognosis following radical or postoperative radiotherapy. *Oncology,* 77**,** 285-92.

LAIN, E., CARNEJAC, S., ESCHER, P., WILSON, M. C., LOMO, T., GAJENDRAN, N. & BRENNER, H. R. 2009. A novel role for embigin to promote sprouting of motor nerve terminals at the neuromuscular junction. *J Biol Chem,* 284**,** 8930-9.

LANGOWSKI, J. L., ZHANG, X., WU, L., MATTSON, J. D., CHEN, T., SMITH, K., BASHAM, B., MCCLANAHAN, T., KASTELEIN, R. A. & OFT, M. 2006. IL-23 promotes tumour incidence and growth. *Nature,* 442**,** 461-5.

LE FLOCH, R., CHICHE, J., MARCHIQ, I., NAIKEN, T., ILC, K., MURRAY, C. M., CRITCHLOW, S. E., ROUX, D., SIMON, M. P. & POUYSSEGUR, J. 2011. CD147 subunit of lactate/H+ symporters MCT1 and hypoxia-inducible MCT4 is critical for

energetics and growth of glycolytic tumors. *Proc Natl Acad Sci U S A,* 108**,** 16663-8.

LEE, E. S., SON, D. S., KIM, S. H., LEE, J., JO, J., HAN, J., KIM, H., LEE, H. J., CHOI, H. Y., JUNG, Y., PARK, M., LIM, Y. S., KIM, K., SHIM, Y., KIM, B. C., LEE, K., HUH, N., KO, C., PARK, K., LEE, J. W., CHOI, Y. S. & KIM, J. 2008. Prediction of recurrence-free survival in postoperative non-small cell lung cancer patients by using an integrated model of clinical information and gene expression. *Clin Cancer Res,* 14**,** 7397-404.

LEWIS, C. A., PARKER, S. J., FISKE, B. P., MCCLOSKEY, D., GUI, D. Y., GREEN, C. R., VOKES, N. I., FEIST, A. M., VANDER HEIDEN, M. G. & METALLO, C. M. 2014. Tracing compartmentalized NADPH metabolism in the cytosol and mitochondria of mammalian cells. *Mol Cell,* 55**,** 253-63.

LEYTUS, S. P., LOEB, K. R., HAGEN, F. S., KURACHI, K. & DAVIE, E. W. 1988. A novel trypsin-like serine protease (hepsin) with a putative transmembrane domain expressed by human liver and hepatoma cells. *Biochemistry,* 27**,** 1067-74.

LI, B., QIU, B., LEE, D. S., WALTON, Z. E., OCHOCKI, J. D., MATHEW, L. K., MANCUSO, A., GADE, T. P., KEITH, B., NISSIM, I. & SIMON, M. C. 2014. Fructose-1,6-bisphosphatase opposes renal carcinoma progression. *Nature,* 513**,** 251-5.

LI, J. H., HUANG, W., LIN, P., WU, B., FU, Z. G., SHEN, H. M., JING, L., LIU, Z. Y., ZHOU, Y., MENG, Y., XU, B. Q., CHEN, Z. N. & JIANG, J. L. 2016. N-linked glycosylation at Asn152 on CD147 affects protein folding and stability: promoting tumour metastasis in hepatocellular carcinoma. *Sci Rep,* 6**,** 35210.

LI, L., KANG, L., ZHAO, W., FENG, Y., LIU, W., WANG, T., MAI, H., HUANG, J., CHEN, S., LIANG, Y., HAN, J., XU, X. & YE, Q. 2017. miR-30a-5p suppresses breast tumor growth and metastasis through inhibition of LDHA-mediated Warburg effect. *Cancer Lett,* 400**,** 89-98.

LI, R., HUANG, L., GUO, H. & TOOLE, B. P. 2001. Basigin (murine EMMPRIN) stimulates matrix metalloproteinase production by fibroblasts. *J Cell Physiol,* 186**,** 371-9.

LIAO, Y., SMYTH, G. K. & SHI, W. 2014. featureCounts: an efficient general purpose program for assigning sequence reads to genomic features. *Bioinformatics,* 30**,** 923-30.

LIGHT, A. & JANSKA, H. 1989. Enterokinase (enteropeptidase): comparative aspects. *Trends Biochem Sci,* 14**,** 110-2.

LIU, Y. C., LI, F., HANDLER, J., HUANG, C. R., XIANG, Y., NERETTI, N., SEDIVY, J. M., ZELLER, K. I. & DANG, C. V. 2008. Global regulation of nucleotide biosynthetic genes by c-Myc. *PLoS One,* 3**,** e2722.

LOCASALE, J. W. 2013. Serine, glycine and one-carbon units: cancer metabolism in full circle. *Nat Rev Cancer,* 13**,** 572-83.

LUNT, S. Y. & VANDER HEIDEN, M. G. 2011. Aerobic glycolysis: meeting the metabolic requirements of cell proliferation. *Annu Rev Cell Dev Biol,* 27**,** 441-64.

LUO, Z., ZANG, M. & GUO, W. 2010. AMPK as a metabolic tumor suppressor: control of metabolism and cell growth. *Future Oncol,* 6**,** 457-70.

LUO, Z., ZHANG, X., ZENG, W., SU, J., YANG, K., LU, L., LIM, C. B., TANG, W., WU, L., ZHAO, S., JIA, X., PENG, C. & CHEN, X. 2016. TRAF6 regulates melanoma invasion and metastasis through ubiquitination of Basigin. *Oncotarget,* 7**,** 7179-92.

MALDONADO-BAEZ, L., COLE, N. B., KRAMER, H. & DONALDSON, J. G. 2013. Microtubule-dependent endosomal sorting of clathrin-independent cargo by Hook1. *J Cell Biol,* 201**,** 233-47.

MANNING, B. D., TEE, A. R., LOGSDON, M. N., BLENIS, J. & CANTLEY, L. C. 2002. Identification of the tuberous sclerosis complex-2 tumor suppressor gene product tuberin as a target of the phosphoinositide 3-kinase/akt pathway. *Mol Cell,* 10**,** 151-62.

MARCHIQ, I., LE FLOCH, R., ROUX, D., SIMON, M. P. & POUYSSEGUR, J. 2015. Genetic disruption of lactate/H+ symporters (MCTs) and their subunit CD147/BASIGIN sensitizes glycolytic tumor cells to phenformin. *Cancer Res,* 75**,** 171-80.

MARIEB, E. A., ZOLTAN-JONES, A., LI, R., MISRA, S., GHATAK, S., CAO, J., ZUCKER, S. & TOOLE, B. P. 2004. Emmprin promotes anchorage-independent growth in human mammary carcinoma cells by stimulating hyaluronan production. *Cancer Res,* 64**,** 1229-32.

MARIN-HERNANDEZ, A., GALLARDO-PEREZ, J. C., RALPH, S. J., RODRIGUEZ-ENRIQUEZ, S. & MORENO-SANCHEZ, R. 2009. HIF-1alpha modulates energy metabolism in cancer cells by inducing over-expression of specific glycolytic isoforms. *Mini Rev Med Chem,* 9**,** 1084-101.

MARJANOVIC, S., WIELBURSKI, A. & NELSON, B. D. 1988. Effect of phorbol myristate acetate and concanavalin A on the glycolytic enzymes of human peripheral lymphocytes. *Biochim Biophys Acta,* 970**,** 1-6.

MASSION, P. P., TAFLAN, P. M., JAMSHEDUR RAHMAN, S. M., YILDIZ, P., SHYR, Y., EDGERTON, M. E., WESTFALL, M. D., ROBERTS, J. R., PIETENPOL, J. A., CARBONE, D. P. & GONZALEZ, A. L. 2003. Significance of p63 amplification and overexpression in lung cancer development and prognosis. *Cancer Res,* 63**,** 7113-21.

MATHUPALA, S. P., HEESE, C. & PEDERSEN, P. L. 1997. Glucose catabolism in cancer cells. The type II hexokinase promoter contains functionally active response elements for the tumor suppressor p53. *J Biol Chem,* 272**,** 22776-80.

MATOBA, S., KANG, J. G., PATINO, W. D., WRAGG, A., BOEHM, M., GAVRILOVA, O., HURLEY, P. J., BUNZ, F. & HWANG, P. M. 2006. p53 regulates mitochondrial respiration. *Science,* 312**,** 1650-3.

MAXWELL, P. H., WIESENER, M. S., CHANG, G. W., CLIFFORD, S. C., VAUX, E. C., COCKMAN, M. E., WYKOFF, C. C., PUGH, C. W., MAHER, E. R. & RATCLIFFE, P. J. 1999. The tumour suppressor protein VHL targets hypoxia-inducible factors for oxygen-dependent proteolysis. *Nature,* 399**,** 271-5.

MAYERS, J. R., TORRENCE, M. E., DANAI, L. V., PAPAGIANNAKOPOULOS, T., DAVIDSON, S. M., BAUER, M. R., LAU, A. N., JI, B. W., DIXIT, P. D., HOSIOS, A. M., MUIR, A., CHIN, C. R., FREINKMAN, E., JACKS, T., WOLPIN, B. M., VITKUP, D. & VANDER HEIDEN, M. G. 2016. Tissue of origin dictates branched-chain amino acid metabolism in mutant Kras-driven cancers. *Science,* 353**,** 1161-5.

MCCLELAND, M. L., ADLER, A. S., DEMING, L., COSINO, E., LEE, L., BLACKWOOD, E. M., SOLON, M., TAO, J., LI, L., SHAMES, D., JACKSON, E., FORREST, W. F.

& FIRESTEIN, R. 2013. Lactate dehydrogenase B is required for the growth of KRAS-dependent lung adenocarcinomas. *Clin Cancer Res,* 19**,** 773-84.

MENDLER, A. N., HU, B., PRINZ, P. U., KREUTZ, M., GOTTFRIED, E. & NOESSNER, E. 2012. Tumor lactic acidosis suppresses CTL function by inhibition of p38 and JNK/c-Jun activation. *Int J Cancer,* 131**,** 633-40.

MENOU, A., DUITMAN, J., FLAJOLET, P., SALLENAVE, J. M., MAILLEUX, A. A. & CRESTANI, B. 2017. Human airway trypsin-like protease, a serine protease involved in respiratory diseases. *Am J Physiol Lung Cell Mol Physiol,* 312**,** L657-L668.

MEUWISSEN, R., LINN, S. C., VAN DER VALK, M., MOOI, W. J. & BERNS, A. 2001. Mouse model for lung tumorigenesis through Cre/lox controlled sporadic activation of the K-Ras oncogene. *Oncogene,* 20**,** 6551-8.

MEYERHOF, O. 1927. Recent Investigations on the Aerobic and an-Aerobic Metabolism of Carbohydrates. *J Gen Physiol,* 8**,** 531-42.

MILLER, G. S., ZORATTI, G. L., MURRAY, A. S., BERGUM, C., TANABE, L. M. & LIST, K. 2014. HATL5: a cell surface serine protease differentially expressed in epithelial cancers. *PLoS One,* 9**,** e87675.

MILLIMAGGI, D., MARI, M., D'ASCENZO, S., CAROSA, E., JANNINI, E. A., ZUCKER, S., CARTA, G., PAVAN, A. & DOLO, V. 2007. Tumor vesicle-associated CD147 modulates the angiogenic capability of endothelial cells. *Neoplasia,* 9**,** 349-57.

MULLEN, A. R., HU, Z., SHI, X., JIANG, L., BOROUGHS, L. K., KOVACS, Z., BORIACK, R., RAKHEJA, D., SULLIVAN, L. B., LINEHAN, W. M., CHANDEL, N. S. & DEBERARDINIS, R. J. 2014. Oxidation of alpha-ketoglutarate is required for

reductive carboxylation in cancer cells with mitochondrial defects. *Cell Rep,* 7**,** 1679-1690.

MUNYON, W. H. & MERCHANT, D. J. 1959. The relation between glucose utilization, lactic acid production and utilization and the growth cycle of L strain fibroblasts. *Exp Cell Res,* 17**,** 490-8.

MURAMATSU, T. & MIYAUCHI, T. 2003. Basigin (CD147): a multifunctional transmembrane protein involved in reproduction, neural function, inflammation and tumor invasion. *Histol Histopathol,* 18**,** 981-7.

NAJJAR, V. A. 1948. The isolation and properties of phosphoglucomutase. *J Biol Chem,* 175**,** 281-90.

NIKIFOROV, M. A., CHANDRIANI, S., O'CONNELL, B., PETRENKO, O., KOTENKO, I., BEAVIS, A., SEDIVY, J. M. & COLE, M. D. 2002. A functional screen for Myc-responsive genes reveals serine hydroxymethyltransferase, a major source of the one-carbon unit for cell metabolism. *Mol Cell Biol,* 22**,** 5793-800.

ORIKAWA, H., KAWAGUCHI, M., BABA, T., YORITA, K., SAKODA, S. & KATAOKA, H. 2012. Activation of macrophage-stimulating protein by human airway trypsin-like protease. *FEBS Lett,* 586**,** 217-21.

PANIERI, E. & SANTORO, M. M. 2016. ROS homeostasis and metabolism: a dangerous liason in cancer cells. *Cell Death Dis,* 7**,** e2253.

PASSONNEAU, J. V. & LOWRY, O. H. 1962. Phosphofructokinase and the Pasteur effect. *Biochem Biophys Res Commun,* 7**,** 10-5.

PATEL, M. S. & ROCHE, T. E. 1990. Molecular biology and biochemistry of pyruvate dehydrogenase complexes. *FASEB J,* 4**,** 3224-33.

PHILP, N. J., OCHRIETOR, J. D., RUDOY, C., MURAMATSU, T. & LINSER, P. J. 2003. Loss of MCT1, MCT3, and MCT4 expression in the retinal pigment epithelium and neural retina of the 5A11/basigin-null mouse. *Invest Ophthalmol Vis Sci,* 44**,** 1305-11.

PISKOUNOVA, E., AGATHOCLEOUS, M., MURPHY, M. M., HU, Z., HUDDLESTUN, S. E., ZHAO, Z., LEITCH, A. M., JOHNSON, T. M., DEBERARDINIS, R. J. & MORRISON, S. J. 2015. Oxidative stress inhibits distant metastasis by human melanoma cells. *Nature,* 527**,** 186-91.

POSSEMATO, R., MARKS, K. M., SHAUL, Y. D., PACOLD, M. E., KIM, D., BIRSOY, K., SETHUMADHAVAN, S., WOO, H. K., JANG, H. G., JHA, A. K., CHEN, W. W., BARRETT, F. G., STRANSKY, N., TSUN, Z. Y., COWLEY, G. S., BARRETINA, J., KALAANY, N. Y., HSU, P. P., OTTINA, K., CHAN, A. M., YUAN, B., GARRAWAY, L. A., ROOT, D. E., MINO-KENUDSON, M., BRACHTEL, E. F., DRIGGERS, E. M. & SABATINI, D. M. 2011. Functional genomics reveal that the serine synthesis pathway is essential in breast cancer. *Nature,* 476**,** 346-50.

POTEMPA, J., KORZUS, E. & TRAVIS, J. 1994. The serpin superfamily of proteinase inhibitors: structure, function, and regulation. *J Biol Chem,* 269**,** 15957-60.

QUENNET, V., YAROMINA, A., ZIPS, D., ROSNER, A., WALENTA, S., BAUMANN, M. & MUELLER-KLIESER, W. 2006. Tumor lactate content predicts for response to fractionated irradiation of human squamous cell carcinomas in nude mice. *Radiother Oncol,* 81**,** 130-5.

RACKER, E. 1950. Spectrophotometric measurements of the enzymatic formation of fumaric and cis-aconitic acids. *Biochim Biophys Acta,* 4**,** 211-4.

RAMIREZ, R. D., SHERIDAN, S., GIRARD, L., SATO, M., KIM, Y., POLLACK, J., PEYTON, M., ZOU, Y., KURIE, J. M., DIMAIO, J. M., MILCHGRUB, S., SMITH, A. L., SOUZA, R. F., GILBEY, L., ZHANG, X., GANDIA, K., VAUGHAN, M. B., WRIGHT, W. E., GAZDAR, A. F., SHAY, J. W. & MINNA, J. D. 2004. Immortalization of human bronchial epithelial cells in the absence of viral oncoproteins. *Cancer Res,* 64**,** 9027-34.

REITZER, L. J., WICE, B. M. & KENNELL, D. 1979. Evidence that glutamine, not sugar, is the major energy source for cultured HeLa cells. *J Biol Chem,* 254**,** 2669-76.

REKHTMAN, N., PAIK, P. K., ARCILA, M. E., TAFE, L. J., OXNARD, G. R., MOREIRA, A. L., TRAVIS, W. D., ZAKOWSKI, M. F., KRIS, M. G. & LADANYI, M. 2012. Clarifying the spectrum of driver oncogene mutations in biomarker-verified squamous carcinoma of lung: lack of EGFR/KRAS and presence of PIK3CA/AKT1 mutations. *Clin Cancer Res,* 18**,** 1167-76.

ROBINSON, M. D., MCCARTHY, D. J. & SMYTH, G. K. 2010. edgeR: a Bioconductor package for differential expression analysis of digital gene expression data. *Bioinformatics,* 26**,** 139-40.

ROMERO, R., SAYIN, V. I., DAVIDSON, S. M., BAUER, M. R., SINGH, S. X., LEBOEUF, S. E., KARAKOUSI, T. R., ELLIS, D. C., BHUTKAR, A., SANCHEZ-RIVERA, F. J., SUBBARAJ, L., MARTINEZ, B., BRONSON, R. T., PRIGGE, J. R., SCHMIDT, E. E., THOMAS, C. J., GOPARAJU, C., DAVIES, A., DOLGALEV, I., HEGUY, A., ALLAJ, V., POIRIER, J. T., MOREIRA, A. L., RUDIN, C. M., PASS, H. I., VANDER HEIDEN, M. G., JACKS, T. & PAPAGIANNAKOPOULOS, T. 2017. Keap1 loss

promotes Kras-driven lung cancer and results in dependence on glutaminolysis. *Nat Med,* 23**,** 1362-1368.

ROSSIER, B. C. & STUTTS, M. J. 2009. Activation of the epithelial sodium channel (ENaC) by serine proteases. *Annu Rev Physiol,* 71**,** 361-79.

SATO, M., LARSEN, J. E., LEE, W., SUN, H., SHAMES, D. S., DALVI, M. P., RAMIREZ, R. D., TANG, H., DIMAIO, J. M., GAO, B., XIE, Y., WISTUBA, II, GAZDAR, A. F., SHAY, J. W. & MINNA, J. D. 2013. Human lung epithelial cells progressed to malignancy through specific oncogenic manipulations. *Mol Cancer Res,* 11**,** 638-50.

SATTLER, U. G., MEYER, S. S., QUENNET, V., HOERNER, C., KNOERZER, H., FABIAN, C., YAROMINA, A., ZIPS, D., WALENTA, S., BAUMANN, M. & MUELLER-KLIESER, W. 2010. Glycolytic metabolism and tumour response to fractionated irradiation. *Radiother Oncol,* 94**,** 102-9.

SCHWARTZENBERG-BAR-YOSEPH, F., ARMONI, M. & KARNIELI, E. 2004. The tumor suppressor p53 down-regulates glucose transporters GLUT1 and GLUT4 gene expression. *Cancer Res,* 64**,** 2627-33.

SEMENZA, G. L. 2008. Tumor metabolism: cancer cells give and take lactate. *J Clin Invest,* 118**,** 3835-7.

SEMENZA, G. L., JIANG, B. H., LEUNG, S. W., PASSANTINO, R., CONCORDET, J. P., MAIRE, P. & GIALLONGO, A. 1996. Hypoxia response elements in the aldolase A, enolase 1, and lactate dehydrogenase A gene promoters contain essential binding sites for hypoxia-inducible factor 1. *J Biol Chem,* 271**,** 32529-37.

SHAW, R. J. & CANTLEY, L. C. 2006. Ras, PI(3)K and mTOR signalling controls tumour cell growth. *Nature,* 441**,** 424-30.

SHEU, K. F. & BLASS, J. P. 1999. The alpha-ketoglutarate dehydrogenase complex. *Ann N Y Acad Sci,* 893**,** 61-78.

SHIM, H., DOLDE, C., LEWIS, B. C., WU, C. S., DANG, G., JUNGMANN, R. A., DALLA-FAVERA, R. & DANG, C. V. 1997. c-Myc transactivation of LDH-A: implications for tumor metabolism and growth. *Proc Natl Acad Sci U S A,* 94**,** 6658-63.

SHIME, H., YABU, M., AKAZAWA, T., KODAMA, K., MATSUMOTO, M., SEYA, T. & INOUE, N. 2008. Tumor-secreted lactic acid promotes IL-23/IL-17 proinflammatory pathway. *J Immunol,* 180**,** 7175-83.

SIBLEY, J. A. & LEHNINGER, A. L. 1949. Determination of aldolase in animal tissues. *J Biol Chem,* 177**,** 859-72.

SILVESTRI, L., PAGANI, A., NAI, A., DE DOMENICO, I., KAPLAN, J. & CAMASCHELLA, C. 2008. The serine protease matriptase-2 (TMPRSS6) inhibits hepcidin activation by cleaving membrane hemojuvelin. *Cell Metab,* 8**,** 502-11.

SLEIN, M. W. 1950. Phosphomannose isomerase. *J Biol Chem,* 186**,** 753-61.

SOM, P., ATKINS, H. L., BANDOYPADHYAY, D., FOWLER, J. S., MACGREGOR, R. R., MATSUI, K., OSTER, Z. H., SACKER, D. F., SHIUE, C. Y., TURNER, H., WAN, C. N., WOLF, A. P. & ZABINSKI, S. V. 1980. A fluorinated glucose analog, 2-fluoro-2-deoxy-D-glucose (F-18): nontoxic tracer for rapid tumor detection. *J Nucl Med,* 21**,** 670-5.

SONVEAUX, P., VEGRAN, F., SCHROEDER, T., WERGIN, M. C., VERRAX, J., RABBANI, Z. N., DE SAEDELEER, C. J., KENNEDY, K. M., DIEPART, C.,

JORDAN, B. F., KELLEY, M. J., GALLEZ, B., WAHL, M. L., FERON, O. & DEWHIRST, M. W. 2008. Targeting lactate-fueled respiration selectively kills hypoxic tumor cells in mice. *J Clin Invest,* 118**,** 3930-42.

SPORN, M. B. & LIBY, K. T. 2012. NRF2 and cancer: the good, the bad and the importance of context. *Nat Rev Cancer,* 12**,** 564-71.

STINE, Z. E., WALTON, Z. E., ALTMAN, B. J., HSIEH, A. L. & DANG, C. V. 2015. MYC, Metabolism, and Cancer. *Cancer Discov,* 5**,** 1024-39.

SU, J., CHEN, X. & KANEKURA, T. 2009. A CD147-targeting siRNA inhibits the proliferation, invasiveness, and VEGF production of human malignant melanoma cells by down-regulating glycolysis. *Cancer Lett,* 273**,** 140-7.

SUTHERLAND, E. W., POSTERNAK, T. & CORI, C. F. 1949. Mechanism of the phosphoglyceric mutase reaction. *J Biol Chem,* 181**,** 153-9.

SZABO, R. & BUGGE, T. H. 2011. Membrane-anchored serine proteases in vertebrate cell and developmental biology. *Annu Rev Cell Dev Biol,* 27**,** 213-35.

SZABO, R., HOBSON, J. P., CHRISTOPH, K., KOSA, P., LIST, K. & BUGGE, T. H. 2009. Regulation of cell surface protease matriptase by HAI2 is essential for placental development, neural tube closure and embryonic survival in mice. *Development,* 136**,** 2653-63.

TAHA, C., LIU, Z., JIN, J., AL-HASANI, H., SONENBERG, N. & KLIP, A. 1999. Opposite translational control of GLUT1 and GLUT4 glucose transporter mRNAs in response to insulin. Role of mammalian target of rapamycin, protein kinase b, and phosphatidylinositol 3-kinase in GLUT1 mRNA translation. *J Biol Chem,* 274**,** 33085-91.

TANG, W., CHANG, S. B. & HEMLER, M. E. 2004. Links between CD147 function, glycosylation, and caveolin-1. *Mol Biol Cell,* 15**,** 4043-50.

TONG, X., ZHAO, F. & THOMPSON, C. B. 2009. The molecular determinants of de novo nucleotide biosynthesis in cancer cells. *Curr Opin Genet Dev,* 19**,** 32-7.

ULLAH, M. S., DAVIES, A. J. & HALESTRAP, A. P. 2006. The plasma membrane lactate transporter MCT4, but not MCT1, is up-regulated by hypoxia through a HIF-1alpha-dependent mechanism. *J Biol Chem,* 281**,** 9030-7.

UTTER, M. F. 1958. Carbohydrate metabolism. *Annu Rev Biochem,* 27**,** 245-84.

UTTER, M. F. & KEECH, D. B. 1963. Pyruvate Carboxylase. I. Nature of the Reaction. *J Biol Chem,* 238**,** 2603-8.

VALIENTE, M., OBENAUF, A. C., JIN, X., CHEN, Q., ZHANG, X. H., LEE, D. J., CHAFT, J. E., KRIS, M. G., HUSE, J. T., BROGI, E. & MASSAGUE, J. 2014. Serpins promote cancer cell survival and vascular co-option in brain metastasis. *Cell,* 156**,** 1002-16.

VESELL, E. S., FRITZ, P. J. & WHITE, E. L. 1968. Effects of buffer,pH, ionic strength and temperatures on lactate dehydrogenase isozymes. *Biochim Biophys Acta,* 159**,** 236-43.

VILORIA, C. G., PEINADO, J. R., ASTUDILLO, A., GARCIA-SUAREZ, O., GONZALEZ, M. V., SUAREZ, C. & CAL, S. 2007. Human DESC1 serine protease confers tumorigenic properties to MDCK cells and it is upregulated in tumours of different origin. *Br J Cancer,* 97**,** 201-9.

VISSER, W. E., FRIESEMA, E. C., JANSEN, J. & VISSER, T. J. 2008. Thyroid hormone transport in and out of cells. *Trends Endocrinol Metab,* 19**,** 50-6.

WALENTA, S., WETTERLING, M., LEHRKE, M., SCHWICKERT, G., SUNDFOR, K., ROFSTAD, E. K. & MUELLER-KLIESER, W. 2000. High lactate levels predict likelihood of metastases, tumor recurrence, and restricted patient survival in human cervical cancers. *Cancer Res,* 60**,** 916-21.

WARBURG, O., WIND, F. & NEGELEIN, E. 1927. The Metabolism of Tumors in the Body. *J Gen Physiol,* 8**,** 519-30.

WEBB, B. A., CHIMENTI, M., JACOBSON, M. P. & BARBER, D. L. 2011. Dysregulated pH: a perfect storm for cancer progression. *Nat Rev Cancer,* 11**,** 671-7.

WEINBERG, F., HAMANAKA, R., WHEATON, W. W., WEINBERG, S., JOSEPH, J., LOPEZ, M., KALYANARAMAN, B., MUTLU, G. M., BUDINGER, G. R. & CHANDEL, N. S. 2010. Mitochondrial metabolism and ROS generation are essential for Kras-mediated tumorigenicity. *Proc Natl Acad Sci U S A,* 107**,** 8788-93.

WEINBERG, S. E. & CHANDEL, N. S. 2015. Targeting mitochondria metabolism for cancer therapy. *Nat Chem Biol,* 11**,** 9-15.

WIDER DE XIFRA, E. A. & BATTLE, A. M. 1973. Mechanism of action of succinyl CoA synthetase. The role of CoA. *Enzyme,* 16**,** 128-37.

WISE, D. R., DEBERARDINIS, R. J., MANCUSO, A., SAYED, N., ZHANG, X. Y., PFEIFFER, H. K., NISSIM, I., DAIKHIN, E., YUDKOFF, M., MCMAHON, S. B. & THOMPSON, C. B. 2008. Myc regulates a transcriptional program that stimulates mitochondrial glutaminolysis and leads to glutamine addiction. *Proc Natl Acad Sci U S A,* 105**,** 18782-7.

WOLD, F. & BALLOU, C. E. 1957. Studies on the enzyme enolase. I. Equilibrium studies. *J Biol Chem,* 227**,** 301-12.

WOOD, I. S. & TRAYHURN, P. 2003. Glucose transporters (GLUT and SGLT): expanded families of sugar transport proteins. *Br J Nutr,* 89**,** 3-9.

WU, R. & RACKER, E. 1959. Regulatory mechanisms in carbohydrate metabolism. III. Limiting factors in glycolysis of ascites tumor cells. *J Biol Chem,* 234**,** 1029-35.

XIAO, Z., JIANG, Q., WILLETTE-BROWN, J., XI, S., ZHU, F., BURKETT, S., BACK, T., SONG, N. Y., DATLA, M., SUN, Z., GOLDSZMID, R., LIN, F., COHOON, T., PIKE, K., WU, X., SCHRUMP, D. S., WONG, K. K., YOUNG, H. A., TRINCHIERI, G., WILTROUT, R. H. & HU, Y. 2013. The pivotal role of IKKalpha in the development of spontaneous lung squamous cell carcinomas. *Cancer Cell,* 23**,** 527-40.

XU, C., FILLMORE, C. M., KOYAMA, S., WU, H., ZHAO, Y., CHEN, Z., HERTER-SPRIE, G. S., AKBAY, E. A., TCHAICHA, J. H., ALTABEF, A., REIBEL, J. B., WALTON, Z., JI, H., WATANABE, H., JANNE, P. A., CASTRILLON, D. H., RUSTGI, A. K., BASS, A. J., FREEMAN, G. J., PADERA, R. F., DRANOFF, G., HAMMERMAN, P. S., KIM, C. F. & WONG, K. K. 2014. Loss of Lkb1 and Pten leads to lung squamous cell carcinoma with elevated PD-L1 expression. *Cancer Cell,* 25**,** 590-604.

YASUOKA, S., OHNISHI, T., KAWANO, S., TSUCHIHASHI, S., OGAWARA, M., MASUDA, K., YAMAOKA, K., TAKAHASHI, M. & SANO, T. 1997. Purification, characterization, and localization of a novel trypsin-like protease found in the human airway. *Am J Respir Cell Mol Biol,* 16**,** 300-8.

YI, W., CLARK, P. M., MASON, D. E., KEENAN, M. C., HILL, C., GODDARD, W. A., 3RD, PETERS, E. C., DRIGGERS, E. M. & HSIEH-WILSON, L. C. 2012. Phosphofructokinase 1 glycosylation regulates cell growth and metabolism. *Science,* 337**,** 975-80.

YOSHIOKA, Y., KOSAKA, N., KONISHI, Y., OHTA, H., OKAMOTO, H., SONODA, H., NONAKA, R., YAMAMOTO, H., ISHII, H., MORI, M., FURUTA, K., NAKAJIMA, T., HAYASHI, H., SUGISAKI, H., HIGASHIMOTO, H., KATO, T., TAKESHITA, F. & OCHIYA, T. 2014. Ultra-sensitive liquid biopsy of circulating extracellular vesicles using ExoScreen. *Nat Commun,* 5**,** 3591.

YU, X. L., HU, T., DU, J. M., DING, J. P., YANG, X. M., ZHANG, J., YANG, B., SHEN, X., ZHANG, Z., ZHONG, W. D., WEN, N., JIANG, H., ZHU, P. & CHEN, Z. N. 2008. Crystal structure of HAb18G/CD147: implications for immunoglobulin superfamily homophilic adhesion. *J Biol Chem,* 283**,** 18056-65.

YUN, J., MULLARKY, E., LU, C., BOSCH, K. N., KAVALIER, A., RIVERA, K., ROPER, J., CHIO, II, GIANNOPOULOU, E. G., RAGO, C., MULEY, A., ASARA, J. M., PAIK, J., ELEMENTO, O., CHEN, Z., PAPPIN, D. J., DOW, L. E., PAPADOPOULOS, N., GROSS, S. S. & CANTLEY, L. C. 2015. Vitamin C selectively kills KRAS and BRAF mutant colorectal cancer cells by targeting GAPDH. *Science,* 350**,** 1391-6.

YUN, J., RAGO, C., CHEONG, I., PAGLIARINI, R., ANGENENDT, P., RAJAGOPALAN, H., SCHMIDT, K., WILLSON, J. K., MARKOWITZ, S., ZHOU, S., DIAZ, L. A., JR., VELCULESCU, V. E., LENGAUER, C., KINZLER, K. W., VOGELSTEIN, B. & PAPADOPOULOS, N. 2009. Glucose deprivation contributes to the development of KRAS pathway mutations in tumor cells. *Science,* 325**,** 1555-9.

YUNEVA, M., ZAMBONI, N., OEFNER, P., SACHIDANANDAM, R. & LAZEBNIK, Y. 2007. Deficiency in glutamine but not glucose induces MYC-dependent apoptosis in human cells. *J Cell Biol,* 178**,** 93-105.

YURCHENKO, V., ZYBARTH, G., O'CONNOR, M., DAI, W. W., FRANCHIN, G., HAO, T., GUO, H., HUNG, H. C., TOOLE, B., GALLAY, P., SHERRY, B. & BUKRINSKY, M. 2002. Active site residues of cyclophilin A are crucial for its signaling activity via CD147. *J Biol Chem,* 277**,** 22959-65.

ZHANG, C., LIU, J., LIANG, Y., WU, R., ZHAO, Y., HONG, X., LIN, M., YU, H., LIU, L., LEVINE, A. J., HU, W. & FENG, Z. 2013. Tumour-associated mutant p53 drives the Warburg effect. *Nat Commun,* 4**,** 2935.

ZHANG, C. S., HAWLEY, S. A., ZONG, Y., LI, M., WANG, Z., GRAY, A., MA, T., CUI, J., FENG, J. W., ZHU, M., WU, Y. Q., LI, T. Y., YE, Z., LIN, S. Y., YIN, H., PIAO, H. L., HARDIE, D. G. & LIN, S. C. 2017. Fructose-1,6-bisphosphate and aldolase mediate glucose sensing by AMPK. *Nature,* 548**,** 112-116.

ZHAO, D., ZOU, S. W., LIU, Y., ZHOU, X., MO, Y., WANG, P., XU, Y. H., DONG, B., XIONG, Y., LEI, Q. Y. & GUAN, K. L. 2013. Lysine-5 acetylation negatively regulates lactate dehydrogenase A and is decreased in pancreatic cancer. *Cancer Cell,* 23**,** 464-76.

ZHAO, H., YANG, L., BADDOUR, J., ACHREJA, A., BERNARD, V., MOSS, T., MARINI, J. C., TUDAWE, T., SEVIOUR, E. G., SAN LUCAS, F. A., ALVAREZ, H., GUPTA, S., MAITI, S. N., COOPER, L., PEEHL, D., RAM, P. T., MAITRA, A. & NAGRATH, D. 2016. Tumor microenvironment derived exosomes pleiotropically modulate cancer cell metabolism. *Elife,* 5**,** e10250.

ZHOU, Y., WU, B., LI, J. H., NAN, G., JIANG, J. L. & CHEN, Z. N. 2017. Rab22a enhances CD147 recycling and is required for lung cancer cell migration and invasion. *Exp Cell Res,* 357**,** 9-16.

ZMORA, P., BLAZEJEWSKA, P., MOLDENHAUER, A. S., WELSCH, K., NEHLMEIER, I., WU, Q., SCHNEIDER, H., POHLMANN, S. & BERTRAM, S. 2014. DESC1 and MSPL activate influenza A viruses and emerging coronaviruses for host cell entry. *J Virol,* 88**,** 12087-97.

ZMORA, P., HOFFMANN, M., KOLLMUS, H., MOLDENHAUER, A. S., DANOV, O., BRAUN, A., WINKLER, M., SCHUGHART, K. & POHLMANN, S. 2018. TMPRSS11A activates the influenza A virus hemagglutinin and the MERS coronavirus spike protein and is insensitive against blockade by HAI-1. *J Biol Chem*.

ZU, X. L. & GUPPY, M. 2004. Cancer metabolism: facts, fantasy, and fiction. *Biochem Biophys Res Commun,* 313**,** 459-65.

ZUCKER, S., HYMOWITZ, M., ROLLO, E. E., MANN, R., CONNER, C. E., CAO, J., FODA, H. D., TOMPKINS, D. C. & TOOLE, B. P. 2001. Tumorigenic potential of extracellular matrix metalloproteinase inducer. *Am J Pathol,* 158**,** 1921-8.

ZUNDEL, W., SCHINDLER, C., HAAS-KOGAN, D., KOONG, A., KAPER, F., CHEN, E., GOTTSCHALK, A. R., RYAN, H. E., JOHNSON, R. S., JEFFERSON, A. B., STOKOE, D. & GIACCIA, A. J. 2000. Loss of PTEN facilitates HIF-1-mediated gene expression. *Genes Dev,* 14**,** 391-6.